Table 2 Comparison of plain MRI-based findings to Gd-DPTA-enhanced MRI-based findings

MRI findings	Gd-enhanced MRI		Total
	Synovitis (+)	Synovitis (−)	
Synovitis			
Plain MRI			
Synovitis (+)	613	316	929
Synovitis (−)	175	312	487
Total	788	628	1416
Bone lesions			
Plain MRI			
Bone lesions (+)	92	9	101
Bone lesions (−)	22	1378	1400
Total	114	1387	1501

Synovitis were evaluated in 1416 sites and bone lesions were evaluated in 1501sites as described in Patients and methods

Gd-DPTA Gadolinium-diethylenetriamine pentaacetic acid, *MRI* magnetic resonance imaging

Table 3 Sensitivity, specificity, PPV, NPV and accuracy of synovitis and bone lesions according to the plain MRI-based findings[a]

	Sensitivity (%)	Specificity (%)	PPV (%)	NPV (%)	Accuracy (%)
Synovitis	77.8	49.7	66.0	64.1	65.3
Bone lesions	80.7	99.4	91.1	98.4	97.9

PPV Positive predictive value, *NPV* negative predictive value

[a] Gd-DTPA enhanced MRI-based findings were considered as gold standard; the accuracy of plain MRI-based findings were compared with Gd-DTPA-enhanced MRI-based findings

(Table 2). These data indicate that some synovitis that appears positive on a plain MR image scan is, in fact, false-positive. Bone lesions were visualized in 1501 sites by both plain and Gd-DTPA-enhanced MRI. In contrast to synovitis, the false-positive rate of bone lesions based on plain MRI findings was very low compared with that based on Gd-DTPA-enhanced MRI findings (Table 2). The rates of sensitivity, specificity, PPV and negative predictive value (NPV), and the accuracy of synovitis and bone lesion readings according to plain MRI were determined (Table 3).

The E-rate in sites of false-positive synovitis was significantly low compared with that in sites of true-positive synovitis

For the purposes of our study, the sites where plain MR scan images were positive for synovitis and Gd-DTPA-enhanced MR scan images were negative were considered

Table 4 Comparison of E-rate in sites of false-positive synovitis with sites of true-positive synovitis

MRI findings	N (sites)	E-rate (mean ± sd, median, range)	*P*-value
A. True positive; plain (+), enhanced (+)	366	8.1±5.1 (6.9, 1.2 – 50.1)	
B. False negative; plain (−), enhanced (+)	57	6.8 ±2.2 (6.5, 3.4 – 14.6)	N.S.
C. False positive; plain (+), enhanced (−)	121	5.7±2.2 (6.0, 1.4 – 14.5)	§
D. True negative; plain (−), enhanced (−)	298	5.5±1.7 (5.5, 1.4 – 12.3)	N.S.

§ § § §

We compared every E-rate by Mann–Whitney *U* test. *P* values are as follows: A vs B, 0.19; A vs C, 9.2×10^{-10}; A vs D, 5.2×10^{-8}; B vs C, 0.00096; B vs D, 5.3×10^{-6} and C vs D, 0.20. It is interesting to note that E-rate of false-negative synovitis sites tended to be low, however, there is no statistical significance as compared with true-positive sites (see A vs B). E-rate of false-negative synovitis sites was high as compared with false-positive synovitis sites (see B vs C)

§ *P* value <0.0001

to be false-positive sites; the sites for which positive results were obtained using both MRI imaging techniques were considered to be true positive sites. The severity of synovitis was compared by the E-rate of Gd-DTPA-enhanced MRI. As shown in Table 4, the E-rate of false-positive synovitis sites was significantly low compared with that of the true positive sites.

Discussion

Recent reviews have reported that plain MRI-based findings of bone lesions can be substituted for Gd-DTPA-enhanced MRI-based findings, although Gd-DTPA enhancement is recommended for the evaluation of synovitis [1]. Since the median disease duration from the onset of articular manifestations to entry in the 51 patients of our study cohort was 5 months, we suggest that our data reflect primarily rheumatoid joint damage, rather than secondary changes due to osteoarthritis. However, there have been few precise comparisons of plain MRI-based findings and Gd-DTPA-enhanced MRI-based findings; i.e., both plain and Gd-DTPA-enhanced sequences of multiple sites in both hands examined simultaneously. Ostergaard et al. reported that Gd-DTPA injection is not important to qualify the MRI scores of bone erosion and bone edema, whereas it is indispensable to diagnose synovitis [14].

Our data also show that plain MRI-based findings are not sufficient alone to evaluate the presence of synovitis. The severity of synovitis, as determined by the E-rate in dynamic Gd-DTPA-enhanced MR scan images, is low in false-positive synovitis sites compared with true-positive

sites. We speculate that cartilage, synovial fluids, or fibrous tissues may be interpreted as synovial hyperplasia in these cases, and we must be aware of the superiority of Gd-DTPA-enhanced MRI over plain MRI in evaluating synovitis, especially in the case of less active lesions. The E-rate of false-negative synovitis sites tended to be low among our patients; however, there was no statistical significance relative to true-positive synovitis sites. Accordingly, the E-rate of false-negative synovitis sites was high as compared with that of false-positive synovitis sites. Since a previous study demonstrated that the E-rate of the wrist correlates with the clinical disease activity in patients with RA [15], we suggest that the E-rate could correlate well with the synovitis score based on the RA MRI scoring system (RAMRIS). Consequently, findings from Gd-DTPA-enhanced MRI are crucial to qualify the presence of synovitis correctly.

Nevertheless, plain MRI is an effective tool for evaluating bone lesions of the wrists and finger joints since false-positivity is very low for this evaluation. In addition to the wrists and metacarpophalangeal joints, we identified three PIP joints as being positively associated with bone lesions out of 114 sites which were identified by Gd-enhanced MRI. There was no false-positive result by plain MRI in these three PIP joints, indicating that plain MRI is able to accurately detect the bone lesions of smaller joints of PIP joints. A recent observation (unpublished data) by our group indicates that the E-rate of sites with bone lesions is significantly high compared with that of those without bone lesions [15]. These data suggest that synovial inflammation is obvious in bone lesion sites and, therefore, that false-positivity is low in these areas.

In summary, our present data confirm the recent results of Ostergaard et al. [14] that bone lesions can be correctly identified by plain MRI-based findings in early-stage RA, while synovitis cannot. Based on our present results, we are currently investigating longitudinal changes in bone lesions by plain MRI of the wrists and finger joints in early arthritis patients during therapeutic interventions. These studies are warranted to establish the value of plain MRI in clinical rheumatology.

Acknowledgments This study was supported in part by a Grant from The Ministry of Health, Labour and Welfare, Japan.

Conflict of interest None.

References

1. Østergaard M, Pedersen SJ, Døhn UM. Imaging in rheumatoid arthritis: status and recent advances for magnetic resonance imaging, ultrasonography, computed tomography and conventional radiography. Best Pract Res Clin Rheumatol. 2008;22:1019–44.
2. Kubassova O, Boesen M, Peloschek P et al. Quantifying disease activity and damage by imaging in rheumatoid arthritis and osteoarthritis. Ann N Y Acad Sci. 2009;1154:207–38.
3. McQueen FM. The use of MRI in early RA. Rheumatology (Oxf). 2008;47:1597–9.
4. McGonagle D, Tan AL. What magnetic resonance imaging has told us about the pathogenesis of rheumatoid arthritis: the first 50 years. Arthritis Res Ther. 2008;10:222.
5. Tamai M, Kawakami A, Uetani M et al. A prediction rule for disease outcome in patients with undifferentiated arthritis using MRI of wrists and finger joints and serologic autoantibodies. Arthritis Rheum. 2009;61:772–8.
6. Tamai M, Kawakami A, Uetani M et al. Bone edema determined by magnetic resonance imaging reflects severe disease status in patients with early-stage rheumatoid arthritis. J Rheumatol. 2007;34:2154–7.
7. Tamai M, Kawakami A, Uetani M et al. Early prediction of rheumatoid arthritis by serological variables and magnetic resonance imaging of the wrists and finger joints: results from prospective clinical examination. Ann Rheum Dis. 2006;65:134–5.
8. Tamai M, Kawakami A, Uetani M et al. The presence of anti-cyclic citrullinated peptide antibody is associated with magnetic resonance imaging detection of bone marrow oedema in early stage rheumatoid arthritis. Ann Rheum Dis. 2006;65:133–4.
9. Ersoy H, Rybicki FJ. Biochemical safety profiles of gadolinium-based extracellular contrast agents and nephrogenic systemic fibrosis. J Magn Reson Imaging. 2007;26:1190–7.
10. Arnett FC, Edworthy SM, Bloch DA et al. The American Rheumatism Association 1987 revised criteria for the classification of rheumatoid arthritis. Arthritis Rheum. 1988;31:315–24.
11. Fujikawa K, Kawakami A, Tamai M et al. High serum cartilage oligomeric matrix protein determines the subset of patients with early-stage rheumatoid arthritis with high serum C-reactive protein, matrix metalloproteinase-3 and MRI-proven bone erosion. J Rheumatol. 2009;36:1126–9.
12. Lassere M, McQueen F, Østergaard M et al. OMERACT Rheumatoid arthritis magnetic resonance imaging studies. Exercise 3: an international multicenter reliability study using the RA-MRI Score. J Rheumatol. 2003;30:1366–75.
13. Conaghan P, Lassere M, Østergaard M, Peterfy C, McQueen F, O'Connor P et al. OMERACT Rheumatoid Arthritis Magnetic Resonance Imaging Studies. Exercise 4: an international multicenter longitudinal study using the RA-MRI Score. J Rheumatol. 2003;30(6):1376–9.
14. Ostergaard M, Conaghan PG, O'Connor P, Szdudlarek M, Klarlund M, Emery P, et al. Reducing invasiveness, duration, and cost of magnetic resonance imaging in rheumatoid arthritis by omitting intravenous contrast injection—does it change the assessment of inflammatory and destructive joint changes by the OMERACT RAMRIS? J Rheumatol. 2009;36:1806–10. (Erratum in: J Rheumatol. 2010;27:2198).
15. Cimmino MA, Innocenti S, Livrone F, Magnaguagno F, Silvestri E, Garlaschi G. Dynamic gadolinium-enhanced magnetic resonance imaging of the wrist in patients with rheumatoid arthritis can discriminate active from in active disease. Arthritis Rheum. 2003;48(5):1207–13.

ARTHRITIS & RHEUMATISM
Vol. 64, No. 1, January 2012, pp 162–172
DOI 10.1002/art.33335
© 2012, American College of Rheumatology

Overexpression of T-bet Gene Regulates Murine Autoimmune Arthritis

Yuya Kondo,[1] Mana Iizuka,[1] Ei Wakamatsu,[2] Zhaojin Yao,[1] Masahiro Tahara,[1] Hiroto Tsuboi,[1] Makoto Sugihara,[1] Taichi Hayashi,[1] Keigyou Yoh,[1] Satoru Takahashi,[1] Isao Matsumoto,[1] and Takayuki Sumida[1]

Objective. To clarify the role of T-bet in the pathogenesis of collagen-induced arthritis (CIA).

Methods. T-bet–transgenic (Tg) mice under the control of the CD2 promoter were generated. CIA was induced in T-bet–Tg mice and wild-type C57BL/6 (B6) mice. Levels of type II collagen (CII)–reactive T-bet and retinoic acid receptor–related orphan nuclear receptor γt (RORγt) messenger RNA expression were analyzed by real-time polymerase chain reaction. Criss-cross experiments using CD4+ T cells from B6 and T-bet–Tg mice, as well as CD11c+ splenic dendritic cells (DCs) from B6 and T-bet–Tg mice with CII were performed, and interleukin-17 (IL-17) and interferon-γ (IFNγ) in the supernatants were measured by enzyme-linked immunosorbent assay. CD4+ T cells from B6, T-bet–Tg, or T-bet–Tg/IFNγ$^{-/-}$ mice were cultured for Th17 cell differentiation, then the proportions of cells producing IFNγ and IL-17 were analyzed by fluorescence-activated cell sorting.

Results. Unlike the B6 mice, the T-bet–Tg mice did not develop CIA. T-bet–Tg mice showed overexpression of *Tbx21* and down-regulation of *Rorc* in CII-reactive T cells. Criss-cross experiments with CD4+ T cells and splenic DCs showed a significant reduction in IL-17 production by CII-reactive CD4+ T cells in T-bet–Tg mice, even upon coculture with DCs from B6 mice, indicating dysfunction of IL-17–producing CD4+ T cells. Inhibition of Th17 cell differentiation under an in vitro condition favoring Th17 cell differentiation was observed in both T-bet–Tg mice and T-bet–Tg/IFNγ$^{-/-}$ mice.

Conclusion. Overexpression of T-bet in T cells suppressed the development of autoimmune arthritis. The regulatory mechanism of arthritis might involve dysfunction of CII-reactive Th17 cell differentiation by overexpression of T-bet via IFNγ-independent pathways.

Rheumatoid arthritis (RA) is a chronic inflammatory disorder characterized by autoimmunity, infiltration of the joint synovium by activated inflammatory cells, and progressive destruction of cartilage and bone. Although the exact cause of RA is not clear, T cells seem to play a crucial role in the initiation and perpetuation of the chronic inflammation in RA.

The Th1 cell subset has long been considered to play a predominant role in inflammatory arthritis, because T cell clones from RA synovium were found to produce large amounts of interferon-γ (IFNγ) (1). Recently, interleukin-17 (IL-17)–producing Th17 cells have been identified, and this newly discovered T cell population appears to play a critical role in the development of various forms of autoimmune arthritis in experimental animals, such as those with glucose-6-phosphate isomerase–induced arthritis (2) and collagen-induced arthritis (CIA) (3). Conversely, IFNγ has antiinflammatory effects on the development of experimental arthritis (4,5). IL-17 is spontaneously produced by RA synovium (6), and the percentage of IL-17–positive CD4+ T cells was increased in the peripheral blood mononuclear cells of patients with RA compared with healthy control subjects (7). It is therefore necessary to determine if autoimmune arthritis is a Th1- or a Th17-associated disorder.

The lineage commitment of each Th cell subset from naive CD4+ T cells is dependent on the expression of specific transcription factors induced under the particular cytokine environment. Differentiation of Th1 cells is dependent on the expression of the transcription factor T-bet, which is induced by IFNγ/STAT-1 signaling pathways and directly activates the production of IFNγ (8,9). Similarly, Th17 cell differentiation in mice is dependent on the transcription factor retinoic acid receptor–related orphan nuclear receptor γt (RORγt) induced by transforming growth factor β (TGFβ) and IL-6 (10). Previous studies showed that these transcription factors negatively regulate the differentiation of other T cell subsets by direct co-interaction and/or indirect effects of cytokines produced from each T cell subset (11,12). How the predominant differentiation of CD4+ T cells affects the development of autoimmune arthritis remains unclear, however.

In the present study, CIA was induced in C57BL/6 (B6) mice and T-bet–transgenic (Tg) mice under the control of the CD2 promoter. The results showed that CIA was significantly suppressed in T-bet–Tg mice as compared with B6 mice. IL-17 production was not detected in type II collagen (CII)–reactive T cells from T-bet–Tg mice, and a significant reduction in IL-17 production by CII-reactive CD4+ T cells from T-bet–Tg mice was observed even when they were cocultured with splenic dendritic cells (DCs) from B6 mice. IFNγ production was also reduced in T-bet–Tg mice as compared with B6 mice, and levels of IFNγ in CII-reactive CD4+ T cells from T-bet–Tg mice were not different from those in B6 mice. Inhibition of Th17 cell differentiation and predominant differentiation of Th1 cells under an in vitro condition favoring Th17 cell differentiation was observed in T-bet–Tg mice, and surprisingly, this inhibition was also observed in T-bet–Tg/IFNγ$^{-/-}$ mice. These results indicate suppression of Th17 cell differentiation by overexpression of T-bet, but not IFNγ. Our findings support the notion that the suppression of autoimmune arthritis in T-bet–Tg mice might be due to the direct inhibition of Th17 cell differentiation by T-bet overexpression in T cells.

MATERIALS AND METHODS

Mice. CD2 T-bet–Tg mice (12) were prepared by backcrossing mice on a C57BL/6 background. IFNγ$^{-/-}$ mice were obtained from The Jackson Laboratory. Littermates of T-bet–Tg mice were used as controls in all experiments. All mice were maintained under specific pathogen–free conditions, and the experiments were conducted in accordance with the institutional ethics guidelines.

Induction of CIA and assessment of arthritis. Native chicken CII (Sigma-Aldrich) was dissolved in 0.01*M* acetic acid and emulsified in Freund's complete adjuvant (CFA). CFA was prepared by mixing 5 mg of heat-killed *Mycobacterium tuberculosis* H37Ra (Difco) and 1 ml of Freund's incomplete adjuvant (Sigma-Aldrich). Mice ages 8–10 weeks were injected intradermally at the base of the tail with 200 μg of CII in CFA on days 0 and 21. Arthritis was evaluated visually, and changes in each paw were scored on a scale of 0–3, where 0 = normal, 1 = slight swelling and/or erythema, 2 = pronounced swelling, and 3 = ankylosis. The scores in the 4 limbs were then summed (maximum score 12).

Histopathologic scoring. For histologic assessment, mice were killed on day 42 after the first immunization, and both rear limbs were removed. After fixation and decalcification, joint sections were cut and stained with hematoxylin and eosin. Histologic features of arthritis were quantified by 2 independent observers (YK and IM) who were blinded with regard to the study group, and a histologic score was assigned to each joint based on the degree of inflammation and erosion, as described previously (13). The severity of inflammation was scored on a scale of 0–5, where 0 = normal, 1 = minimal inflammatory infiltration, 2 = mild infiltration with no soft tissue edema or synovial lining cell hyperplasia, 3 = moderate infiltration with surrounding soft tissue edema and some synovial lining cell hyperplasia, 4 = marked infiltration, edema, and synovial lining cell hyperplasia, and 5 = severe infiltration with extended soft tissue edema and marked synovial lining cell hyperplasia. The severity of bone erosion was also scored on a scale of 0–5, where 0 = none, 1 = minimal, 2 = mild, 3 = moderate, 4 = marked, and 5 = severe erosion with full-thickness defects in the cortical bone.

Analysis of cytokine profiles and cytokine and transcriptional factor gene expression. Inguinal and popliteal lymph nodes were harvested from each mouse on day 10 after the first immunization with CII. Single-cell suspensions were prepared, and lymph node cells (2×10^5/well on a 96-well round-bottomed plate) were cultured for 72 hours in RPMI 1640 medium (Sigma-Aldrich) containing 10% fetal bovine serum, 100 units/ml of penicillin, 100 μg/ml of streptomycin, and 50 μ*M* 2-mercaptoethanol in the presence of 100 μg/ml of denatured chicken CII. The supernatants were analyzed for IFNγ, IL-4, IL-10, and IL-17 by enzyme-linked immunosorbent assay (ELISA) using specific Quantikine ELISA kits (R&D Systems).

Lymphocytes harvested on day 10 after immunization were used to obtain complementary DNA (cDNA) by reverse transcription, using a commercially available kit. A TaqMan Assay-on-Demand gene expression product was used for real-time polymerase chain reaction (PCR; Applied Biosystems). The expression levels of *Ifng*, *Il17a*, *Tbx21*, *Rorc*, *Il12a*, and *Il23a* were normalized relative to the expression of *gapdh*. Analyses were performed with an ABI Prism 7500 apparatus (Applied Biosystems).

Criss-cross coculture with CD4+ T cells and CD11c+ splenic dendritic cells. Ten days after the first CII immunization, CD4+ cells in draining lymph nodes were isolated by

Supported in part by the Japanese Ministry of Science and Culture and by the Japanese Ministry of Health, Labor, and Welfare.

[1]Yuya Kondo, MD, Mana Iizuka, MSc, Zhaojin Yao, MSc, Masahiro Tahara, BSc, Hiroto Tsuboi, MD, PhD, Makoto Sugihara, MD, PhD, Taichi Hayashi, MD, PhD, Keigyou Yoh, MD, PhD, Satoru Takahashi, MD, PhD, Isao Matsumoto, MD, PhD, Takayuki Sumida, MD, PhD: Graduate School of Comprehensive Human Sciences, University of Tsukuba, Tsukuba City, Ibaraki, Japan; [2]Ei Wakamatsu, PhD: Graduate School of Comprehensive Human Sciences, University of Tsukuba, Tsukuba City, Ibaraki, Japan, and Harvard Medical School, Boston, Massachusetts.

Address correspondence to Takayuki Sumida, MD, PhD, Division of Clinical Immunology, Doctoral Programs in Clinical Sciences, Graduate School of Comprehensive Human Science, University of Tsukuba, 1-1-1 Tennodai, Tsukuba City, Ibaraki 305-8575, Japan. E-mail: tsumida@md.tsukuba.ac.jp.

Submitted for publication January 4, 2011; accepted in revised form September 1, 2011.

positive selection, using a magnetic-activated cell sorter (MACS) system with anti-CD4 monoclonal antibody (mAb; Miltenyi Biotec). After treatment with mitomycin C, CD11c+ cells were isolated from the spleen by positive selection, using a MACS system with anti-CD11c mAb (Miltenyi Biotec). Criss-cross coculture for 72 hours was performed with 1×10^5 CD4+ cells and 2×10^4 CD11c+ cells in 100 μg/ml of denatured CII-containing medium. Cytokine production and transcription factor expression were then analyzed.

Measurement of collagen-specific immunoglobulin titers. Serum was collected from the mice on day 56 after the first immunization. A total of 10 μg/ml of CII in phosphate buffered saline (PBS) was coated overnight at 4°C onto 96-well plates (Nunc MaxiSorp; Nalge Nunc). After washes with washing buffer (0.05% Tween 20 in PBS), the blocking solution, including 1% bovine serum albumin in PBS, was applied for 1 hour. After washing, 100 μl of diluted serum was added, and the plates were incubated for 1 hour at room temperature. After further washing, horseradish peroxidase–conjugated anti-mouse IgG, IgG1, IgG2a, or IgG2b (1:5,000 dilution) in blocking solution was added, and the plates were incubated for 1 hour at room temperature. After washing, tetramethylbenzidine was added, and the optical density was read at 450 nm using a microplate reader.

Purification of CD4+ cells and in vitro T cell cultures. CD4+ cells (1×10^6/well) were cultured in medium with 1 μg/ml of soluble anti-CD3ε mAb (eBioscience), 1 μg/ml of soluble anti-CD28 mAb (BioLegend), 10 μg/ml of anti-IFNγ mAb (BioLegend), and 10 μg/ml of anti-IL-4 mAb (BioLegend) for a neutral condition. For Th17 cell differentiation, CD4+ cells (1×10^6/well) were cultured in medium with 1 μg/ml of soluble anti-CD3ε mAb, 1 μg/ml of soluble anti-CD28 mAb, 3 ng/ml of human TGFβ (R&D Systems), 20 ng/ml of mouse IL-6 (eBioscience), 10 μg/ml of anti-IFNγ mAb, and 10 μg/ml of anti–IL-4 mAb. On day 4, cells were restimulated for 4 hours with 50 ng/ml of phorbol myristate acetate and 500 ng/ml of ionomycin and used in the experiments.

Surface and intracellular staining and fluorescence-activated cell sorter (FACS) analysis. GolgiStop (BD PharMingen) was added during the last 6 hours of each culture. Cells were stained extracellularly, fixed, and permeabilized with Cytofix/Cytoperm solution (BD PharMingen). Then, intracellular cytokine staining was performed according to the manufacturer's protocol, using fluorescein isothiocyanate (FITC)–conjugated anti-IFNγ (BD PharMingen) and phycoerythrin (PE)–conjugated anti–IL-17 (BD PharMingen) or FITC-conjugated anti–IL-17 (BioLegend). A Treg cell staining kit (eBioscience) was used to stain T-bet, RORγt, and FoxP3 in cultured cells according to the manufacturer's protocol, using PE-conjugated anti–T-bet (eBioscience), allophycocyanin-conjugated anti-RORγt (eBioscience), and PE-conjugated anti-FoxP3 (eBioscience). Samples were analyzed with a FACSCalibur flow cytometer (Becton Dickinson), and data were analyzed with FlowJo software (Tree Star).

Statistical analysis. Data are expressed as the mean ± SEM or the mean ± SD. Differences between groups were examined for statistical significance using Student's *t*-test. *P* values less than 0.05 were considered significant.

RESULTS

Construction of the T-bet transgene and tissue distribution of transcription factors and cytokine production in naive mice. To generate transgenic mouse lines that express high levels of T-bet specifically in T cells, mouse T-bet cDNA was inserted into a VA vector containing a human CD2 transgene cassette (14). To confirm the expression of the transgene, reverse transcription–PCR (RT-PCR) was performed to monitor the expression of *Tbx21* (coding for T-bet) in organs from the T-bet–Tg mice. *Tbx21* messenger RNA (mRNA) expression was detected in the lymphatic system and in nonlymphatic organs in T-bet–Tg mice, and the expression levels were higher than those in B6 mice (data available upon request from the author). Analysis by semiquantitative RT-PCR and quantitative PCR (data not shown) revealed that the expression levels of other transcription factors (*Gata3*, *Rorc*, and *Foxp3*) in T-bet–Tg mice were not different from those in B6 mice. As previously reported by Ishizaki et al (14), high production of IFNγ was observed even when CD4+ T cells isolated from the spleen of T-bet–Tg mice were cultured under neutral conditions (data available upon request from the author).

Failure to induce CIA and low CII-specific IgG production in T-bet–Tg mice. To assess whether T cell–specific T-bet expression affects the development of arthritis, we induced CIA in T-bet–Tg mice and in wild-type B6 mice. The incidence and severity of arthritis in T-bet–Tg mice were markedly suppressed compared with those in B6 mice (Figure 1A). Surprisingly, the majority of T-bet–Tg mice were essentially free of arthritis, and even when arthritis was present, it was of the mild type. Consistent with these findings, histologic analyses of the joints obtained from each mouse 42 days after immunization revealed that joint inflammation and destruction were significantly suppressed in T-bet–Tg mice compared with B6 mice (Figures 1B and C). These results indicated that enforced expression of T-bet in T cells suppressed the development of CIA.

Because the levels of CII-specific IgG correlate well with the development of arthritis (15), we examined CII-specific IgG production in T-bet–Tg mice. CII-specific IgG, IgG1, IgG2a, and IgG2b levels were significantly lower in T-bet–Tg mice than in B6 mice, as determined by ELISA (Figure 1D). Thus, enforced expression of T-bet in T cells suppresses the development of CIA and CII-specific IgG production.

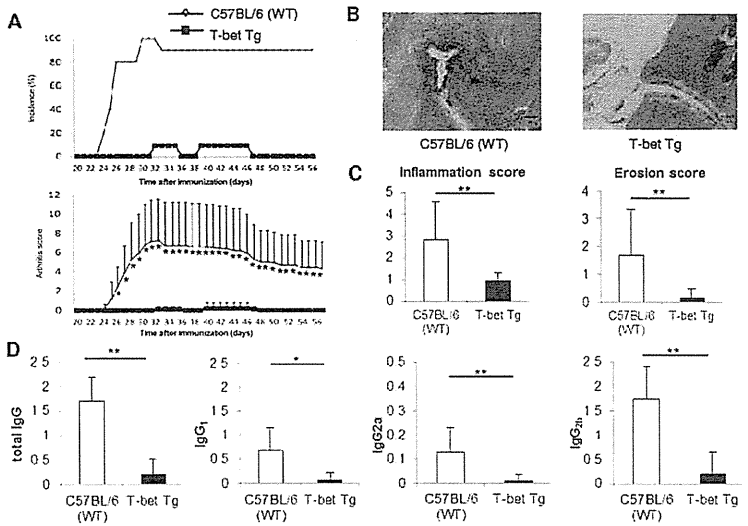

Figure 1. Significant suppression of collagen-induced arthritis (CIA) and type II collagen (CII)–specific IgG production in T-bet–transgenic (Tg) mice. On days 0 and 21, mice were immunized intradermally at several sites at the base of the tail with chicken CII emulsified with Freund's complete adjuvant. **A**, Incidence and severity of CIA. The arthritis score was determined as described in Materials and Methods. Data were obtained from 2 independent experiments involving 10 C57BL/6 (wild-type [WT]) mice and 11 T-bet–Tg mice. **B**, Hematoxylin and eosin–stained sections of the hind paws of mice obtained 6 weeks after the first immunization. Original magnification × 40. **C**, Inflammation and bone erosion scores in 7 C57BL/6 mice and 5 T-bet–Tg mice 6 weeks after the first immunization. Scores were determined as described in Materials and Methods. **D**, Serum levels of CII-specific IgG, IgG1, IgG2a, and IgG2b levels in 10 C57BL/6 mice and 11 T-bet–Tg mice 8 weeks after the first immunization, as measured by enzyme-linked immunosorbent assay. Values in **A**, **C**, and **D** are the mean ± SD. * = $P < 0.05$; ** = $P < 0.01$ by Student's *t*-test.

Suppression of CII-reactive IL-17 production and IL-17 mRNA expression in T-bet–Tg mice. Because enforced T-bet expression in T cells suppressed the development CIA, we examined antigen-specific cytokine production and transcription factor expression in mice with CIA. CD4+ T cells harvested from draining lymph nodes were stimulated with CII in vitro, and then various cytokine levels in the supernatants were measured by ELISA. IL-17 production by CII-reactive T cells was significantly reduced in T-bet–Tg mice as compared with B6 mice (Figure 2A). IFNγ production by CII-reactive T cells also tended to be decreased in T-bet–Tg mice.

We analyzed CII-reactive cytokine and transcription factor mRNA expression levels by real-time PCR (Figure 2B). Similar to the ELISA results, *Il17a* expression tended to be lower in T-bet–Tg mice than in B6 mice. No difference in *Ifng* expression was observed between B6 and T-bet–Tg mice (Figure 2B). *Tbx21* expression tended to be higher in T-bet–Tg mice, whereas *Rorc* expression was lower in T-bet–Tg mice than in B6 mice ($P < 0.05$). The level of expression of *Il12a* (coding for IL-12p35) was also higher in T-bet–Tg mice than in B6 mice ($P < 0.05$). However, there was no difference in the expression levels of *Il23a* (coding for IL-23p19) between B6 mice and T-bet–Tg mice. These

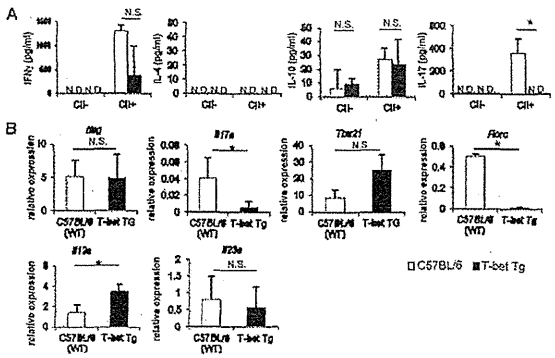

Figure 2. No production of interleukin-17 (IL-17) and low production of interferon-γ (IFNγ) in type II collagen (CII)–reactive CD4+ T cells. A, Ten days after the first CII immunization, lymphocytes derived from the draining lymph nodes of C57BL/6 (wild-type [WT]) mice and T-bet–transgenic (Tg) mice were cultured for 72 hours in the presence or absence of 100 μg/ml of denatured CII. Levels of IL-17, IFNγ, IL-4, and IL-10 in the supernatants were measured by enzyme-linked immunosorbent assay. B, After culture of lymphocytes with CII, cDNA was obtained, and levels of *Ifng*, *Il17a*, *Tbx21*, *Rorc*, *Il12a*, and *Il23a* expression were analyzed by real-time polymerase chain reaction. Values are the mean ± SD of 3 mice. * = $P < 0.05$ by Student's *t*-test. ND = not detected; NS = not significant.

results suggest that overexpression of T-bet on CD4+ T cells suppressed the expression of RORγt and IL-17.

No reduction of RORγt expression on CII-reactive CD4+ T cells in T-bet–Tg mice. CD4+ T cells from T-bet–Tg and B6 mice were cultured in vitro with CII, and analyses of T-bet and RORγt expression on CD4+ T cells were carried out by the intracellular staining method. T-bet expression on CII-reactive CD4+ T cells was significantly higher in T-bet–Tg mice than in B6 mice (Figure 3A). Surprisingly, the majority of T-bet+ CII-reactive T cells expressed RORγt in both the B6 mice and the T-bet–Tg mice (Figure 3A). Although there was no significant difference in the mean fluorescence intensity of RORγt between B6 mice and T-bet–Tg mice, the number of RORγt+ cells tended to be lower in T-bet–Tg mice (data available upon request from the author).

Moreover, in the case of CD4+ T cells examined under conditions favoring Th17 differentiation, RORγt expression on CD4+ T cells from T-bet–Tg mice was lower than that on cells from B6 mice (Figure 3B). Interestingly, most of the RORγt+ cells also expressed T-bet in the T-bet–Tg mice, and the proportion of IL-17–producing RORγt+ CD4+ T cells was lower in the T-bet–Tg mice than in the B6 mice. These findings support the notion that overexpression of T-bet not only suppresses RORγt expression on CD4+ T cells but also inhibits the production of IL-17 from RORγt+ T cells.

To investigate whether the suppression of arthritis and low antigen-specific cytokine production observed in T-bet–Tg mice was related to Treg cells, the next experiment analyzed FoxP3 expression on CD4+ T cells harvested from draining lymph nodes 10 days after immunization. There was no significant difference in the percentage of FoxP3+ cells among the CD4+ T cells between B6 mice and T-bet–Tg mice (data available upon request from the author). Thus, Treg cells do not seem to be involved in the suppression of CIA in T-bet–Tg mice.

Decreased numbers of T cells in the lymph nodes, spleen, and thymus of T-bet–Tg mice. To evaluate the low cytokine response and the low population of CII-reactive RORγt+CD4+ T cells in T-bet–Tg mice with CIA, we analyzed the lymphocyte subsets in the draining lymph nodes and spleen after immunization. The percentage and absolute number of CD3+ T cells were lower in both the draining lymph nodes and the

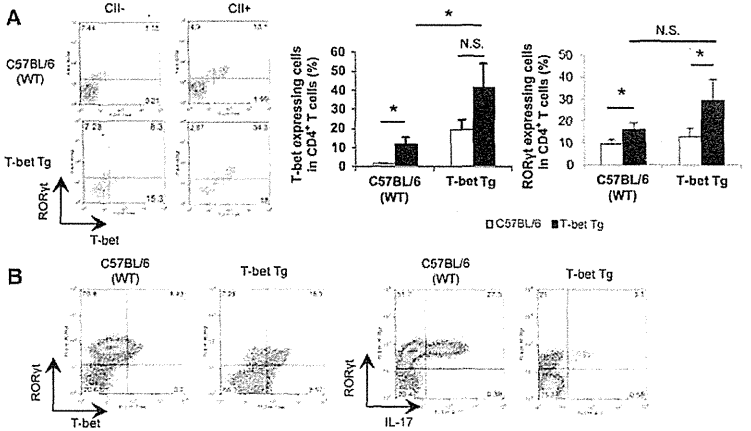

Figure 3. Suppression of Th17 cell differentiation by enforced expression of T-bet in T cells despite expression of retinoic acid receptor–related orphan nuclear receptor γt (RORγt). A, Ten days after the first type II collagen (CII) immunization, lymphocytes derived from the draining lymph nodes of C57BL/6 (wild-type [WT]) and T-bet–transgenic (Tg) mice were cultured for 72 hours in the presence or absence of 100 μg/ml of denatured CII. Levels of T-bet and RORγt expression on CD4+ T cells were analyzed by intracellular staining. Numbers in each compartment of the histograms are the percentage of transcription factor–expressing cells gated on CD4+ T cells. Values in the bar graphs are the mean ± SD of 3 mice per group. * = $P < 0.05$ by Student's *t*-test. NS = not significant. B, CD4+ T cells were isolated from the spleen of C57BL/6 and T-bet–Tg mice by magnetic-activated cell sorting and were then cultured for 96 hours with soluble anti-CD3 antibody, soluble anti-CD28 antibody, interleukin-6 (IL-6), and transforming growth factor β. Cytokine production and transcription factor expression on CD4+ T cells were analyzed by intracellular staining. Representative histograms from flow cytometric analysis of T-bet and RORγt expression with IL-17 production are shown. Numbers in each compartment are the percentage of positive cells gated on CD4+ T cells.

spleen of T-bet–Tg mice as compared with B6 mice (Figures 4A and B). The absolute number of CD4+ and CD8+ T cells also tended to be lower in T-bet–Tg mice (Figure 4B). Moreover, analysis of the thymus showed a significantly low number of total thymocytes in T-bet–Tg mice and the presence of an abnormal proportion of T precursor cells, such as a low number of double-positive T cells and CD4 single-positive T cells in T-bet–Tg mice (Figure 4C). These results suggest abnormal T cell development in the thymus of T-bet–Tg mice.

Inhibition of IL-17 production by CII-reactive CD4+ T cells in T-bet–Tg mice. To clarify whether T-bet overexpression on CD4+ T cells directly affects cytokine production, we performed criss-cross experiments using CD4+ T cells from B6 and T-bet–Tg mice, as well as DCs from B6 and T-bet–Tg mice in CII-containing medium, and measured IL-17 and IFNγ levels in the supernatants by ELISA. IL-17 production was detected in CII-reactive CD4+ T cells from B6 mice and in DCs from T-bet–Tg mice. Interestingly, IL-17 production was significantly reduced, even when CD4+ T cells from T-bet–Tg mice were cocultured with DCs from B6 mice (Figure 5A). These observations suggest that T-bet overexpression on CD4+ T cells is responsible for the inhibition of CII-reactive IL-17 production. No difference in IFNγ production was noted among the experimental conditions (Figure 5A), suggesting that reduced IFNγ production by CII-reactive CD4+ T cells from T-bet–Tg mice (Figure 2) was probably related to the reduced numbers of CD4+ T cells in draining lymph nodes. Moreover, intracellular staining revealed that RORγt expression was suppressed and T-bet expression was increased, even when CD4+ T cells from T-bet–Tg

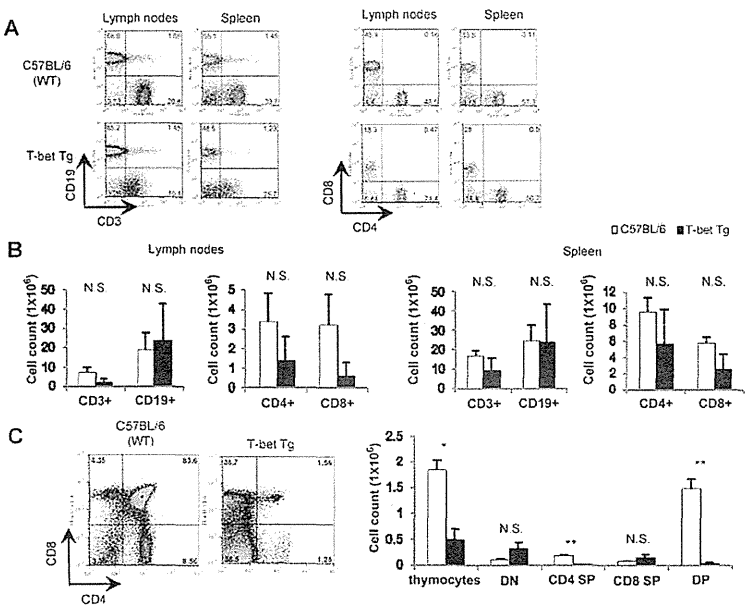

Figure 4. Decreased number of CD3+ T cells in spleen and lymph nodes and abnormal development of T precursor cells in the thymus in T-bet–transgenic (Tg) mice. A, Ten days after first immunization, the proportion of lymphocytes in draining lymph nodes and spleen were analyzed by fluorescence-activated cell sorting (FACS), and the absolute numbers of cells were calculated. Numbers in each compartment are the percentage of the parent population. B, The absolute numbers of CD3+, CD19+, CD4+, and CD8+ T cells in the lymph nodes and spleen of C57BL/6 (wild-type [WT]) and T-bet–Tg mice were determined. Values are the mean ± SD of 3 mice per group. NS = not significant. C, The proportion of T precursor cells in the thymus of nonimmunized mice was analyzed by FACS, and the absolute numbers of thymocytes, double-negative (DN) T cells, CD4 and CD8 single-positive (SP) T cells, and double-positive (DP) T cells were determined. Values in the bar graphs are the mean ± SD of 3 mice per group. * = $P < 0.05$; ** = $P < 0.01$ by Student's t-test.

mice were cocultured with DCs from B6 mice (Figure 5B). These results indicate that T-bet overexpression on CD4+ T cells suppressed CII-reactive IL-17 production by inhibition of the expression of RORγt.

Overexpression of T-bet directly suppresses Th17 cell differentiation via IFNγ-independent mechanisms. To clarify whether IFNγ production influences Th17 cell differentiation, we generated T-bet–Tg/IFNγ$^{-/-}$ mice. CD4+ T cells were isolated from the spleen of T-bet–Tg, T-bet–Tg/IFNγ$^{-/-}$, and B6 mice and were then cultured for Th17 cell differentiation. FACS analysis demonstrated that the proportion of IL-17–producing CD4+ T cells was lower in T-bet–Tg mice than in B6 mice, whereas the proportion of IFNγ-producing CD4+ T cells was higher in T-bet–Tg mice. Similarly, the proportion of IL-17–producing CD4+ T cells was also lower in T-bet–Tg/IFNγ$^{-/-}$ mice, although no IFNγ-producing CD4+ T cells were detected in

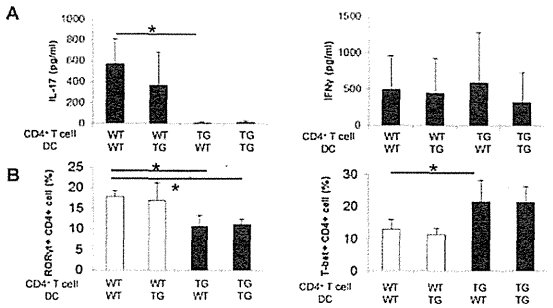

Figure 5. Impaired antigen-specific Th17 cell responses in T-bet–transgenic (Tg) mice with collagen-induced arthritis (CIA). Ten days after the first type II collagen (CII) immunization, CD4+ cells were isolated from draining lymph nodes of C57BL/6 (wild-type [WT]) mice and T-bet–Tg (TG) mice by positive selection using magnetic-activated cell sorting (MACS) with anti-CD4 monoclonal antibody (mAb). After treatment with mitomycin C, CD11c+ cells were isolated from the spleen by positive selection using a MACS system with anti-CD11c mAb. Criss-cross coculture for 72 hours was performed with 1×10^5 CD4+ cells and 2×10^4 CD11c+ cells in 100 μg/ml of denatured CII–containing medium. A, Levels of interleukin-17 (IL-17) and interferon-γ (IFNγ) in culture supernatants were measured by enzyme-linked immunosorbent assay. B, Expression of retinoic acid receptor–related orphan nuclear receptor γt (RORγt) and T-bet expression on CD4+ T cells were analyzed by intracellular staining. Representative data from flow cytometric analysis of the percentage of RORγt+ or T-bet+ cells in the CD4+ T cell subset are shown. Values are the mean ± SD of 3 mice per group. * = $P < 0.05$ by Student's t-test. DC = dendritic cells.

T-bet–Tg/IFNγ$^{-/-}$ mice (Figure 6). These results strongly support the view that inhibition of Th17 cell differentiation in T-bet–Tg mice cannot be due to overproduction of IFNγ, indicating that overexpression of T-bet directly suppresses Th17 cell differentiation in T-bet–Tg mice.

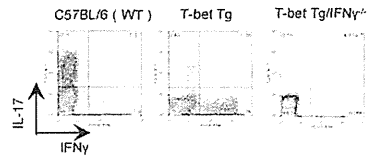

Figure 6. Suppressed expression of interleukin-17 (IL-17) by T-bet overexpression independently of interferon-γ (IFNγ) in T-bet–transgenic (Tg) mice. CD4+ T cells were isolated from the spleen of C57BL/6 (wild-type [WT]), T-bet–Tg, and T-bet–Tg/IFNγ$^{-/-}$ mice by magnetic-activated cell sorting and then cultured for 96 hours with soluble anti-CD3 monoclonal antibody (mAb), soluble anti-CD28 mAb, IL-6, and transforming growth factor β. IFNγ and IL-17 production by CD4+ cells was analyzed by intracellular cytokine staining. Numbers in each compartment are the percentage of cells secreting cytokines.

DISCUSSION

Recent studies showed that IL-17 plays a crucial role in the development of CIA (3) and other types of experimental arthritis (2). In contrast, it has been reported that IFNγ can suppress IL-17 production in vitro (16) and has antiinflammatory effects on the development of experimental arthritis (4,5). T-bet is a transcription factor known to induce the differentiation of naive CD4+ T cells to Th1 cells (8). Although the absence of T-bet can result in severe IL-17–mediated experimental autoimmune myocarditis via dysregulation of IFNγ (17), several studies have shown that T-bet is essential for the development of several models of autoimmunity, such as experimental autoimmune encephalitis (18,19), colitis (20), and diabetes mellitus (21). Nevertheless, the effect of T-bet expression on Th17 cell differentiation and function during arthritis remains unclear.

T-bet–Tg mice overexpress T-bet and mainly produce IFNγ in their T cells (14). Previous studies in T-bet–Tg mice suggested that overexpression of T-bet and a predominant Th1 response affect the pathogenesis of various diseases (14,22,23). To examine whether T-bet overexpression on T cells affects the regulation of

autoimmune arthritis, we induced CIA in T-bet–Tg mice and found marked suppression of CIA in T-bet–Tg mice.

To determine the reason for the low incidence of CIA in T-bet–Tg mice, we measured CII-reactive cytokine production and expression in vitro. IL-17 production from CII-reactive CD4+ T cells and *Il17a* expression were reduced in T-bet–Tg mice as compared with B6 mice. Although a predominant Th1 cell response was reported by Ishizuka et al (14), CII-specific IFNγ production was reduced in T-bet–Tg mice, and no significant difference was observed in *Ifng* expression between B6 mice and T-bet–Tg mice. Furthermore, *Il12a* expression was significantly higher in T-bet–Tg mice than in B6 mice, suggesting that overexpression of T-bet on T cells seems to affect innate immune cells, because the main producers of IL-12 are DCs and macrophages, not CD4+ T cells.

In criss-cross coculture experiments with CD4+ T cells and splenic DCs from B6 mice and T-bet–Tg mice, CII-reactive IL-17 production was also reduced even when CD4+ T cells from T-bet–Tg mice were cocultured with DCs from B6 mice, although there was no significant difference in IL-17 production by CD4+ T cells from B6 mice cocultured with DCs from either B6 mice or T-bet–Tg mice. In contrast, no difference in IFNγ production was observed under all coculture conditions examined. Moreover, suppression of RORγt expression and high expression of T-bet on CD4+ T cells were observed even when CD4+ T cells from T-bet–Tg mice were cocultured with DCs from B6 mice. These findings indicate that T-bet overexpression on CD4+ T cells might suppress CII-reactive IL-17 production resulting from suppression of RORγt expression in an IFNγ-independent manner, and that overexpression of T-bet has no direct effect on DC function.

CII-specific IgG levels correlate well with the development of arthritis (15). We observed significant suppression of CII-specific IgG production in the T-bet–Tg mice as compared with the B6 mice. A previous study showed that IL-17 is required for anti-CII antibody production (3). Therefore, the suppression of anti-CII antibody formation might be due to lower CII-reactive IL-17 production in T-bet–Tg mice.

To evaluate the low cytokine response to CII in T-bet–Tg mice, we analyzed lymphocytes obtained after immunization from draining lymph nodes and spleen. The percentage and absolute number of T cells tended to be lower in both the draining lymph nodes and spleen of T-bet–Tg mice compared with B6 mice. Moreover, significantly lower numbers of total thymocytes and an abnormal proportion of T precursor cells were observed in T-bet–Tg mice. The latter phenomenon could be due to T-bet transgene expression on double-negative thymic cells in T-bet–Tg mice. Because previous observations showed that T-bet interferes with GATA-3 function (11) and that GATA-3 was required for the development of early thymic T cells (24), one of the reasons for abnormal T cell development in the thymus might be the dysfunction of GATA-3 by overexpression of T-bet. These results suggest that overexpression of T-bet in thymic T cells affects T cell development, is responsible for the low number of T cells in spleen and lymph nodes, and is related to the low cytokine production against CII in T-bet–Tg mice.

To assess the effect of T-bet on CD4+ T cell differentiation in T-bet–Tg mice, we performed in vitro induction of Th17 cells. Analysis of T-bet–Tg mice showed a reduction in IL-17–producing CD4+ T cells and an increase in IFNγ-producing CD4+ T cells in spite of the condition favoring Th17 differentiation, which indicates suppression of Th17 cell differentiation and predominance of Th1 cell differentiation in vitro in T-bet–Tg mice. These results did not contradict the previous findings that the phenotype of polarized Th1 cells was not affected by Th cell–polarizing conditions (25). It is possible that suppression of CII-reactive IL-17 production in T-bet–Tg mice was not associated with IFNγ. For this reason, we generated T-bet–Tg/IFNγ$^{-/-}$ mice and performed in vitro induction of Th17 cells in these mice. Surprisingly, in T-bet–Tg/IFNγ$^{-/-}$ mice, the levels of IL-17–producing CD4+ T cells were also markedly reduced under Th17 cell differentiation–favoring conditions, indicating an IFNγ-independent suppressive pathway against Th17 cell differentiation. Although previous studies showed that suppression of Th17 cell differentiation was mediated through IFNγ signal transduction (16), our findings allow us to propose a new hypothesis: Th17 cell differentiation is regulated by a pathway that is distinct from the IFNγ signaling pathway. Therefore, we suggest that T-bet expression either directly or indirectly suppresses Th17 cell differentiation via an IFNγ-independent mechanism.

Tbx21 expression was significantly higher in T-bet–Tg mice as compared with B6 mice, and FACS analysis of CII-reactive CD4+ T cells revealed a significantly higher percentage of T-bet+ cells among the CD4+ T cell subset in T-bet–Tg mice. While there was no significant difference in the percentage of RORγt+ cells among the CD4+ T cell subset in T-bet–Tg mice as compared with B6 mice, *Rorc* expression was down-regulated on CII-reactive CD4+ T cells in T-bet–Tg mice. In the case of CD4+ T cells under conditions favoring Th17 cell differentiation, RORγt expression on CD4+ T cells from T-bet–Tg mice was lower than that on cells from B6 mice. Interestingly, most of the RORγt+ cells also expressed T-bet in T-bet–Tg mice, and the proportion of IL-17–producing RORγt+ T cells in the CD4+ cell subset was lower in T-bet–Tg mice than in B6 mice. These findings support the notion that overexpression of T-bet not only suppresses RORγt expression on CD4+ T cells, but also inhibits the production of IL-17 from RORγt+ T cells.

Previous studies showed that RORγt expression is positively regulated by several transcription factors, such as runt-related transcription factor 1 (RUNX-1), interferon regulatory factor 4, and STAT-3 (26–28). Lazarevic et al (29) recently reported that T-bet prevented RUNX-1–mediated activation of the gene encoding RORγt, followed by the suppression of Th17 cell differentiation. In addition to direct promotion of RORγt expression, RUNX-1 also acts as a coactivator, together with RORγt, and induces the expression of *Il17a* and *Il17f* (26); therefore, T-bet inhibits IL-17 production by RORγt+ cells induced by RUNX-1 (29). Although further studies will be required to identify the effect of T-bet overexpression on the function of RUNX-1, it might be associated with the suppression of Th17 cell differentiation that was observed in the T-bet–Tg mice.

In conclusion, our results demonstrated that overexpression of T-bet in T cells suppressed the development of autoimmune arthritis. The regulatory mechanism of CIA might involve dysfunction of CII-reactive Th17 cell differentiation by overexpression of T-bet via IFNγ-independent pathways. These findings should enhance our understanding of the pathogenesis of autoimmune arthritis and help in the development of new therapies for RA.

ACKNOWLEDGMENT

We thank Dr. F. G. Issa for critical reading of the manuscript.

AUTHOR CONTRIBUTIONS

All authors were involved in drafting the article or revising it critically for important intellectual content, and all authors approved the final version to be published. Dr. Sumida had full access to all of the data in the study and takes responsibility for the integrity of the data and the accuracy of the data analysis.

Study conception and design. Sugihara, Hayashi, Yoh, Takahashi, Matsumoto, Sumida.

Acquisition of data. Kondo, Yao, Tahara.

Analysis and interpretation of data. Kondo, Iizuka, Wakamatsu, Tsuboi, Matsumoto.

REFERENCES

1. Miltenburg AM, van Laar JM, de Kuiper R, Daha MR, Breedveld FC. T cells cloned from human rheumatoid synovial membrane functionally represent the Th 1 subset. Scand J Immunol 1992;35:603–10.
2. Iwanami K, Matsumoto I, Tanaka-Watanabe Y, Inoue A, Mihara M, Ohsugi Y, et al. Crucial role of the interleukin-6/interleukin-17 cytokine axis in the induction of arthritis by glucose-6-phosphate isomerase. Arthritis Rheum 2008;58:754–63.
3. Nakae S, Nambu A, Sudo K, Iwakura Y. Suppression of immune induction of collagen-induced arthritis in IL-17-deficient mice. J Immunol 2003;171:6173–7.
4. Chu CQ, Swart D, Alcorn D, Tocker J, Elkon KB. Interferon-γ regulates susceptibility to collagen-induced arthritis through suppression of interleukin-17. Arthritis Rheum 2007;56:1145–51.
5. Geboes L, De Klerck B, Van Balen M, Kelchtermans H, Mitera T, Boon L, et al. Freund's complete adjuvant induces arthritis in mice lacking a functional interferon-γ receptor by triggering tumor necrosis factor α–driven osteoclastogenesis. Arthritis Rheum 2007;56:2595–607.
6. Chabaud M, Durand JM, Buchs N, Fossiez F, Page G, Frappart L, et al. Human interleukin-17: a T cell–derived proinflammatory cytokine produced by the rheumatoid synovium. Arthritis Rheum 1999;42:963–70.
7. Shen H, Goodall JC, Gaston JS. Frequency and phenotype of peripheral blood Th17 cells in ankylosing spondylitis and rheumatoid arthritis. Arthritis Rheum 2009;60:1647–56.
8. Szabo SJ, Kim ST, Costa GL, Zhang X, Fathman CG, Glimcher LH. A novel transcription factor, T-bet, directs Th1 lineage commitment. Cell 2000;100:655–69.
9. Afkarian M, Sedy JR, Yang J, Jacobson NG, Cereb N, Yang SY, et al. T-bet is a STAT1-induced regulator of IL-12R expression in naive CD4+ T cells. Nat Immunol 2002;57:549–57.
10. Ivanov II, McKenzie BS, Zhou L, Tadokoro CE, Lepelley A, Lafaille JJ, et al. The orphan nuclear receptor RORγt directs the differentiation program of proinflammatory IL-17+ T helper cells. Cell 2006;126:1121–33.
11. Hawng ES, Szabo SJ, Schwartzberg PL, Glimcher LH. T helper cell fate specified by kinase-mediated interaction of T-bet with GATA-3. Science 2005;307:430–3.
12. Zhou L, Lopes JE, Chong MM, Ivanov II, Min R, Victora GD, et al. TGF-β-induced Foxp3 inhibits T_H17 cell differentiation by antagonizing RORγt function. Nature 2008;453:236–41.
13. Buttgereit F, Zhou H, Kalak R, Gaber T, Spies CM, Huscher D, et al. Transgenic disruption of glucocorticoid signaling in mature osteoblasts and osteocytes attenuates K/BxN mouse serum–induced arthritis in vivo. Arthritis Rheum 2009;60:1998–2007.
14. Ishizaki K, Yamada A, Yoh K, Nakano T, Shimohata H, Maeda A, et al. Th1 and type 1 cytotoxic T cells dominate responses in T-bet overexpression transgenic mice that develop contact dermatitis. J Immunol 2007;178:605–12.
15. Cho YG, Cho ML, Min SY, Kim HY. Type II collagen autoimmunity in a model of human rheumatoid arthritis. Autoimmun Rev 2007;7:65–70.
16. Tanaka K, Ichiyama K, Hashimoto M, Yoshida H, Takimoto T, Takaesu G, et al. Loss of suppressor of cytokine signaling 1 in helper T cells leads to defective Th17 differentiation by enhancing antagonistic effects of IFN-γ on STAT3 and Smads. J Immunol 2008;180:3746–56.
17. Kiwamoto T, Ishii Y, Morishima Y, Yoh K, Maeda A, Ishizaki K, et al. Transcription factor T-bet and GATA-3 regulate development of airway remodeling. Am J Respir Crit Care Med 2006;174:142–51.
18. Shimohata H, Yamada A, Yoh K, Ishizaki K, Morito N, Yamagata K, et al. Overexpression of T-bet in T cells accelerates auto-

immune glomerulonephritis in mice with a dominant Th1 background. J Nephrol 2009;22:123–9.
19. Rangachari M, Mauermann N, Marty RR, Dirnhofer S, Kurrer MO, Komnenovic V, et al. T-bet negatively regulates autoimmune myocarditis by suppressing local production of interleukin 17. J Exp Med 2006;203:2009–19.
20. Nath N, Prasad R, Giri S, Singh AK, Singh I. T-bet is essential for the progression of experimental autoimmune encephalomyelitis. Immunology 2006;118:384–91.
21. Yang Y, Weiner J, Liu Y, Smith AJ, Huss DJ, Winger R, et al. T-bet is essential for encephalitogenicity of both Th1 and Th17 cells. J Exp Med 2009;206:1549–64.
22. Neurath MF, Weigmann B, Finotto S, Glickman J, Nieuwenhuis E, Iijima H, et al. The transcription factor T-bet regulates mucosal T cell activation in experimental colitis and Crohn's disease. J Exp Med 2002;195:1129–43.
23. Juedes AE, Rodrigo E, Togher L, Glimcher LH, von Herrath MG. T-bet controls autoaggressive CD8 lymphocyte responses in type 1 diabetes. J Exp Med 2004;199:1153–62.
24. Hosoya T, Kuroha T, Moriguchi T, Cummings D, Maillard I, Lim KC, et al. GATA-3 is required for early T lineage progenitor development. J Exp Med 2009;206:2987–3000.
25. Shi G, Wang Z, Jin H, Chen YW, Wang Q, Qian Y. Phenotype switching by inflammation-inducing polarized Th17 cells, but not by Th1 cells. J Immunol 2008;181:7205–13.
26. Zhang F, Meng G, Strober W. Interactions among the transcription factors Runx1, RORγt and Foxp3 regulate the differentiation of interleukin 17–producing T cells. Nat Immunol 2008;9:1297–306.
27. Brustle A, Heink S, Huber M, Rosenplanter C, Stadelmann C, Yu P, et al. The development of inflammatory T_H17 cells requires interferon-regulatory factor 4. Nat Immunol 2007;8:958–66.
28. Durant L, Watford WT, Ramos HL, Laurence A, Vahedi G, Wei L, et al. Diverse targets of the transcription factor STAT3 contribute to T cell pathogenicity and homeostasis. Immunity 2010;32:605–15.
29. Lazarevic V, Chen X, Shim JH, Hwang ES, Jang E, Bolm AN, et al. T-bet represses T_H17 differentiation by preventing Runx1-mediated activation of the gene encoding RORγt. Nat Immunol 2011;12:96–104.

p16^{INK4a} Exerts an Anti-Inflammatory Effect through Accelerated IRAK1 Degradation in Macrophages

Yousuke Murakami,*[,1] Fumitaka Mizoguchi,* Tetsuya Saito,* Nobuyuki Miyasaka,*[,†] and Hitoshi Kohsaka*[,†]

Induction of cyclin-dependent kinase (CDK) inhibitor gene p16^{INK4a} into the synovial tissues suppresses rheumatoid arthritis in animal models. In vitro studies have shown that the cell-cycle inhibitor p16^{INK4a} also exerts anti-inflammatory effects on rheumatoid synovial fibroblasts (RSF) in CDK activity-dependent and -independent manners. The present study was conducted to discern how p16^{INK4a} modulates macrophages, which are the major source of inflammatory cytokines in inflamed synovial tissues. We found that p16^{INK4a} suppresses LPS-induced production of IL-6 but not of TNF-α from macrophages. This inhibition did not depend on CDK4/6 activity and was not observed in RSF. p16^{INK4a} gene transfer accelerated LPS-triggered IL-1R–associated kinase 1 (IRAK1) degradation in macrophages but not in RSF. The degradation inhibited the AP-1 pathway without affecting the NF-κB pathway. Treatment with a proteosome inhibitor prevented the acceleration of IRAK1 degradation and downregulation of the AP-1 pathway. THP-1 macrophages with forced IRAK1 expression were resistant to the p16^{INK4a}-induced IL-6 suppression. Senescent macrophages with physiological expression of p16^{INK4a} upregulated IL-6 production when p16^{INK4a} was targeted by specific small interfering RNA. These findings indicate that p16^{INK4a} promotes ubiquitin-dependent IRAK1 degradation, impairs AP-1 activation, and suppresses IL-6 production. Thus, p16^{INK4a} senescence gene upregulation inhibits inflammatory cytokine production in macrophages in a different way than in RSF. *The Journal of Immunology*, 2012, 189: 5066–5072.

Rheumatoid arthritis (RA) is a chronic inflammatory disease characterized by synovial inflammation, hyperplasia, and destruction of the cartilage and bone. In rheumatoid synovial tissues, lymphocytes and macrophages are recruited and activated. These cells, especially activated macrophages, release a large amount of inflammatory cytokines. In response to these cytokines, synovial fibroblasts proliferate vigorously and form villous hyperplastic synovial tissues called pannus. These fibroblasts also secrete inflammatory mediators that further attract inflammatory cells and stimulate growth of the synovial fibroblasts as well as vascular endothelial cells (1). The pannus becomes the source of tissue-degrading proteinases and activators of osteoclasts, leading to destruction of the affected joints (2, 3).

The pannus formation results from proliferation of the synovial fibroblasts driven by the inflammatory processes in RA. This fact led us to explore a new therapeutic approach that directly controls the cell cycle of synovial fibroblasts. If the synovial fibroblasts become refractory to the proliferative stimuli, no pannus should develop (4). It has been known that the master molecules that control cell cycling are cyclin-dependent kinases (CDK) (5). Especially CDK4/6 phosphorylates retinoblastoma gene product (pRb), which liberates active E2F transcription factors for cell-cycle progression. CDK inhibitors (CDKI) are intracellular proteins that inhibit kinase activity of cyclin/CDK complexes. CDKI p16^{INK4a} inhibits CDK4/6 specifically, whereas CDK p21^{CIP1} inhibits a broad spectrum of CDK (5). The intra-articular gene transfer of p16^{INK4a} as well as p21^{CIP1} suppressed RA in animal models (4, 6). It inhibited histological findings characteristic to RA: synovial hyperplasia, mononuclear cell infiltration, and destruction of the bone and cartilage of the joints. Comparable therapeutic effects were observed when the small-molecule (sm)CDKI was administered orally or i.p. (7). A separate series of our experiments disclosed that cell-cycle progression is not the only function of CDK (8). CDK kinase activity also regulates production of inflammatory molecules in a pRb-independent manner. Also, it has been suggested that CDKI can affect expression of inflammatory molecules in a CDK kinase-independent manner.

The above studies were all carried out with synovial fibroblasts. In rheumatoid synovial tissues, macrophages are the major source of inflammatory cytokines that are critical for the resultant pathology (9–11). The present study was conducted to explore how p16^{INK4a} affects expression of inflammatory cytokines from activated macrophages. We found that p16^{INK4a} suppresses IL-6 production in macrophages. The effect was mediated by accelerated degradation of IL-1R–associated kinase 1 (IRAK1).

*Department of Medicine and Rheumatology, Graduate School of Medical and Dental Sciences, Tokyo Medical and Dental University, Tokyo 113-8519, Japan; and †Global Center of Excellence Program, International Research Center for Molecular Science in Tooth and Bone Disease, Graduate School of Medical and Dental Sciences, Tokyo Medical and Dental University, Tokyo 113-8519, Japan

[1]Current address: Receptor Cell Biology Section, Laboratory of Immunogenetics, National Institute of Allergy and Infectious Diseases, National Institutes of Health, Bethesda, MD.

Received for publication November 7, 2011. Accepted for publication September 12, 2012.

Address correspondence and reprint requests to Dr. Hitoshi Kohsaka, Department of Medicine and Rheumatology, Graduate School of Medical and Dental Sciences, Tokyo Medical and Dental University, 1-5-45 Yushima, Bunkyo-ku, Tokyo 113-8519, Japan. E-mail address: kohsaka.rheu@tmd.ac.jp

The online version of this article contains supplemental material.

Abbreviations used in this article: BMM, bone marrow-derived macrophage; CDK, cyclin-dependent kinase; CDKI, cyclin-dependent kinase inhibitor; IKK, IκB kinase; IRAK1, IL-1R–associated kinase 1; miR146a, micro-RNA 146a; MKK4, MAPK kinase 4; MMP, matrix metalloproteinase; pRb, retinoblastoma gene product; RA, rheumatoid arthritis; RSF, rheumatoid synovial fibroblast; shCDK4, murine cyclin-dependent kinase 4-specific short hairpin RNA; shIRAK1, murine IL-1R–associated kinase 1-specific short hairpin RNA; shNC, short hairpin RNA vector for negative control; siRNA, small interfering RNA; sm, small molecule.

Copyright © 2012 by The American Association of Immunologists, Inc. 0022-1767/12/$16.00

www.jimmunol.org/cgi/doi/10.4049/jimmunol.1103156

Downloaded from http://www.jimmunol.org/ at Sangyo Ika Daigaku on February 23, 2014

Materials and Methods

Reagents

Anti-p-p38 MAPK, anti-p-JNK, anti-p-IκB kinase (IKK)α/β, anti-p-MAPK kinase 4 (MKK4), and anti-IκBα Abs were purchased from Cell Signaling Technology (Danvers, MA). Biotin-labeled anti-TLR4 Ab and PE-labeled streptavidin were purchased from eBioscience (San Diego CA). Biotin-labeled IgG1 was purchased from Beckman Coulter (Tokyo, Japan). Anti-actin Ab and MG132 were purchased from Sigma-Aldrich (St. Louis, MO). Anti-p16^{INK4a} Ab was purchased from Millipore (Billerica, MA). Anti-IRAK1 Ab was kindly provided by Dr. Shizuo Akira [Osaka University, Osaka, Japan (12)]. An smCDK4/6 selective inhibitor, PD0332991, was provided by Pfizer (Boston, MA) (13). IRAK1 wild-type and knockout bone marrow-derived macrophage (BMM) lysates were kindly provided by Dr. James A. Thomas (University of Texas Southwestern Medical Center, Dallas, TX).

Cells

BMM were isolated from 6–8-wk-old DBA1/J mice (Charles River Laboratories, Yokohama, Japan) and cultured as described previously (14). They were cultured in RPMI 1640 medium containing rM-CSF (50 ng/ml) or 10% CMG14-12–conditioned media as a source of M-CSF (15). Human synovial tissues were derived from RA patients undergoing total joint replacement surgery or synovectomy at Shimoshizu National Hospital. Consent forms were completed by the patients prior to the surgery. RA was diagnosed according to the 1988 criteria of the American College of Rheumatology (16). Human synovial cells were prepared as described previously (8). Human acute monocytic leukemia cell line THP-1 cells were cultured and differentiated to macrophages as described elsewhere (17). RAW264.7 cells were cultured as described elsewhere (18). For activation, cells were stimulated with the optimal doses of LPS, which were minimum dose to induce maximum IL-6 production in each cell type.

Western blot analyses and electrophoresis mobility shift assay

Total cell lysate of BMM and rheumatoid synovial fibroblasts (RSF) were subject to Western blot analyses with specific Abs. A primary Ab against mouse actin was used for loading control. Peroxidase-conjugated anti-mouse or rat IgG Abs were used as secondary Abs.

After preparation of nuclear lysates with the Nuclear Extraction kit (Active Motif, Carlsbad, CA), EMSA was performed with the second-generation gel shift assay kit (Roche, Tokyo, Japan). AP-1 and NF-κB consensus sequence was purchased from Promega (Madison, WI).

Proliferation assay

Measurement of [^{3}H]thymidine uptake by RSF and BMM was performed as described elsewhere (8, 14).

Flow cytometry analysis

BMM were stained with biotin-labeled anti-TLR4 mAb or biotin-labeled isotype-matched IgG1 followed by PE-labeled streptavidin. Data were acquired with the FACSCalibur system (BD Biosciences, San Jose, CA) and analyzed by CellQuest (BD Biosciences) and FlowJo software (Tree Star, Ashland, OR).

Preparation of retroviral and adenoviral vectors

The human p16^{INK4a} and IRAK1 genes were cloned into the retroviral expression vectors, pMX-IP and pMX-IN, respectively (pMX-p16^{INK4a} and pMX-IRAK1). They had an internal ribosomal entry site and a resistance gene for pharmacological selection (19). Using pSilencer5.1 (Applied Biosystems, Tokyo, Japan), recombinant retroviral vectors containing murine CDK4- and IRAK1-specific short hairpin (sh)RNA sequences (IRAK1 sense, 5′-GATCCAGAGCCCATCCCTCCCCGTTTCAAGAGAACGGGGAGGGATGGGCTCTTTTTTTGGAAA-3′, and IRAK1 antisense, 5′-AGCTTTTCCAAAAAAAGAGCCCATCCCTCCCCGTTCTCTTGAAACGGGGAGGGATGGGCTCTG-3′; CDK4 sense, 5′-GATCCGGTTGAGGTCATTGAGGATCTTCCTGTCAATCCTTAATGGTCTCAACCGGTTTTTTGGAAA-3′, and CDK4 antisense 5′-AGCTTTTCCAAAAAACCGGTTGAGACCATTAAGGATTGACAGGAAGATCCTCAATGACCTCAACCG-3′) were constructed (murine CDK4 short hairpin [shCDK4] and murine IRAK1 short hairpin [shIRAK1]). Short hairpin RNA vector for negative control (shNC) was purchased from Applied Biosystems. Recombinant retroviruses were prepared as described previously (20). Cells were infected with the retroviruses in the presence of 6 μg/ml polybrene. One day after the infection, they were exposed to puromycine (6 μg/ml) or neomycine (500 μg/ml).

Replication-defective adenoviruses containing a human p16 gene (AxCA-p16) and LacZ gene (AxCA-LacZ) were prepared as described previously (8).

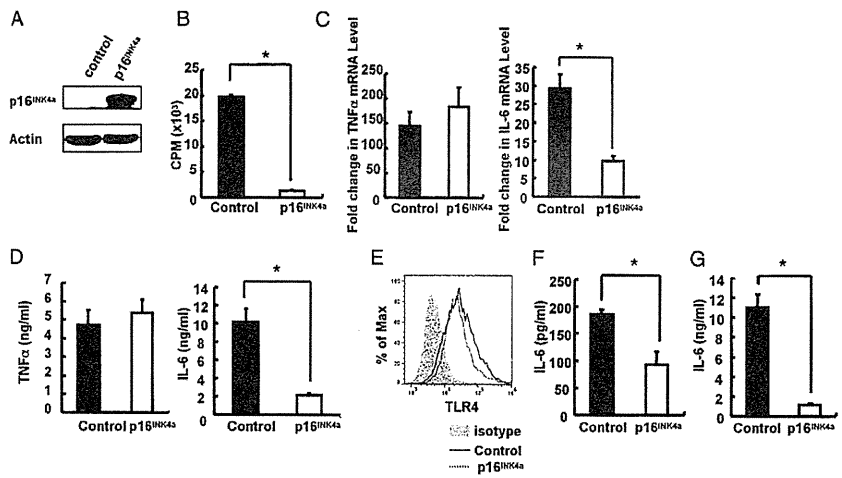

FIGURE 1. Effect of p16^{INK4a} expression on IL-6 production in LPS-stimulated macrophages. BMM, THP-1, and RAW264.7 cells were infected with pMX-IP (control) and pMX-p16^{INK4a} (p16^{INK4a}) retroviruses. **(A)** Cellular proteins were harvested. p16^{INK4a} and actin expression were detected with Western blot analyses. **(B)** [^{3}H]thymidine was added to culture media of the BMM transductants. Incorporation of [^{3}H]thymidine was assessed after 8 h. **(C)** The BMM transductants were stimulated with LPS (10 ng/ml). Total RNA were harvested for TNF-α and IL-6, and mRNA was quantified with real-time PCR. The amounts of the cytokine mRNA were normalized to that of GAPDH mRNA and presented as fold change relative to nontreated control cells. The TNF-α levels at 3 h and IL-6 levels at 6 h after stimulation were depicted because they were highest during the observation. **(D)** The BMM transductants were stimulated with LPS (10 ng/ml) for 24 h. Culture supernatants were collected, and IL-6 and TNF-α levels quantified with ELISA. **(E)** TLR4 surface expression on BMM transductants was detected by flow cytometry analyses. **(F)** Differentiated THP-1 macrophages were stimulated with LPS (1 μg/ml) for 24 h for quantification of IL-6 in the culture supernatants. **(G)** RAW264.7 cells were treated in the same way with LPS (100 ng/ml). Data are representative of three independent experiments and expressed as the mean ± SD of triplicate wells. *$p < 0.01$.

Downloaded from http://www.jimmunol.org/ at Sangyo Ika Daigaku on February 23, 2014

Quantification of cytokine and IRAK1 expression

Specific ELISA kits to quantify human and murine IL-6 and TNF-α in the culture supernatants were purchased from R&D Systems (Minneapolis, MN). Quantitative real-time PCRs for IL-6, TNF-α, IRAK1, and GAPDH were carried out as previously described (21, 22). A p16^{INK4a} gene-specific primer set was purchased from Qiagen (Tokyo, Japan).

Small interfering RNA transfection

To introduce small interfering RNA (siRNA) into BMM, 2×10^5 BMM was incubated with 200 μl 1.2 μM siRNA containing 24 μl FuGENE-HD transfection reagent (Roche) in Opti-MEM for 16 h. p16^{INK4a}-specific siRNA (si-p16A and B) and control siRNA were purchased from Qiagen.

Statistic analyses

[^{3}H]Thymidine uptake, IRAK1 and cytokine mRNA measurements, and IL-6 concentrations in the supernatants were compared with the Mann–Whitney *U* test.

Results

p16^{INK4a} suppressed IL-6 expression in LPS-stimulated macrophages

To study the effect of p16^{INK4a} on macrophages, BMM were infected with pMX-p16 or control pMX-IP retroviruses. Ectopic p16^{INK4a} protein expression in the pMX-p16^{INK4a}-infected cells had been confirmed with Western blot analyses (Fig. 1A). [^{3}H]Thymidine uptake by the p16^{INK4a}-expressing BMM was almost completely suppressed compared with control virus-treated BMM (Fig. 1B). Quantitative PCR showed that p16^{INK4a} gene transfer significantly suppressed IL-6 mRNA expression by BMM stimulated with LPS, whereas TNF-α mRNA expression was not affected (Fig. 1C). IL-6, but not TNF-α, production at the protein level was also suppressed significantly in BMM expressing p16^{INK4a} (Fig. 1D). LPS recognition receptor TLR4 expression was not modified by p16^{INK4a} overexpression, showing that IL-6 reduction was not due to the TLR4 downmodulation (Fig. 1E). The murine macrophage cell line RAW264.7 cells as well as human THP-1 cells that had been induced to differentiate to macrophages produce IL-6 in response to LPS. This response was also reduced by the p16^{INK4a} gene transfer (Fig. 1F, 1G). Thus, p16^{INK4a} gene transfer suppressed IL-6 expression in murine and human macrophages.

CDK4/6 inhibition did not affect IL-6 expression in LPS-stimulated macrophages

Our previous study demonstrated that p16^{INK4a} inhibited matrix metalloproteinase (MMP)-3 expression in RSF by suppressing CDK4/6 kinase activity (8). To determine if the inhibitory effect of p16^{INK4a} on LPS-induced IL-6 production in BMM depends on CDK4/6 kinase activity, CDK4/6 selective inhibitor (PD0332991) was added to the BMM culture. The CDK4/6 inhibitor suppressed [^{3}H]thymidine uptake of BMM in a dose-dependent manner. Maximal inhibition was observed at 2 μM PD0332991 (Fig. 2A), which did not affect viability of BMM (data not shown). The CDK4/6 inhibitor did not modulate LPS-induced IL-6 expression and production by BMM, but it completely suppressed BMM proliferation

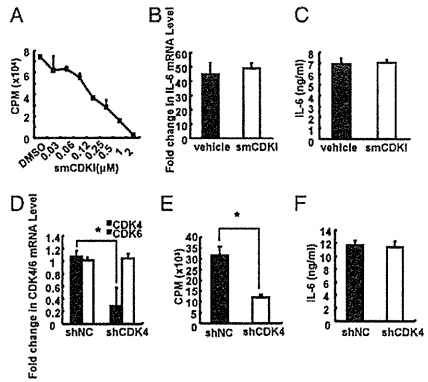

FIGURE 2. Effects of direct CDK4/6 inhibition on IL-6 production in LPS-stimulated BMM. **(A)** BMM were treated with or without indicated concentrations of smCDK4/6-selective inhibitor PD0332991 (smCDKI) for 24 h, and [^{3}H]thymidine uptake was assessed for the last 8 h. **(B)** BMM were treated with or without 2 mM smCDKI for 1 h prior to LPS stimulation (10 ng/ml) for 6 h. IL-6 mRNA in the treated BMM were quantified with real-time PCR. The amounts of the mRNA were normalized to that of GAPDH mRNA and presented as fold change relative to nontreated cells. **(C)** BMM were pretreated in the same manner and then stimulated with LPS (10 ng/ml) for 24 h. IL-6 in the culture supernatants was measured with ELISA. **(D)** BMM were transduced with shCDK4 or shNC. CDK4 and CDK6 mRNA in the BMM were quantified with real-time PCR. **(E)** BMM infected with shCDK4 and shNC were examined for [^{3}H]thymidine uptake during 8 h incubation. **(F)** BMM infected with shCDK4 and shNC were stimulated with LPS (10 ng/ml) for 24 h. IL-6 in the culture supernatants was measured with ELISA. Data are representative of three independent experiments and expressed as the mean ± SD of triplicate wells. *$p < 0.01$.

(Fig. 2B, 2C). To suppress CDK4 specifically, a retroviral vector containing shCDK4 was prepared. In contrast with shNC transfer, shCDK4 transfer suppressed CDK4 expression significantly, but not CDK6 expression, by BMM (Fig. 2D). As the [^{3}H]thymidine incorporation by BMM was inhibited by shCDK4, BMM depended primarily on CDK4 for phosphorylation of pRb (Fig. 2E). Consistent with the effect of PD0332991, CDK4 knockdown by shCDK4 did not affect LPS-induced IL-6 production (Fig. 2F). Thus, inhibition of LPS-induced IL-6 production by p16^{INK4a} did not depend on the CDK kinase activity.

p16^{INK4a} expression in BMM promoted IRAK1 degradation

TLR4 signaling is mediated by quite a few signaling molecules. To explore how p16^{INK4a} inhibits IL-6 production in LPS-stimulated BMM, we studied the expression of signaling molecules with Western blot analyses and found that p16^{INK4a} gene transfer affected IRAK1 protein expression (Fig. 3A). Upon ligand binding to TLR, MyD88 is recruited to the receptor and brings IRAK1 and IRAK4 to the receptor. This leads to phosphorylation of IRAK1, which activates kinase activity of IRAK1 and then triggers degradation of IRAK1 itself (23). The IRAK1 protein level in p16^{INK4a}-expressing BMM was comparable to that in control cells at the unstimulated status. Upon LPS stimulation, the IRAK1 expression was significantly downmodulated in p16^{INK4a}-expressing cells as compared with control cells (Fig. 3A). The specific band was observed in wild-type BMM but not in IRAK1 knockout cells, dem-

Downloaded from http://www.jimmunol.org/ at Sangyo Ika Daigaku on February 23, 2014

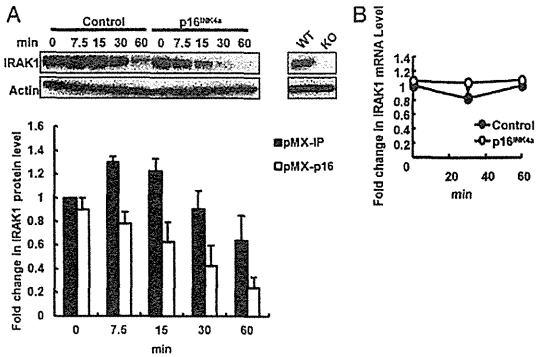

FIGURE 3. Promotion of IRAK1 degradation by exogenous $p16^{INK4a}$. BMM transduced with pMX-IP (control) and pMX-$p16^{INK4a}$ ($p16^{INK4a}$) were stimulated with LPS (10 ng/ml). **(A)** Cellular proteins were harvested at the indicated time points. IRAK1 and actin expression was detected with Western blot analyses (*top panel*). The density of the IRAK1 bands were normalized to that of actin and presented as fold change relative to nontreated control cells (*bottom panel*). Data are representative of three experiments and expressed as the mean ± SD of three independent experiments. **(B)** IRAK1 mRNA in the BMM was quantified with real-time PCR. The amount of the IRAK1 mRNA were normalized to that of GAPDH mRNA and presented as fold change relative to nontreated control cells. Data are representative of three experiments and expressed as the mean ± SD of triplicate wells.

onstrating that binding of anti-IRAK1 Abs was specific (Fig. 3A). $p16^{INK4a}$ expression did not affect IRAK1 mRNA levels, arguing that the decrease of the IRAK1 protein was not due to the decrease in gene transcription (Fig. 3B).

To discern if the same suppression is observed in RSF, $p16^{INK4a}$ or control LacZ were transduced using an adenoviral vector to RSF and IL-6 production was measured after LPS stimulation. Although [^{3}H]thymidine uptake was inhibited in the $p16^{INK4a}$-infected RSF, IL-6 production was not altered (Supplemental Fig. 1A, 1B). In accordance with this, IRAK1 expression in RSF in $p16^{INK4a}$-expressing and control RSF was comparable throughout the LPS stimulation (Supplemental Fig. 1C).

$p16^{INK4a}$ suppressed the AP-1 signaling pathway without suppressing the NF-κB signaling pathway

Upon LPS stimulation of macrophages, activated IRAK1 triggers phosphorylation of p38 MAPK/JNK and IKKα/β, which leads to activation of the AP-1 and NF-κB transcription factors (24). Western blot analyses illustrated that ectopic $p16^{INK4a}$ expression suppressed phosphorylation of p38 MAPK and JNK but not of IKKα/β in BMM stimulated with LPS (Fig. 4A). Phosphorylation of MKK4, which is upstream of JNK, was suppressed by $p16^{INK4a}$ (Fig. 4A). Downstream AP-1 binding activity was also reduced in $p16^{INK4a}$-expressing BMM (Fig. 4B). In contrast, IκB degradation, which is downstream of IKKα/β, as well as NF-κB–binding activity were not affected by $p16^{INK4a}$ overexpression (Fig. 4A, 4B).

We assumed that the impairment of the AP-1 pathway in $p16^{INK4a}$-expressing BMM should be directly due to reduced IRAK1 protein expression. To substantiate this, shIRAK1 was retrovirally transduced in BMM. IRAK1 protein was downregulated in the shIRAK1-transduced cells in comparison with control cells (Fig. 4C). When these cells were stimulated with LPS, AP-1 activation, but not IκB degradation, was significantly suppressed in the shIRAK1-

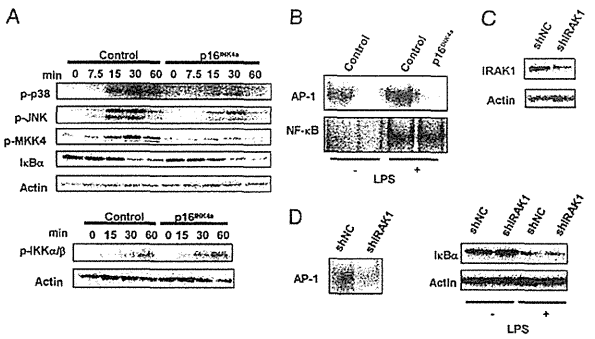

FIGURE 4. Suppression of phosphorylation of p38 MAPK and JNK without affecting the IKKα/β–IκB pathway by $p16^{INK4a}$. **(A)** Transduction of BMM with pMX-IP (control) and pMX-$p16^{INK4a}$ ($p16^{INK4a}$) retroviruses was followed by LPS (10 ng/ml) stimulation. Total cell lysates were collected at the indicated time points and examined for p-p38 MAPK, p-JNK, p-MKK4, p-IKKα/β, IκBα, and actin expression with Western blot analyses. **(B)** Nuclear extracts of the control and $p16^{INK4a}$-expressing BMM stimulated with LPS (10 ng/ml) for 1 h were examined for AP-1 and NF-κB binding activity with EMSA. **(C)** shIRAK1 or shNC were transduced retrovirally into BMM. Protein levels of IRAK1 and actin in total cell lysates were determined with Western blot analyses. **(D)** Cells were stimulated with LPS (10 ng/ml). After 1 h, the cells were lysed, and AP-1 binding activity in the nuclear extracts was examined with EMSA. After 30 min stimulation, the protein levels of IκBα in total cell lysates were determined with Western blot analyses. Data are representative of three independent experiments.

Downloaded from http://www.jimmunol.org/ at Sangyo Ika Daigaku on February 23, 2014

transduced cells (Fig. 4D). Thus, reduction of the IRAK1 protein in BMM resulted in inhibition of the AP-1 signaling pathway without affecting the NF-κB signaling pathway.

$p16^{INK4a}$-induced IRAK1 degradation was mediated by proteosome pathway

It was reported that IRAK1 degradation is modulated by the ubiquitin-dependent proteosome pathway in LPS-stimulated monocyte/macrophages (23). To inhibit this degradation pathway, a proteosome-specific inhibitor, MG132, was added to the $p16^{INK4a}$-expressing BMM culture. This treatment prevented acceleration of IRAK1 degradation in $p16^{INK4a}$-transduced cells (Fig. 5A). It also restored p38 MAPK and JNK phosphorylation in $p16^{INK4a}$-expressing BMM, indicating that $p16^{INK4a}$-induced IRAK1 degradation depends on the proteosome degradation pathway.

To determine if the observed IL-6 downregulation is a direct consequence of accelerated IRAK1 degradation, the $p16^{INK4a}$ gene was retrovirally transferred to THP-1 macrophages with or without the exogenous IRAK1 gene. THP-1 macrophages were used because primary BMM are too sensitive to neomycin and puromycin treatment to select the transduced cells. As in BMM, $p16^{INK4a}$ suppressed LPS-induced IL-6 production by THP-1 cells. This suppression was abrogated by cotransduction of the exogenous IRAK1 gene. Thus, IL-6 production was not downregulated without reduction of IRAK1 (Fig. 5B).

Inhibitory effect of endogenous $p16^{INK4a}$ on IL-6 production

To discern if expression of endogenous $p16^{INK4a}$ exerts the same inhibitory effects, BMM were cultured to senescence as was described previously (25). No endogenous $p16^{INK4a}$ protein was detectable in log-phase growing BMM, whereas the senescent BMM substantially upregulated the protein and mRNA of $p16^{INK4a}$ (Fig. 6A). These cells were then treated with two different siRNAs against $p16^{INK4a}$ to reduce $p16^{INK4a}$ expression levels (Fig. 6B). IL-6 production from BMM was upregulated by LPS stimulation and inversely proportional to $p16^{INK4a}$ mRNA expression levels (Fig. 6C). Thus, endogenous physiological $p16^{INK4a}$ expression can contribute to the suppression of the LPS-induced IL-6 production.

Discussion

$p16^{INK4a}$ expression in macrophages suppressed LPS-induced production of IL-6 but not of TNF-α in a CDK4/6-independent manner. This was not observed in synovial fibroblasts. Molecular analyses disclosed that it was due to the acceleration of proteosome-mediated IRAK1 degradation and following suppression of the AP-1 signaling pathway. Thus, $p16^{INK4a}$ gene transfer or its induction in synovial cells inhibits production of a part of macrophage-derived cytokines in addition to proliferation of synovial cells.

Recently, it was shown that TLR triggering is relevant in rheumatoid inflammation. Endogenous ligands for TLR-2 and TLR-4 are found in RA joints. These include gp96, fibrinogen, Hsp60, Hsp70, hyaluronic acid, mycloid-related protein 8/14, and high mobility group box chromosomal protein 1 (26). Indeed, TLR inhibition by a dominant-negative form of the Toll/IL-1R domain containing adaptor protein molecules suppressed the spontaneous production of proinflammatory cytokines and MMPs from RSF (27). LPS was used as a TLR stimulator in this study.

$p16^{INK4a}$ gene transfer suppressed IL-6 production via the promoted IRAK1 reduction, because IRAK1 coexpression prevented the IL-6 reduction. Indeed, the upstream molecule of IRAK1, IKKα/β, was phosphorylated equally in $p16^{INK4a}$-expressing cells and control cells. These findings also indicated that neither

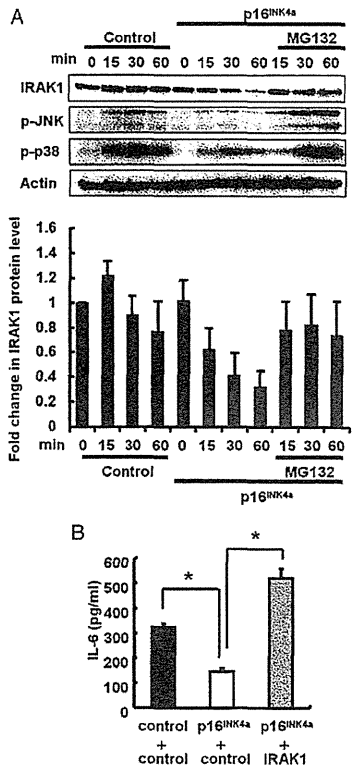

FIGURE 5. Proteome dependency of $p16^{INK4a}$-induced suppression of IL-6 production. **(A)** BMM transduced with pMX-IP (control) and pMX-$p16^{INK4a}$ ($p16^{INK4a}$) retroviruses were pretreated with the proteasome inhibitor MG132 (20 μM) for 1 h then stimulated with LPS (10 ng/ml) for the indicated times. p-p38 MAPK, p-JNK, IRAK1, and actin in the total cell lysates were detected with Western blot analyses (*top panel*). The density of the IRAK1 bands were normalized to that of actin and presented as fold change relative to nontreated control cells (*bottom panel*). Data are representative of three experiments and expressed as the mean ± SD of three independent experiments. **(B)** THP-1 cells were double-transduced with empty vectors (pMX-IP and pMX-IN controls; black bar), pMX-$p16^{INK4a}$ with pMX-IN empty vector control (white bar), or pMX-$p16^{INK4a}$ and pMX-IRAK1 (gray bar). THP-1 cells were treated with PMA for 2 d to induce macrophage differentiation and then stimulated with LPS (1 μg/ml) for 24 h. IL-6 in the culture supernatants was measured with ELISA. Data are representative of three experiments and expressed as the mean ± SD of triplicate wells. $*p < 0.01$.

downstream nor upstream molecule of IRAK1 was affected by $p16^{INK4a}$.

Studies of IRAK1-deficient cells showed that IRAK1 activation is an essential step in the TLR signaling pathways that leads to NF-κB and AP-1 activation and subsequent production of proinflammatory cytokines (23, 28, 29). IRAK1 activation causes degra-

Downloaded from http://www.jimmunol.org/ at Sangyo Ika Daigaku on February 23, 2014

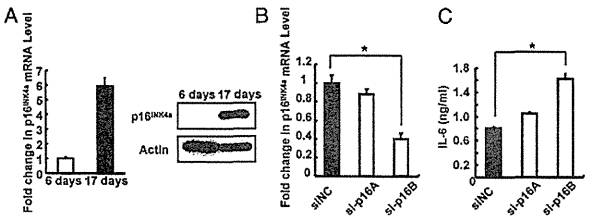

FIGURE 6. Inhibitory effect of endogenous $p16^{INK4a}$ on IL-6 production. (**A**) BMM cultured for 6 d were still in a logarithmic growth phase (6 d), whereas those cultured for 17 d reached replicative senescence (17 d). Endogenous $p16^{INK4a}$ and actin were detected with Western blotting analyses. $p16^{INK4a}$ mRNA expression in these cells was quantified with real-time PCR. The amounts of the $p16^{INK4a}$ mRNA were normalized to that of GAPDH mRNA and presented as fold change relative to BMM cultured for 6 d. (**B**) BMM were transfected with siRNA against $p16^{INK4a}$ (si-p16A and B) and siNC. $p16^{INK4a}$ mRNA expression in the treated BMM was measured with real-time PCR. The amounts of the $p16^{INK4a}$ mRNA were presented as fold change relative to siNC-treated cells. (**C**) These cells were stimulated with LPS (100 ng/ml) for 24 h. IL-6 in the culture supernatants was measured with ELISA. Data are representative of two independent experiments and expressed as the mean ± SD of triplicate wells. $^*p < 0.01$.

dation of IRAK1 itself, which induces tolerance against restimulation of TLR. Tolerant cells do not express IRAK1 and thus fail to activate both the NF-B and AP-1 signaling pathways in response to repeated TLR ligation (30, 31). In contrast with IRAK1-deficient cells and LPS-induced tolerant cells, $p16^{INK4a}$-expressing macrophages express a reduced but significant level of the IRAK1 protein. These cells as well as macrophages with partial IRAK1 knockdown by siRNA had selective impairment of AP-1 signaling pathway. These results are in concordance with previous observations that siRNA against IRAK1 downregulated IL-1β–induced production of inflammatory cytokines without interfering with IκB degradation and that IRAK1 knockdown impaired the AP-1 signaling pathway (32, 33). It was of interest that different transcription factors depend differentially on the IRAK1 level.

IL-6 expression in monocytes/macrophages depends on NF-κB and AP-1 pathways because loss of either pathway severely impaired IL-6 expression (34, 35). In contrast, TNF-α expression in monocytes/macrophages depends primarily on NF-κB because mutation of the AP-1 binding site in the TNF-α promoter sequence did not alter its expression (36). This difference in AP-1 dependency should account for the differential effect on IL-6 and TNF-α expression in $p16^{INK4a}$-expressing macrophages.

$p16^{INK4a}$ can make complexes not only with CDK4/6 but also with other signaling molecules. In mouse embryonic fibroblasts, $p16^{INK4a}$ bound to JNK prevents its interaction with c-Jun, which resulted in suppression of AP-1 activation induced by UV irradiation (37). In contrast to $p16^{INK4a}$ expression in macrophages, its expression in mouse embryonic fibroblasts did not disturb JNK phosphorylation. Another report demonstrated that $p16^{INK4a}$ in HeLa cells was associated with RelA, which is a component of NK-κB (38). This association inhibited NF-κB activation in HeLa cells, although we did not observe suppression of the NF-κB signaling pathway in macrophages. Thus, the inhibition of signal transduction by $p16^{INK4a}$ appeared to depend on the cell types.

The promoted IRAK1 degradation by $p16^{INK4a}$ could be accelerated by either IRAK1 ubiquitination or by recruitment to the proteasome. Polyubiquitination of signaling molecules triggers either proteosome-dependent protein degradation or activation of downstream signaling molecules (39). K48 ubiquitination causes the degradation of target molecules, whereas K63 ubiquitination activates downstream signaling molecules. K48 ubiquitination of IRAK1 appears to trigger degradation because treatment with a proteosome inhibitor, MG132, prevented the IRAK1 degradation in HEK293 cells stimulated with IL-1 (40). This agrees with the previous observation that MG132 treatment prevented LPS-induced IRAK1 degradation and enhanced activation of the AP-1 signaling pathway in THP-1 cells (17). These findings suggested that $p16^{INK4a}$ might enhance the K48 ubiquitination of IRAK1. Unlike the ubiquitination processes, processes of IRAK1 recruitment to the proteasome are unknown. Because some specific ubiquitin-receptor proteins may escort the ubiquitinated proteins to the proteasome, $p16^{INK4a}$ might enhance the function of the ubiquitin-receptor proteins. A recent report revealed that LPS-induced IRAK1 degradation was regulated partly by micro-RNA 146a (miR146a) (41). However, the miR146a level in $p16^{INK4a}$-expressing cells was close to that in control cells (data not shown), suggesting that miR146a was not a primary contributor to the downregulation of IRAK1 in the $p16^{INK4a}$-expressing cells.

Cellular senescence is a potent anticancer mechanism that arrests proliferation of cells at risk for neoplastic transformation. Fibroblasts in senescence develop a complex senescence-associated secretory phenotype in vitro and in vivo (42–45). An increase in IL-6 production is one of the principal indicators of senescence-associated secretory phenotype. However, $p16^{INK4a}$ senescence gene transfer did not affect IL-6 production from human fibroblasts (46). Another report demonstrated that IL-6 production was upregulated in oncogene-induced senescent fibroblasts even when $p16^{INK4a}$ induction was abolished with short hairpin RNA (47). These findings indicated that $p16^{INK4a}$ does not impact IL-6 production from senescent fibroblasts. In contrast, our present study has revealed that exogenous and endogenous $p16^{INK4a}$ expression suppresses IL-6 production in senescent macrophages, showing that $p16^{INK4a}$ has inhibitory effect in macrophages. Furthermore, induction of endogenous $p16^{INK4a}$ in RSF suppressed the arthritis model by systemic treatment of histone deacetylase inhibitor, suggesting that induction of endogenous $p16^{INK4a}$ in macrophages as well as RSF can be useful for therapy of RA (48).

Our previous studies demonstrated that $p16^{INK4a}$ could suppress proliferation and MCP-1 and MMP-3 production of RSF in a CDK4/6-dependent manner (8). Thus, $p16^{INK4a}$ should exert anti-arthritic effects in multiple ways. Retroviral and adenoviral $p16^{INK4a}$ gene transfer have advantages and disadvantages in clinical settings. Pharmacological means to induce endogenous $p16^{INK4a}$ in synovial cells of the arthritis joints should be investigated in future studies.

Downloaded from http://www.jimmunol.org/ at Sangyo Ika Daigaku on February 23, 2014

Acknowledgments

We thank John E. Coligan, Konrad Krzewski, and Jennifer Weck for providing language help.

Disclosures

The authors have no financial conflicts of interest.

References

1. Arend, W. P. 2001. Physiology of cytokine pathways in rheumatoid arthritis. *Arthritis Rheum.* 45: 101–106.
2. Müller-Ladner, U., T. Pap, R. E. Gay, M. Neidhart, and S. Gay. 2005. Mechanisms of disease: the molecular and cellular basis of joint destruction in rheumatoid arthritis. *Nat. Clin. Pract. Rheumatol.* 1: 102–110.
3. Feldmann, M., F. M. Brennan, and R. N. Maini. 1996. Rheumatoid arthritis. *Cell* 85: 307–310.
4. Taniguchi, K., H. Kohsaka, N. Inoue, Y. Terada, H. Ito, K. Hirokawa, and N. Miyasaka. 1999. Induction of the p16INK4a senescence gene as a new therapeutic strategy for the treatment of rheumatoid arthritis. *Nat. Med.* 5: 760–767.
5. Sherr, C. J., and J. M. Roberts. 1999. CDK inhibitors: positive and negative regulators of G1-phase progression. *Genes Dev.* 13: 1501–1512.
6. Nasu, K., H. Kohsaka, Y. Nonomura, Y. Terada, H. Ito, K. Hirokawa, and N. Miyasaka. 2000. Adenoviral transfer of cyclin-dependent kinase inhibitor genes suppresses collagen-induced arthritis in mice. *J. Immunol.* 165: 7246–7252.
7. Sekine, C., T. Sugihara, S. Miyake, H. Hirai, M. Yoshida, N. Miyasaka, and H. Kohsaka. 2008. Successful treatment of animal models of rheumatoid arthritis with small-molecule cyclin-dependent kinase inhibitors. *J. Immunol.* 180: 1954–1961.
8. Nonomura, Y., K. Nagasaka, H. Hagiyama, C. Sekine, T. Nanki, M. Tamamori-Adachi, N. Miyasaka, and H. Kohsaka. 2006. Direct modulation of rheumatoid inflammatory mediator expression in retinoblastoma protein-dependent and -independent pathways by cyclin-dependent kinase 4/6. *Arthritis Rheum.* 54: 2074–2083.
9. Szekanecz, Z., and A. E. Koch. 2007. Macrophages and their products in rheumatoid arthritis. *Curr. Opin. Rheumatol.* 19: 289–295.
10. McCoy, J. M., J. R. Wicks, and L. P. Audoly. 2002. The role of prostaglandin E2 receptors in the pathogenesis of rheumatoid arthritis. *J. Clin. Invest.* 110: 651–658.
11. McInnes, I. B., B. P. Leung, M. Field, X. Q. Wei, F. P. Huang, R. D. Sturrock, A. Kinninmonth, J. Weidner, R. Mumford, and F. Y. Liew. 1996. Production of nitric oxide in the synovial membrane of rheumatoid and osteoarthritis patients. *J. Exp. Med.* 184: 1519–1524.
12. Sato, S., O. Takeuchi, T. Fujita, H. Tomizawa, K. Takeda, and S. Akira. 2002. A variety of microbial components induce tolerance to lipopolysaccharide by differentially affecting MyD88-dependent and -independent pathways. *Int. Immunol.* 14: 783–791.
13. Fry, D. W., P. J. Harvey, P. R. Keller, W. L. Elliott, M. Meade, E. Trachet, M. Albassam, X. Zheng, W. R. Leopold, N. K. Pryer, and P. L. Toogood. 2004. Specific inhibition of cyclin-dependent kinase 4/6 by PD 0332991 and associated antitumor activity in human tumor xenografts. *Mol. Cancer Ther.* 3: 1427–1438.
14. Xaus, J., M. Comalada, M. Cardó, A. F. Valledor, and A. Celada. 2001. Decorin inhibits macrophage colony-stimulating factor proliferation of macrophages and enhances cell survival through induction of p27(Kip1) and p21(Waf1). *Blood* 98: 2124–2133.
15. Azuma, Y., K. Kaji, R. Katogi, S. Takeshita, and A. Kudo. 2000. Tumor necrosis factor-alpha induces differentiation of and bone resorption by osteoclasts. *J. Biol. Chem.* 275: 4858–4864.
16. Arnett, F. C., S. M. Edworthy, D. A. Bloch, D. J. McShane, J. F. Fries, N. S. Cooper, L. A. Healey, S. R. Kaplan, M. H. Liang, H. S. Luthra, et al. 1988. The American Rheumatism Association 1987 revised criteria for the classification of rheumatoid arthritis. *Arthritis Rheum.* 31: 315–324.
17. Cuschieri, J., D. Gourlay, I. Garcia, S. Jelacic, and R. V. Maier. 2004. Implications of proteasome inhibition: an enhanced macrophage phenotype. *Cell. Immunol.* 227: 140–147.
18. Oh, Y. J., J. H. Youn, Y. Ji, S. E. Lee, K. J. Lim, J. E. Choi, and J. S. Shin. 2009. HMGB1 is phosphorylated by classical protein kinase C and is secreted by a calcium-dependent mechanism. *J. Immunol.* 182: 5800–5809.
19. Kitamura, T., Y. Koshino, F. Shibata, T. Oki, H. Nakajima, T. Nosaka, and H. Kumagai. 2003. Retrovirus-mediated gene transfer and expression cloning: powerful tools in functional genomics. *Exp. Hematol.* 31: 1007–1014.
20. Ohata, J., T. Miura, T. A. Johnson, S. Hori, S. F. Ziegler, and H. Kohsaka. 2007. Enhanced efficacy of regulatory T cell transfer against increasing resistance, by elevated Foxp3 expression induced in arthritic murine hosts. *Arthritis Rheum.* 56: 2947–2956.
21. Urdinguio, R. G., L. Lopez-Serra, P. Lopez-Nieva, M. Alaminos, R. Diaz-Uriarte, A. F. Fernandez, and M. Esteller. 2008. Mecp2-null mice provide new neuronal targets for Rett syndrome. *PLoS ONE* 3: e3669.
22. Murakami, Y., T. Akahoshi, N. Aoki, M. Toyomoto, N. Miyasaka, and H. Kohsaka. 2009. Intervention of an inflammation amplifier, triggering receptor expressed on myeloid cells 1, for treatment of autoimmune arthritis. *Arthritis Rheum.* 60: 1615–1623.
23. Gottipati, S., N. L. Rao, and W. P. Fung-Leung. 2008. IRAK1: a critical signaling mediator of innate immunity. *Cell. Signal.* 20: 269–276.
24. Moynagh, P. N. 2009. The Pellino family: IRAK E3 ligases with emerging roles in innate immune signalling. *Trends Immunol.* 30: 33–42.
25. Randle, D. H., F. Zindy, C. J. Sherr, and M. F. Roussel. 2001. Differential effects of p19(Arf) and p16(Ink4a) loss on senescence of murine bone marrow-derived preB cells and macrophages. *Proc. Natl. Acad. Sci. USA* 98: 9654–9659.
26. Huang, Q. Q., and R. M. Pope. 2009. The role of toll-like receptors in rheumatoid arthritis. *Curr. Rheumatol. Rep.* 11: 357–364.
27. Sacre, S. M., E. Andreakos, S. Kiriakidis, P. Amjadi, A. Lundberg, G. Giddins, M. Feldmann, F. Brennan, and B. M. Foxwell. 2007. The Toll-like receptor adaptor proteins MyD88 and Mal/TIRAP contribute to the inflammatory and destructive processes in a human model of rheumatoid arthritis. *Am. J. Pathol.* 170: 518–525.
28. Kanakaraj, P., P. H. Schafer, D. E. Cavender, Y. Wu, K. Ngo, P. F. Grealish, S. A. Wadsworth, P. A. Peterson, J. J. Siekierka, C. A. Harris, and W. P. Fung-Leung. 1998. Interleukin (IL)-1 receptor-associated kinase (IRAK) requirement for optimal induction of multiple IL-1 signaling pathways and IL-6 production. *J. Exp. Med.* 187: 2073–2079.
29. Swantek, J. L., M. F. Tsen, M. H. Cobb, and J. A. Thomas. 2000. IL-1 receptor-associated kinase modulates host responsiveness to endotoxin. *J. Immunol.* 164: 4301–4306.
30. Li, L., S. Cousart, J. Hu, and C. E. McCall. 2000. Characterization of interleukin-1 receptor-associated kinase in normal and endotoxin-tolerant cells. *J. Biol. Chem.* 275: 23340–23345.
31. Jacinto, R., T. Hartung, C. McCall, and L. Li. 2002. Lipopolysaccharide- and lipoteichoic acid-induced tolerance and cross-tolerance: distinct alterations in IL-1 receptor-associated kinase. *J. Immunol.* 168: 6136–6141.
32. Liu, G., Y. J. Park, and E. Abraham. 2008. Interleukin-1 receptor-associated kinase (IRAK) -1-mediated NF-kappaB activation requires cytosolic and nuclear activity. *FASEB J.* 22: 2285–2296.
33. Ahmad, R., J. Sylvester, and M. Zafarullah. 2007. MyD88, IRAK1 and TRAF6 knockdown in human chondrocytes inhibits interleukin-1-induced matrix metalloproteinase-13 gene expression and promoter activity by impairing MAP kinase activation. *Cell. Signal.* 19: 2549–2557.
34. Dendorfer, U., P. Oettgen, and T. A. Libermann. 1994. Multiple regulatory elements in the interleukin-6 gene mediate induction by prostaglandins, cyclic AMP, and lipopolysaccharide. *Mol. Cell. Biol.* 14: 4443–4454.
35. Seshadri, S., Y. Kannan, S. Mitra, J. Parker-Barnes, and M. D. Wewers. 2009. MAIL regulates human monocyte IL-6 production. *J. Immunol.* 183: 5358–5368.
36. Yao, J., N. Mackman, T. S. Edgington, and S. T. Fan. 1997. Lipopolysaccharide induction of the tumor necrosis factor-alpha promoter in human monocytic cells. Regulation by Egr-1, c-Jun, and NF-kappaB transcription factors. *J. Biol. Chem.* 272: 17795–17801.
37. Choi, B. Y., H. S. Choi, K. Ko, Y. Y. Cho, F. Zhu, B. S. Kang, S. P. Ermakova, W. Y. Ma, A. M. Bode, and Z. Dong. 2005. The tumor suppressor p16(INK4a) prevents cell transformation through inhibition of c-Jun phosphorylation and AP-1 activity. *Nat. Struct. Mol. Biol.* 12: 699–707.
38. Wolff, B., and M. Naumann. 1999. INK4 cell cycle inhibitors direct transcriptional inactivation of NF-kappaB. *Oncogene* 18: 2663–2666.
39. Pickart, C. M., and D. Fushman. 2004. Polyubiquitin chains: polymeric protein signals. *Curr. Opin. Chem. Biol.* 8: 610–616.
40. Newton, K., M. L. Matsumoto, I. E. Wertz, D. S. Kirkpatrick, J. R. Lill, J. Tan, D. Dugger, N. Gordon, S. S. Sidhu, F. A. Fellouse, et al. 2008. Ubiquitin chain editing revealed by polyubiquitin linkage-specific antibodies. *Cell* 134: 668–678.
41. Taganov, K. D., M. P. Boldin, K. J. Chang, and D. Baltimore. 2006. NF-kappaB-dependent induction of microRNA miR-146, an inhibitor targeted to signaling proteins of innate immune responses. *Proc. Natl. Acad. Sci. USA* 103: 12481–12486.
42. Bavik, C., I. Coleman, J. P. Dean, B. Knudsen, S. Plymate, and P. S. Nelson. 2006. The gene expression program of prostate fibroblast senescence modulates neoplastic epithelial cell proliferation through paracrine mechanisms. *Cancer Res.* 66: 794–802.
43. Krtolica, A., S. Parrinello, S. Lockett, P. Y. Desprez, and J. Campisi. 2001. Senescent fibroblasts promote epithelial cell growth and tumorigenesis: a link between cancer and aging. *Proc. Natl. Acad. Sci. USA* 98: 12072–12077.
44. Liu, D., and P. J. Hornsby. 2007. Senescent human fibroblasts increase the early growth of xenograft tumors via matrix metalloproteinase secretion. *Cancer Res.* 67: 3117–3126.
45. Coppé, J. P., C. K. Patil, F. Rodier, Y. Sun, D. P. Muñoz, J. Goldstein, P. S. Nelson, P. Y. Desprez, and J. Campisi. 2008. Senescence-associated secretory phenotypes reveal cell-nonautonomous functions of oncogenic RAS and the p53 tumor suppressor. *PLoS Biol.* 6: 2853–2868.
46. Rodier, F., J. P. Coppé, C. K. Patil, W. A. Hoeijmakers, D. P. Muñoz, S. R. Raza, A. Freund, E. Campeau, A. R. Davalos, and J. Campisi. 2009. Persistent DNA damage signalling triggers senescence-associated inflammatory cytokine secretion. [Published erratum appears in 2009. *Nat. Cell Biol.* 11: 1272.] *Nat. Cell Biol.* 11: 973–979.
47. Kuilman, T., C. Michaloglou, L. C. Vredeveld, S. Douma, R. van Doorn, C. J. Desmet, L. A. Aarden, W. J. Mooi, and D. S. Peeper. 2008. Oncogene-induced senescence relayed by an interleukin-dependent inflammatory network. *Cell* 133: 1019–1031.
48. Nishida, K., T. Komiyama, S. Miyazawa, Z. N. Shen, T. Furumatsu, H. Doi, A. Yoshida, J. Yamana, M. Yamamura, Y. Ninomiya, et al. 2004. Histone deacetylase inhibitor suppression of autoantibody-mediated arthritis in mice via regulation of p16INK4a and p21(WAF1/Cip1) expression. *Arthritis Rheum.* 50: 3365–3376.

Downloaded from http://www.jimmunol.org/ at Sangyo Ika Daigaku on February 23, 2014

Rheumatology Advance Access published September 18, 2013
RHEUMATOLOGY 53, 270

Review

doi:10.1093/rheumatology/ket311

Sonographic synovial vascularity of synovitis in rheumatoid arthritis

Jun Fukae[1], Kazuhide Tanimura[1], Tatsuya Atsumi[2] and Takao Koike[2]

Abstract

RA is a condition of multiple synovitis. Abnormal synovial vascularity (SV) is evident with the onset of joint inflammation. The idea of estimating the level of joint inflammation by sonographic SV was conceived with the advancement of US. The ideal treatment strategy, called treat to target (T2T), requires early diagnosis and assessment of RA. Detection of positive SV can be useful for proving the presence of synovitis and finally diagnosing RA. In the assessment of RA, US-based global scores aimed at assessing overall disease activity have the potential to be useful for the achievement of T2T because US can directly detect changes in synovitis. Remaining SV in local joints increases the risk of structural deterioration. RA requires both improvement of overall disease activity and the disappearance of local SV for remission. The evaluation of SV provides various information and contributes to the clinical treatment of RA.

Key words: rheumatoid arthritis, ultrasound, power Doppler sonography, synovitis, synovial vascularity, treat to target.

Introduction

Today, why are rheumatologists enthusiastic to evaluate synovial vascularity (SV) in patients with RA in daily practice? RA is a condition of multiple cryptogenic synovitis characterized by expansion of soft tissue and destructive bone invasion at various joint sites that results in systemic musculoskeletal dysfunction. The pathogenesis of rheumatoid synovitis has been strongly associated with SV (Fig. 1).

Pathological explorations have tried to discover the characteristic pathogenesis of rheumatoid synovitis, and in recent years it has become apparent that with the onset of inflammation, abnormal vascularization is evident in the synovium due to vasodilation or angiogenesis [1–5]. A close relation between SV and synovitis has been confirmed. Presently SV is one of the hottest topics in rheumatology clinics.

Various factors such as the variety of afflicted joint sites or the diversity of disease progression may affect evaluation of the disease activity of RA. Composite scoring, which comprises clinical findings such as tender or swollen joint counts, has been established to evaluate the overall disease activity of RA. Clinical composite scores such as the 28-joint DAS (DAS28), the Simplified Disease Activity Index and the Clinical Disease Activity Index have been proven to be useful by various clinical trials [6, 7]. Although these clinical composite scores assess overall disease activity, they do not satisfactorily alert the clinician to changes in local joints due to their dichotomous judgment for each joint. To achieve deep remission of RA and to halt all abnormal joint destruction, the focus must be on detecting changes in local joint inflammation.

Progress in digital technology has resulted in US systems that produce high-quality images that enable observation of small joints. The novel idea of estimating the level of joint inflammation by sonographic SV was conceived with advancements in power Doppler US (PDS). Newman *et al.* [8, 9] first reported the use of PDS to detect abnormal SV, and Szkudlarek *et al.* [10] compared PDS with dynamic MRI to assess synovitis in finger joints and showed equivalency with both techniques.

With advancements in treatments for RA, early diagnosis and treatment have come to the forefront [11–14]. In response to this, new ACR/ European League Against Rheumatism (EULAR) classification criteria were introduced in 2010 [15, 16]. These criteria specify that patients with probable synovitis are first screened according to clinical findings. SV reflects the presence of synovitis in the early stage with high specificity.

Here we review the potential of SV detected by PDS for use in the diagnosis and assessment of RA.

[1]Hokkaido Medical Center for Rheumatic Diseases, Department of Rheumatology and [2]Department of Medicine II, Hokkaido University Graduate School of Medicine, Sapporo, Japan.

Submitted 30 April 2013; revised version accepted 1 August 2013.

Correspondence to: Jun Fukae, Hokkaido Medical Center for Rheumatic Diseases, 1-45, 3-Chome, 1-Jo, Kotoni, Nishi-ku, Sapporo 063-0811, Japan. E-mail: jun.fukae@ryumachi-jp.com

© The Author 2013. Published by Oxford University Press on behalf of the British Society for Rheumatology. All rights reserved. For Permissions, please email: journals.permissions@oup.com

FIG. 1 Longitudinal US image of a metacarpophalangeal joint in a patient with RA.

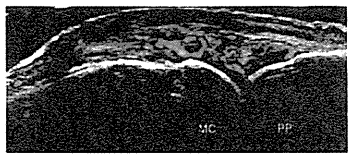

The multicolour fusion image of grey-scale and corresponding power Doppler images shows inflamed hypertrophic synovial tissue digitally stained in blue and abnormal SV stained in red. MC: metacarpal head; PP: proximal phalanx.

Assessment of SV

PDS is essentially a flexible and sonographer-dependent examination. Although PDS is useful for the assessment of SV, reproducibility is a major problem [17]. Settings of US machines and the scanning technique of the sonographer can greatly influence the visualization of SV, which affects reproducibility. Among the various US machine settings, US parameters such as pulse repetition frequency influence the quality of PDS imaging. Further, deterioration of the US transducer can adversely affect PDS imaging. Thus appropriate machine settings and maintenance are critical to ensure stable and reproducible PDS imaging. To minimize problems of the scanning technique, standardization of joint scanning has been studied by the EULAR [18, 19]. Education of the sonographer and proficiency in scanning are important for stable PDS imaging and improves reproducibility.

To measure SV by PDS, a semi-quantitative scoring system has been described [20] that comprises four scoring categories (0, none; 1, mild; 2, moderate; 3, severe) determined by the area of SV and grossly scored from the PDS images. This simple method has the advantage of no requirement for additional devices or special software, but reproducibility and reliability are problematic. Several clinical trials, most performed by members of the EULAR, have addressed these issues [21–24]. These studies found that appropriate training in scanning technique and reading of PDS images could improve and stabilize the reproducibility and reliability of scoring. However, this semi-quantitative scoring system might not be satisfactory to assess joint inflammation because it includes only four scoring categories. Therefore quantitative methods were established to measure SV in more detail [25–27]. Several groups reported a quantitative method to measure pixel counts of SV in the region of interest, which was located at in synovial tissue. Quantitative measurement could show the level or changes of SV numerically.

Because US is fundamentally a two-dimensional (2D) assessment, the images reflect a cross section of volumetric synovial tissue. Therefore the question of a discrepancy between sonographic assessment and the level of practical inflammation always exists. Recently three-dimensional (3D) PDS has been developed that enables assessment of SV at a volumetric level [28, 29]. This method may have several advantages, including image reproducibility and fewer training requirements for scanning joints or reading images. Naredo *et al.* [30] reported that 3D PDS showed repeatability such that it could be used in multicentre cohort studies of RA.

Abnormal SV in the early diagnosis of RA

Because abnormal SV is strongly associated with the pathology of synovitis, logically, detecting abnormal SV at symptomatic joints may be useful for proving the presence of synovitis and in finally diagnosing RA. We previously reported that when the sum of the levels of SV at the finger joints in each undiagnosed patient exceeded a certain level, the patient was ultimately diagnosed as having RA [31]. This result indicated the potential for detection of SV to become a first-stage screening test for RA. Importantly, diagnosis of RA requires not only detection of synovitis, but also systemic evaluation including serological or clinical tests.

The new 2010 ACR/EULAR classification criteria for RA were introduced with the aim of diagnosing RA earlier than with conventional methods [15, 16]. Attempts to combine the 2010 ACR/EULAR classification criteria with detection of synovitis by US to improve diagnostic power were reported from several groups [32–34]. Kawashiri *et al.* [33] reported that positive signs of sonographically abnormal SV in patients with undefined arthritis were a stronger prognostic factor for developing RA than were MRI findings or the presence of sonographic synovial hypertrophy. Nakagomi *et al.* [34] reported that US findings, including positive SV, had the power to confirm the presence of synovitis and increased the accuracy of the classification criteria. Thus, in the early diagnosis of RA, detection of abnormal SV has the potential to be used as a screening test or to confirm clinical findings.

Change in SV for assessment of overall disease activity in RA

Estimation of SV can be useful for assessment of disease activity in RA [35]. Although the semi-quantitative scoring system comprises only four categories, and thus is inadequate to assess changes in local joints, it could be useful for assessment of overall disease activity in combination with US estimation at several joints. US-based global scores aimed at assessing overall disease activity consist of the synovial hypertrophy score and SV score. These

REVIEW
Downloaded from http://rheumatology.oxfordjournals.org/ by guest on January 23, 2014
Downloaded from http://rheumatology.oxfordjournals.org/ by guest on January 23, 2014

methods are expected to be more accurate and sensitive than the clinical composite score, with numerous basic studies in this area [36, 37]. However, this method may have the disadvantages of high cost or being time consuming in practical use. Several research groups have produced unique US-based global scores that targeted limited joint sites to prove these disadvantages [38–44]. At present, there is no consensus as to which score should be used for clinical trials or in daily practice [45]. Additional and confirmatory trials are required to establish a US-based global score. Of note, Backhaus *et al.* produced a unique US-based composite score called the US7, which targets seven joints to reflect disease activity. They reported results of several trials and have steadily progressed in their study of this score [43, 44].

Treat to target (T2T) is a concept of ideal treatment of RA that has become widespread internationally [46]. It emphasizes that RA must be treated in the early phase and tightly controlled by appropriate measurement of disease activity so that patients will receive maximum therapeutic impact and achieve the goal of remission. The US-based global scores have the potential to be useful for the achievement of T2T because US can directly detect changes in synovitis. The various US-based composite scores mentioned here are now in the evaluation process, and additional detailed analyses are anticipated.

Change in SV for assessment of local joints in RA

In our investigation focusing on local joints, we reported that remaining SV at local joints increases the risk of structural deterioration, despite the fact that anti-rheumatoid therapy achieved low disease activity (LDA) clinically at 8 weeks [25, 47]. Interestingly, these joints tended to show improvement in clinical signs such as joint pain or swelling and thus clinical composite scores also showed improvement. Similar findings were reported by another group [48]. Subclinical synovitis and sonography were first reviewed by Bresnihan *et al.* [49], and Brown *et al.* [50, 51] reported that detailed sonographic observation detected subclinical synovitis in patients with long-term clinical remission. These joints with a poor prognosis were asymptomatic or mildly symptomatic but showed positive SV at the local level. Joints with remaining SV might be related to subclinical synovitis. Further longitudinal observation may clarify this relation.

We also reported that joints with a disappearance of SV with simultaneous overall disease improvement showed an improvement in joint prognosis [52]. Dougados *et al.* [53] reported a similar conclusion in their multicentre prospective trial. These results indicate that RA requires both an improvement in overall disease activity and the disappearance of local SV for remission and achievement of T2T. Remaining SV at a local joint indicates ongoing structural alteration. Recently the EULAR published recommendations for the use of joint imaging in RA [54] in which monitoring of inflammatory activity and prediction of response to treatment by imaging were discussed. Although PDS was considered useful for these purposes, more detailed data are needed for PDS to became an established examination tool. We have focused on the response of SV to treatment that may predict structural deterioration in local joints. Multicentre studies are necessary to establish the mechanism of response of SV to treatment.

In RA, accumulation of inflammation leads to the progression of joint damage and, logically, time-integrated SV consequently relates to a change in structural alteration. Naredo *et al.* [55] showed that in the body overall, time-integrated joint counts with positive SV are related to the change in total Sharp score. We also reported that local joints showed poor prognosis when SV remained despite achievement of LDA clinically. However, changes in structural alteration of the joint are not related to time-integrated quantitative SV [52]. The reason for this unexpected result is unknown. We speculated that local synovitis might change to heterogeneous inflammation in a condition of LDA that is neither that of simple reduction of acute inflammation nor of prolonged recovery. Further studies are needed to confirm these results.

In daily clinical practice, joints with remaining SV are often detected by PDS, however, there are no definitive methods to treat them. Although these asymptomatic or mildly symptomatic joints with poor prognosis, namely those showing subclinical synovitis, need to be treated, it is unclear whether systemic intensive therapy or topical therapy are effective. Recently a research group called the Targeted Ultrasound Initiative started a multicentre international study called Targeted Ultrasound in RA to investigate the effect of corticosteroid injection in joints with remaining positive SV [56]. T2T emphasizes optimizing treatment by appropriate disease assessment, and clinical composite scores reflecting systemic disease activity are mostly used at present. The use of local assessment with US will help to achieve T2T.

Conclusion

Why should rheumatologists evaluate SV in RA? Early diagnosis and assessment of disease activity are at the heart of the T2T approach in RA. In the early diagnosis of RA, detection of SV to discover synovitis could be used as a screening test for entry into the ACR/EULAR classification algorithm. A US-based global score consisting of both the SV score and synovial hypertrophy score used to assess overall disease activity may be more sensitive and objective than the clinical composite score and thus may be useful as a guide for optimizing disease treatment. Also, changes in local SV have prognostic value for local joint destruction that may lead to meticulous control of inflammation. The evaluation of SV provides various important information and contributes to the clinical practice of RA (Fig. 2).

Downloaded from http://rheumatology.oxfordjournals.org/ by guest on January 23, 2014

FIG. 2 Usefulness of SV in the clinical practice of RA.

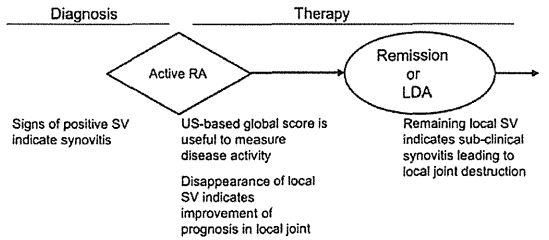

Information obtained from SV at each clinical point is shown.

Rheumatology key messages

- Abnormal SV is strongly associated with synovitis of RA.
- Detection of SV is useful for proving the presence of synovitis and diagnosing RA.
- RA remission requires an improvement of overall disease activity and disappearance of local SV.

Disclosure statement: The authors have declared no conflicts of interest.

References

1 Firestein GS. Starving the synovium: angiogenesis and inflammation in rheumatoid arthritis. J Clin Invest 1999; 103:3–4.

2 Hutton CW, Hinton C, Dieppe PA. Intra-articular variation of synovial changes in knee arthritis: biopsy study comparing changes in patellofemoral synovium and the medial tibiofemoral synovium. Br J Rheumatol 1987;26:5–8.

3 Knight AD, Levick JR. The density and distribution of capillaries around a synovial cavity. Q J Exp Physiol 1983; 68:629–44.

4 Koch AE. Review: angiogenesis: implications for rheumatoid arthritis. Arthritis Rheum 1998;41:951–62.

5 Walsh DA. Angiogenesis and arthritis. Rheumatology 1999;38:103–12.

6 Aletaha D, Smolen J. The Simplified Disease Activity Index (SDAI) and the Clinical Disease Activity Index (CDAI): a review of their usefulness and validity in rheumatoid arthritis. Clin Exp Rheumatol 2005;23(Suppl 39):S100–8.

7 Prevoo ML, van 't Hof MA, Kuper HH *et al.* Modified disease activity scores that include twenty-eight-joint counts. Development and validation in a prospective longitudinal study of patients with rheumatoid arthritis. Arthritis Rheum 1995;38:44–8.

8 Newman JS, Adler RS, Bude RO *et al.* Detection of soft-tissue hyperemia: value of power Doppler sonography. AJR Am J Roentgenol 1994;163:385–9.

9 Newman JS, Laing TJ, McCarthy CJ *et al.* Power Doppler sonography of synovitis: assessment of therapeutic response—preliminary observations. Radiology 1996;198: 582–4.

10 Szkudlarek M, Court-Payen M, Strandberg C *et al.* Power Doppler ultrasonography for assessment of synovitis in the metacarpophalangeal joints of patients with rheumatoid arthritis: a comparison with dynamic magnetic resonance imaging. Arthritis Rheum 2001;44: 2018–23.

11 Finckh A, Liang MH, van Herckenrode CM *et al.* Long-term impact of early treatment on radiographic progression in rheumatoid arthritis: a meta-analysis. Arthritis Rheum 2006;55:864–72.

12 Goekoop-Ruiterman YP, de Vries-Bouwstra JK, Allaart CF *et al.* Clinical and radiographic outcomes of four different treatment strategies in patients with early rheumatoid arthritis (the BeSt study): a randomized, controlled trial. Arthritis Rheum 2008;58(Suppl):S126–35.

13 Quinn MA, Conaghan PG, O'Connor PJ *et al.* Very early treatment with infliximab in addition to methotrexate in early, poor-prognosis rheumatoid arthritis reduces magnetic resonance imaging evidence of synovitis and damage, with sustained benefit after infliximab withdrawal: results from a twelve-month randomized, double-blind, placebo-controlled trial. Arthritis Rheum 2005;52: 27–35.

14 Vermeer M, Kuper HH, Hoekstra M *et al.* Implementation of a treat-to-target strategy in very early rheumatoid arthritis: results of the Dutch Rheumatoid Arthritis Monitoring remission induction cohort study. Arthritis Rheum 2011;63:2865–72.

15 Aletaha D, Neogi T, Silman AJ *et al.* 2010 Rheumatoid arthritis classification criteria: an American College of Rheumatology/European League Against Rheumatism collaborative initiative. Arthritis Rheum 2010;62:2569–81.

16 Aletaha D, Neogi T, Silman AJ *et al.* 2010 rheumatoid arthritis classification criteria: an American College of Rheumatology/European League Against Rheumatism collaborative initiative. Ann Rheum Dis 2010;69:1580–8.

17 Albrecht K, Muller-Ladner U, Strunk J. Quantification of the synovial perfusion in rheumatoid arthritis using

Downloaded from http://rheumatology.oxfordjournals.org/ by guest on January 23, 2014

Doppler ultrasonography. Clin Exp Rheumatol 2007;25: 630–8.

18 Wakefield RJ, D'Agostino MA. Essential applications of musculoskeletal ultrasound in rheumatology: expert consult premium edition. Philadelphia: Saunders, 2010.

19 Backhaus M, Burmester GR, Gerber T *et al.* Guidelines for musculoskeletal ultrasound in rheumatology. Ann Rheum Dis 2001;60:641–9.

20 Szkudlarek M, Court-Payen M, Jacobsen S *et al.* Interobserver agreement in ultrasonography of the finger and toe joints in rheumatoid arthritis. Arthritis Rheum 2003;48:955–62.

21 Koski JM, Saarakkala S, Helle M *et al.* Assessing the intra- and inter-reader reliability of dynamic ultrasound images in power Doppler ultrasonography. Ann Rheum Dis 2006;65: 1658–60.

22 Naredo E, Möller I, Moragues C *et al.* Interobserver reliability in musculoskeletal ultrasonography: results from a "Teach the Teachers" rheumatologist course. Ann Rheum Dis 2006;65:14–9.

23 Wakefield RJ, D'Agostino MA, Iagnocco A *et al.* The OMERACT Ultrasound Group: status of current activities and research directions. J Rheumatol 2007;34:848–51.

24 Scheel AK, Schmidt WA, Hermann KG *et al.* Interobserver reliability of rheumatologists performing musculoskeletal ultrasonography: results from a EULAR "Train the trainers" course. Ann Rheum Dis 2005;64:1043–9.

25 Fukae J, Kon Y, Henmi M *et al.* Change of synovial vascularity in a single finger joint assessed by power Doppler sonography correlated with radiographic change in rheumatoid arthritis: comparative study of a novel quantitative score with a semiquantitative score. Arthritis Care Res 2010;62:657–63.

26 Terslev L, Torp-Pedersen S, Savnik A *et al.* Doppler ultrasound and magnetic resonance imaging of synovial inflammation of the hand in rheumatoid arthritis: a comparative study. Arthritis Rheum 2003;48:2434–41.

27 Larche MJ, Seymour M, Lim A *et al.* Quantitative power Doppler ultrasonography is a sensitive measure of metacarpophalangeal joint synovial vascularity in rheumatoid arthritis and declines significantly following a 2-week course of oral low-dose corticosteroids. J Rheumatol 2010;37:2493–501.

28 Naredo E, Möller I, Acebes C *et al.* Three-dimensional volumetric ultrasonography. Does it improve reliability of musculoskeletal ultrasound?. Clin Exp Rheumatol 2010; 28:79–82.

29 Strunk J, Lange U. Three-dimensional power Doppler sonographic visualization of synovial angiogenesis in rheumatoid arthritis. J Rheumatol 2004;31:1004–6.

30 Naredo E, Acebes C, Brito E *et al.* Three-dimensional volumetric ultrasound: a valid method for blinded assessment of response to therapy in rheumatoid arthritis. J Rheumatol 2013;40:253–60.

31 Fukae J, Shimizu M, Kon Y *et al.* Screening for rheumatoid arthritis with finger joint power Doppler ultrasonography: quantification of conventional power Doppler ultrasonographic scoring. Mod Rheumatol 2009;19:502–6.

32 Freeston JE, Wakefield RJ, Conaghan PG *et al.* A diagnostic algorithm for persistence of very early inflammatory arthritis: the utility of power Doppler ultrasound when added to conventional assessment tools. Ann Rheum Dis 2010;69:417–9.

33 Kawashiri SY, Suzuki T, Okada A *et al.* Musculoskeletal ultrasonography assists the diagnostic performance of the 2010 classification criteria for rheumatoid arthritis. Mod Rheumatol 2013;23:36–43.

34 Nakagomi D, Ikeda K, Okubo A *et al.* Ultrasound can improve the accuracy of the 2010 American College of Rheumatology/European League Against Rheumatism classification criteria for rheumatoid arthritis to predict the requirement for methotrexate requirement. Arthritis Rheum 2013;65:890–8.

35 Taylor PC, Steuer A, Gruber J *et al.* Comparison of ultrasonographic assessment of synovitis and joint vascularity with radiographic evaluation in a randomized, placebo-controlled study of infliximab therapy in early rheumatoid arthritis. Arthritis Rheum 2004;50:1107–16.

36 Dougados M, Jousse-Joulin S, Mistretta F *et al.* Evaluation of several ultrasonography scoring systems for synovitis and comparison to clinical examination: results from a prospective multicentre study of rheumatoid arthritis. Ann Rheum Dis 2010;69:828–33.

37 Mandl P, Balint PV, Brault Y *et al.* Clinical and ultrasound-based composite disease activity indices in rheumatoid arthritis: results from a multicenter, randomized study. Arthritis Care Res 2013;65:879–87.

38 Hameed B, Pilcher J, Heron C *et al.* The relation between composite ultrasound measures and the DAS28 score, its components and acute phase markers in adult RA. Rheumatology 2008;47:476–80.

39 Hammer HB, Kvien TK. Comparisons of 7- to 78-joint ultrasonography scores: all different joint combinations show equal response to adalimumab treatment in patients with rheumatoid arthritis. Arthritis Res Ther 2011; 13:R78.

40 Perricone C, Ceccarelli F, Modesti M *et al.* The 6-joint ultrasonographic assessment: a valid, sensitive-to-change and feasible method for evaluating joint inflammation in RA. Rheumatology 2012;51:866–73.

41 Scheel AK, Hermann KG, Kahler E *et al.* A novel ultrasonographic synovitis scoring system suitable for analyzing finger joint inflammation in rheumatoid arthritis. Arthritis Rheum 2005;52:733–43.

42 Filer A, de Pablo P, Allen G *et al.* Utility of ultrasound joint counts in the prediction of rheumatoid arthritis in patients with very early synovitis. Ann Rheum Dis 2011;70: 500–7.

43 Backhaus M, Ohrndorf S, Kellner H *et al.* Evaluation of a novel 7-joint ultrasound score in daily rheumatologic practice: a pilot project. Arthritis Rheum 2009;61: 1194–201.

44 Ohrndorf S, Fischer IU, Kellner H *et al.* Reliability of the novel 7-joint ultrasound score: results from an inter- and intraobserver study performed by rheumatologists. Arthritis Care Res 2012;64:1238–43.

45 Mandl P, Naredo E, Wakefield RJ *et al.* OMERACT Ultrasound Task Force. A systematic literature review analysis of ultrasound joint count and scoring systems to assess synovitis in rheumatoid arthritis according to the OMERACT filter. J Rheumatol 2011;38:2055–62.

Downloaded from http://rheumatology.oxfordjournals.org/ by guest on January 23, 2014

46 Smolen JS, Aletaha D, Bijlsma JW *et al.* Treating rheumatoid arthritis to target: recommendations of an international task force. Ann Rheum Dis 2010;69:631–7.

47 Fukae J, Isobe M, Kitano A *et al.* Radiographic prognosis of finger joint damage predicted by early alteration in synovial vascularity in patients with rheumatoid arthritis: potential utility of power Doppler sonography in clinical practice. Arthritis Care Res 2011;63:1247–53.

48 Saleem B, Brown AK, Keen H *et al.* Should imaging be a component of rheumatoid arthritis remission criteria? A comparison between traditional and modified composite remission scores and imaging assessments. Ann Rheum Dis 2011;70:792–8.

49 Bresnihan B, Kane D. Sonography and subclinical synovitis. Ann Rheum Dis 2004;63:333–4.

50 Brown AK, Quinn MA, Karim Z *et al.* Presence of significant synovitis in rheumatoid arthritis patients with disease-modifying antirheumatic drug-induced clinical remission: evidence from an Imaging study may explain structural progression. Arthritis Rheum 2006;54:3761–73.

51 Brown AK, Conaghan PG, Karim Z *et al.* An explanation for the apparent dissociation between clinical remission and continued structural deterioration in rheumatoid arthritis. Arthritis Rheum 2008;58:2958–67.

52 Fukae J, Isobe M, Kitano A *et al.* Positive synovial vascularity in patients with low disease activity indicates smouldering inflammation leading to joint damage in rheumatoid arthritis: time-integrated joint inflammation estimated by synovial vascularity in each finger joint. Rheumatology 2013;52:523–8.

53 Dougados M, Devauchelle-Pensec V, Ferlet JF *et al.* The ability of synovitis to predict structural damage in rheumatoid arthritis: a comparative study between clinical examination and ultrasound. Ann Rheum Dis 2013;72: 665–71.

54 Colebatch AN, Edwards CJ, Østergaard M *et al.* EULAR recommendations for the use of imaging of the joints in the clinical management of rheumatoid arthritis. Ann Rheum Dis 2013;72:804–14.

55 Naredo E, Collado P, Cruz A *et al.* Longitudinal power Doppler ultrasonographic assessment of joint inflammatory activity in early rheumatoid arthritis: predictive value in disease activity and radiologic progression. Arthritis Rheum 2007;57:116–24.

56 Wakefield RJ, D'Agostino MA, Naredo E *et al.* After treat-to-target: can a targeted ultrasound initiative improve RA outcomes? Ann Rheum Dis 2012;71: 799–803.

Downloaded from http://rheumatology.oxfordjournals.org/ by guest on January 23, 2014

Arthritis Care & Research
Vol. 63, No. 9, September 2011, pp 1247–1253
DOI 10.1002/acr.20517
© 2011, American College of Rheumatology

ORIGINAL ARTICLE

Radiographic Prognosis of Finger Joint Damage Predicted by Early Alteration in Synovial Vascularity in Patients With Rheumatoid Arthritis: Potential Utility of Power Doppler Sonography in Clinical Practice

JUN FUKAE,[1] MASATO ISOBE,[1] AKEMI KITANO,[1] MIHOKO HENMI,[1] FUMIHIKO SAKAMOTO,[1] AKIHIRO NARITA,[1] TAKEYA ITO,[1] AKIO MITSUZAKI,[1] MASATO SHIMIZU,[1] KAZUHIDE TANIMURA,[1] MEGUMI MATSUHASHI,[1] TAMOTSU KAMISHIMA,[2] TATSUYA ATSUMI,[3] AND TAKAO KOIKE[3]

Objective. To investigate the relationship between synovial vascularity and progression of structural bone damage in each finger joint in patients with rheumatoid arthritis (RA) and to demonstrate synovial vascularity as a potential therapeutic marker.

Methods. We studied 250 metacarpophalangeal (MCP) and 250 proximal interphalangeal (PIP) joints of 25 patients with active RA who were administered adalimumab or tocilizumab. Patients were examined with clinical and laboratory assessments. Power Doppler sonography was performed at baseline and at the fourth and eighth weeks. Synovial vascularity was evaluated according to quantitative measurement. Hand and foot radiography was performed at baseline and the twentieth week.

Results. Clinical indices such as the 28-joint Disease Activity Score, the Clinical Disease Activity Index, and the Simplified Disease Activity Index were significantly decreased by biologic agents. The MCP and PIP joints with no response in synovial vascularity between baseline and the eighth week (vascularity improvement of ≤70% at the eighth week) showed a higher risk of radiographic progression compared with responsive joints (vascularity improvement of >70% at the eighth week: relative risk 2.33–9). Radiographic progression at the twentieth week was significantly lower in responsive joints than in nonresponsive joints.

Conclusion. The improvement of synovial vascularity following treatment with biologic agents led to suppression of radiographic progression of RA in each finger joint. The alteration in synovial vascularity numerically reflected therapeutic efficacy. Using vascularity as a marker to determine the most suitable therapeutic approach would be beneficial for patients with active RA.

INTRODUCTION

Several biologic agents against rheumatoid arthritis (RA) have been developed for clinical application in the last decade. For clinical trials and/or clinical practice, clinical indices such as the American College of Rheumatology (ACR) core data set or the European League Against Rheumatism (EULAR) 28-joint Disease Activity Score (DAS28) (1,2) have been utilized as markers of disease activity. Although those general comprehensive markers have been well established, neither the ACR core data set nor the DAS28 predict precisely the destruction of each individual joint. Brown et al reported that some joints with poor prognosis were detected in an individual patient, even if systemic improvement had been obtained (3). Considering that one of the current goals of treatment for RA is to prevent joint destruction (radiologic remission), establishing new markers to reflect local inflammation precisely and predict bone destruction in each joint have been the subjects of enthusiastic research.

Appearance and increase of synovial vascularity related to vasodilation and angiogenesis indicate active joint inflammation (4). Power Doppler sonography (PDS) enables the visualization of synovial vascularity and has the ability to represent local inflammation numerically (5). PDS has been reported as a useful tool to detect arthritis in the early stages and monitor disease activity (6,7). PDS has been studied as a clinical device having the potential to provide supplemented joint information in clinical practice (8,9). While 4-graded semiquantitative scoring has been widely used to evaluate synovial vascularity, we previously established quantitative measurement of joint PDS that enables the detection of detailed changes in local finger joints (10). In this study, we used quantitative PDS to investigate the relationship between synovial vascularity and bone destruction for patients treated with disease-modifying antirheumatic drug (DMARD) therapy. The results showed that improvement in synovial vascularity in response to DMARDs leads to suppression of radiographic progression in each local finger joint. To extend our previous findings, we focused on biologic agent therapies that were more drastic in their control of joint inflammation than DMARDs. In this study, we investigated a potential relationship between synovial vascularity and bone destruction during therapy with 2 different biologic agents, adalimumab (ADA) or tocilizumab (TCZ).

Significance & Innovations

- In clinical practice recommendations for treatment of rheumatoid arthritis, tight control of disease activity would lead to better joint prognosis.
- Accurate and direct markers of the joint inflammation are essential for tight control of disease activity in place of traditional composite clinical indices.
- Synovial vascularity reflects local joint inflammation. The early alteration in synovial vascularity by antirheumatic therapy has potential to be a therapeutic marker of joint destruction. Using synovial vascularity as a guide to make therapeutic decisions could be possible in the near future.

PATIENTS AND METHODS

Patients. Twenty-five patients with RA who had ADA or TCZ therapies were enrolled. All patients satisfied the ACR 1987 revised criteria for the classification of RA (11). The patients had been pretreated with DMARDs (ADA group: 6 patients with methotrexate [MTX], 1 patient with tacrolimus [TAC], 1 patient with bucillamine [BUC] + TAC, and 1 patient with MTX + TAC; TCZ group: 8 patients with MTX, 1 patient with BUC, and 1 patient with TAC) or pretreated with biologic agents (ADA group: 1 patient with MTX + infliximab [IFX]; TCZ group: 3 patients with MTX + IFX, 1 patient with MTX + etanercept, and 1 patient with MTX + ADA). Despite these pretreatments, all patients had at least 1 swollen joint of the metacarpophalangeal (MCP)/proximal interphalangeal (PIP) joints and showed a DAS28–erythrocyte sedimentation rate (ESR) of >2.7 mm/hour. Demographic, clinical, and laboratory characteristics of the patients are shown in Table 1. After baseline examinations, ADA was given to 10 patients and TCZ to 15 patients. The biologic agents were given according to the standard protocols (ADA 40 mg subcutaneous injection biweekly, TCZ 8 mg/kg intravenous infusion every 4 weeks). Biologic agent therapies were continued throughout the study. None of the patients received an additional or escalating dose of DMARDs or steroid after the eighth week in the study. We performed clinical and imaging examinations as described in each section.

The study was conducted in accordance with the Helsinki Declaration. Informed consent to the protocol ap-

Table 1. Clinical and laboratory characteristics of patients at baseline*

	Adalimumab	Tocilizumab	All
Age, mean (range) years	52 (30–69)	57 (34–75)	55 (30–75)
Sex, no. female/male	10/0	14/1	24/1
Duration of symptoms, months	78 (42–225)	96 (51–144)	78 (48–150)
ESR, mm/hour	39 (23–52)	55 (35–69)	48 (33–64)
CRP level, mg/dl	0.29 (0.08–0.69)	1.77 (0.53–2.9)	0.66 (0.22–2.48)
Swollen joint count	3 (2–5)	5 (3–6)	4 (2–6)
Tender joint count	4 (2–9)	7 (4–10)	6 (3–9)
Patient's global assessment by VAS	57 (41–76)	65 (40–74)	64 (40–75)
Examiner's global assessment by VAS	45 (40–75)	50 (33–70)	50 (35–70)
DAS28-ESR, mean ± SD	5.27 ± 1.21	5.34 ± 1.13	5.31 ± 1.14
CDAI, mean ± SD	22.6 ± 10.4	23 ± 11.8	22.8 ± 11.1
SDAI, mean ± SD	23.3 ± 10.7	24.9 ± 12.1	24.3 ± 11.4

* Values are the median (interquartile range) unless otherwise indicated. ESR = erythrocyte sedimentation rate; CRP = C-reactive protein; VAS = visual analog scale; DAS28 = 28-joint Disease Activity Score; CDAI = Clinical Disease Activity Index; SDAI = Simplified Disease Activity Index.

UMIN-CTR: UMIN000004476.
[1]Jun Fukae, MD, PhD, Masato Isobe, MD, PhD, Akemi Kitano, MT, Mihoko Henmi, MT, Fumihiko Sakamoto, MT, Akihiro Narita, MT, Takeya Ito, MD, Akio Mitsuzaki, MD, Masato Shimizu, MD, Kazuhide Tanimura, MD, Megumi Matsuhashi, MD: Hokkaido Medical Center for Rheumatic Diseases, Sapporo, Japan; [2]Tamotsu Kamishima, MD, PhD: Hokkaido University Hospital, Sapporo, Japan; [3]Tatsuya Atsumi, MD, PhD, Takao Koike, MD, PhD: Hokkaido University Graduate School of Medicine, Sapporo, Japan.
Address correspondence to Jun Fukae, MD, PhD, Hokkaido Medical Center for Rheumatic Diseases, 1-45, 3-Chome, 1-Jo, Kotoni, Nishi-ku, Sapporo 063-0811, Japan. E-mail: jun.fukae@ryumachi-jp.com.
Submitted for publication February 15, 2011; accepted in revised form May 26, 2011.

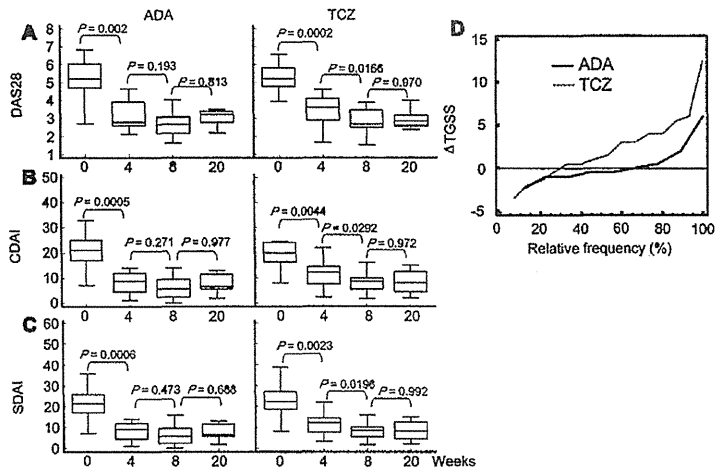

Figure 1. The change in clinical indices and radiographic progression for adalimumab (ADA) and tocilizumab (TCZ). The graphs of the 28-joint Disease Activity Score (DAS28) (A), Clinical Disease Activity Index (CDAI) (B), and Simplified Disease Activity Index (SDAI) (C) are shown. The left side of each graph is the course of ADA and right side of each graph is the course of TCZ. The cumulative probability plots for change in total Genant-modified Sharp score (ΔTGSS) for ADA and TCZ (D) are also shown.

proved by the local ethics committee was obtained from all patients.

Clinical examination. Swollen, tender joints and global assessment on a visual analog scale were assessed at baseline and at the fourth, eighth, and twentieth weeks by rheumatologists (JF, MS, MM, KT) who were blinded to ultrasonographic results. Blood tests for ESR and C-reactive protein were performed at each visit.

Ultrasonography and assessment. Ultrasonography was performed at baseline and at the fourth, eighth, and twentieth weeks by 1 of the 3 ultrasonographers (MH, FS, AN) specialized in musculoskeletal ultrasonography who were blinded to other clinical information. A 13 MHz linear array transducer was used (Hitachi EUP-L34P). Pulse Doppler settings were standardized for the detection of synovial blood flow by adjusting color gain, pulse repetition, and flow optimization parameters according to a previous study (12). Power Doppler settings (75 dB dynamic range, medium persistence, medium frame rate, low wall filter, 1,300 Hz pulse repetition frequency, flow optimization: medium vein, 1,300 Hz speed velocity) were identical throughout the examinations. Room temperature was kept at 25°C. The patients were positioned comfortably, and examinations were then started after 10 minutes of stabilization of pulse rate. The scanning technique on each finger joint was standardized and fixed as follows: first through fifth MCP and first through fifth PIP joint scanning was performed in the longitudinal plane over the dorsal surface of the joint with light skin pressure. The basic scanning technique followed the EULAR guidelines (13). The synovial vascular area with the most pronounced power Doppler activity was identified from the cine-loop and stored. The PDS images were recorded in the hard disk of the ultrasonographic machine. All examinations were completed within 15 minutes. The quantitative PDS method was established in a previous report (10). A synovial vascularity value was determined by counting the number of vascular flow pixels in the region of interest (ROI). The ROI was a standardized box type (5 mm × 10 mm) that was located to contain as many of the vascular flow pixels as possible. Vascular flow pixels in the ROI were measured automatically using the program's vascularity mode in the ultrasonographic machine (Hitachi EUB-7500).

Radiography and assessment. Plain radiographs of the hands, wrists, and feet were obtained at baseline and the twentieth week. Radiologic assessments were examined according to the Genant-modified Sharp score by a rheumatologist (MS) who was blinded to other clinical information (14).

Statistical analysis. Statistical analyses were calculated with the use of the Excel program (Microsoft) and MedCalc program 11.5.0.0. Differences between the 2 groups were examined using either the Student's *t*-test or a nonparametric test (Wilcoxon's signed rank test, Mann-Whitney U test), as applicable. Categorical data of clinical improvements were analyzed by the chi-square test or by Fisher's exact test. Intra- and interobserver reliability of quantitative PDS was estimated using calculations of intraclass correlation coefficients (ICCs). The smallest detectable change (SDC) for the radiographic score change was calculated according to a previous study (15).

RESULTS

Clinical disease activity. The disease activity of the patients at baseline is described in Table 1. In both the ADA and TCZ groups, the DAS28-ESR, Clinical Disease Activity Index (CDAI), and Simplified Disease Activity Index (SDAI) were significantly decreased from baseline (Figure 1). There were no significant differences in any disease activity markers between the ADA and TCZ groups for the change from baseline to the fourth week (DAS28: P = 0.879, CDAI: P = 0.319, SDAI: P = 0.580) and for the change from baseline to the eighth week (DAS28: P = 0.853, CDAI: P = 0.907, SDAI: P = 0.90).

Radiographic evaluation of joint damage. The radiographic images of the hands, wrists, and feet at baseline and the twentieth week in 25 patients were evaluated. The medians of the total Genant-modified Sharp score (TGSS) for the ADA and TCZ groups at baseline were 95.8 (interquartile range [IQR] 48.4—154.5) and 60 (IQR 47.8—128), respectively. In both the ADA and TCZ groups, the TGSS did not progress significantly from baseline to the twentieth week (P = 0.636 and P = 0.843, respectively). The cumulative probability plots of the change in TGSS (ΔTGSS) from baseline to the twentieth week are shown in Figure 1. At the twentieth week, 60% of patients treated with ADA and 27% of patients treated with TCZ had no radiographic progression (ΔTGSS ≤0). There was no significant difference in the rate of number of patients with no progression of TGSS (ΔTGSS ≤0) between the ADA and TCZ groups (P = 0.122).

We next focused on local finger joints. Two hundred fifty MCP joints and 250 PIP joints of 25 patients were evaluated for changes in synovial vascularity and the local Genant-modified Sharp score (LGSS). The medians of the LGSS in ADA therapy at baseline for the MCP and PIP joints were 2 (IQR 1–4.25) and 1.5 (IQR 0.5–4), respectively. The medians of LGSS in TCZ therapy at baseline for the MCP and PIP joints were 2 (IQR 1–4) and 1.5 (IQR 1–6), respectively. The SDC values were calculated for the LGSS for single MCP and PIP joints (0.35 and 0.28, respectively). None of the calculated SDCs exceeded the smallest unit of the scoring (0.5).

Relationship between change of synovial vascularity and radiographic progression in local finger joints. Finger joints with positive synovial vascularity at baseline were selected (ADA: MCP n = 28, PIP n = 22; TCZ: MCP n = 60, PIP n = 47). The medians of the MCP joint synovial vascularity were 355 (range 71–3,053) for the ADA group and 1,207 (range 80–4,686) for the TCZ group, showing no significant difference between the 2 groups (P = 0.0547).

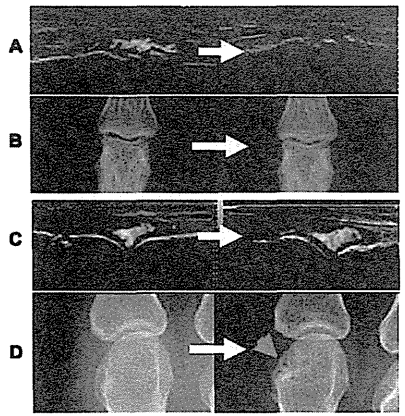

Figure 2. The change in synovial vascularity and bone destruction. In the left second proximal interphalangeal joint, images for synovial vascularity improvement (baseline to eighth week) (A) and halting radiographic progression (baseline to twentieth week) (B) are shown. In the right second metacarpophalangeal joint, images for synovial vascularity persistence (baseline to eighth week) (C) and radiographic progression (baseline to twentieth week) (D) are shown. **White arrows** show the time course. The **red arrow** indicates the occurrence of bone erosion.

The medians of PIP joint synovial vascularity were 497 (range 65–2,414) for the ADA group and 781 (range 74–4,260) for the TCZ group, showing no significant difference between the 2 groups (P = 0.994). At the eighth week, the medians of MCP joint synovial vascularity were 0 (range 0–1,917) for the ADA group and 142 (range 0–3,621) for the TCZ group, showing a significant decrease from baseline (P = 0.0001 and P < 0.0001, respectively). The medians of PIP joint synovial vascularity were 0 (range 0–213) for the ADA group and 0 (range 0–2,201) for the TCZ group, showing a significant decrease from baseline (P < 0.0001 in both cases).

We arbitrarily categorized these finger joints into 2 groups: the response group (R-group), with vascularity improvement of >70% at the eighth week (ADA: MCP n = 21, PIP n = 18; TCZ: MCP n = 36, PIP n = 36), and the no response group (NR-group), with vascularity improvement of ≤70% at the eighth week (ADA: MCP n = 7, PIP n = 4; TCZ: MCP n = 24, PIP n = 11). Representative pictures for change in Doppler sonographic images and corresponding radiographic images are shown in Figure 2. In the ADA group, 95% (20 of 21) of the MCP joints and 89% (16 of 18) of the PIP joints in the R-group had no significant radiographic progression (change in LGSS [ΔLGSS] ≤0) compared with 57% (4 of 7) and 25% (1 of 4), respectively, in the NR-group (P = 0.0376 and P = 0.0209, respectively). In the TCZ group, 75% (27 of 36) of the MCP joints and 83% (30 of 36) of the PIP joints in the R-group had no significant radiographic progression compared with 42% (10 of 24)

Table 2. Change in synovial vascularity and radiographic progression in local finger joints*

	Joints with progression (ΔLGSS >0)/total number			
	R-group	NR-group	RR (95% CI)	*P*
Adalimumab				
MCP joints	1/21	3/7	9 (1.11–73.2)	0.0398
PIP joints	2/18	3/4	6.75 (1.63–28.0)	0.0086
Tocilizumab				
MCP joints	9/36	14/24	2.33 (1.21–4.51)	0.0118
PIP joints	6/36	6/11	3.27 (1.32–8.11)	0.0105
All				
MCP joints	10/57	17/31	3.13 (1.64–5.97)	0.0006
PIP joints	8/54	9/15	4.05 (1.89–8.67)	0.0003

* ΔLGSS = change in local Genant-modified Sharp score; R-group = synovial vascularity response group; NR-group = synovial vascularity no response group; RR = relative risk; 95% CI = 95% confidence interval; MCP = metacarpophalangeal; PIP = proximal interphalangeal.

and 45% (5 of 11), respectively, of the NR-group (P = 0.0145 and P = 0.0198, respectively). Assuming no response in synovial vascularity (NR-group) as a risk factor for radiographic progression, the NR-group had a significantly higher risk compared with the R-group in both the ADA and TCZ groups (Table 2). In the period from baseline to the twentieth week, the ΔLGSS in the R-group was significantly lower compared with the NR-group for both the ADA and TCZ groups (Figure 3).

Intra- and interobserver reliability for power Doppler PDS. Representative PDS images for 20 MCP joints and 20 PIP joints were randomly chosen, and synovial vascularity was measured 3 times each by the 3 ultrasonographers (MH, FS, AN). The obtained intraobserver ICC values were 0.997–0.998 for MCP joints and 0.995–0.999 for PIP joints. The interobserver ICC values were 0.991–0.995 for MCP joints and 0.992–0.999 for PIP joints.

DISCUSSION

In this pilot study, we found that synovial vascularity was a direct marker of local joint inflammation and the early alteration in synovial vascularity by antirheumatic therapy was a potential therapeutic marker of joint destruction.

Recent biologic agents exert strong antiinflammatory effects in the short term; therefore, accurate and sensitive measurement of their therapeutic efficacy is essential for their appropriate usage (16,17). Although composite scores such as the DAS28, CDAI, SDAI, and ACR core data set had been widely used for RA assessment, such markers do not directly reflect local joint inflammation. To closely control disease activity, direct and sensitive evaluation for local joint abnormality would be useful as well as those general disease activity markers. For this purpose, we focused on synovial vascularity as an index of local joint inflammation.

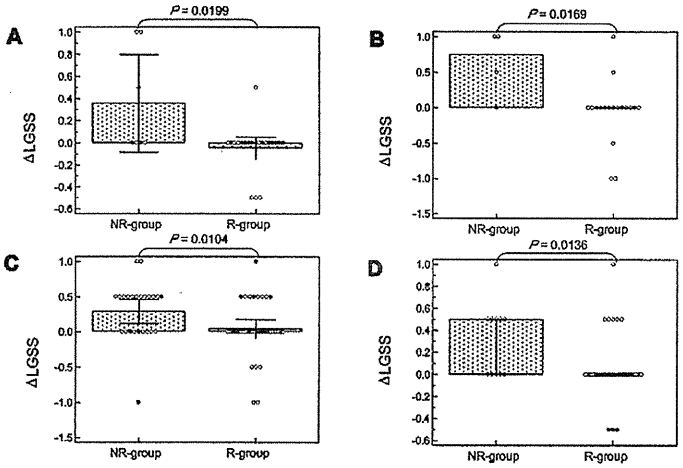

Figure 3. The change in the local Genant-modified Sharp score (ΔLGSS). Metacarpophalangeal (MCP) joints and proximal interphalangeal (PIP) joints that were positive for synovial vascularity at baseline were categorized into the synovial vascularity response group (R-group) and no response group (NR-group; see Results). For the adalimumab treatment, the ΔLGSS of MCP joints (A) and PIP joints (B) are shown. For the tocilizumab treatment, the ΔLGSS of MCP joints (C) and PIP joints (D) are shown.

In this study, we selected ADA and TCZ for the investigation so as not to limit the clinical significance of synovial vascularity to a single drug. While ADA is a representative biologic agent inhibiting tumor necrosis factor α, TCZ has a different mechanism and reduces inflammation by neutralizing the interleukin-6 receptor (18,19). There was no difference between ADA and TCZ therapies in clinical indices such as the DAS28, CDAI, and SDAI at baseline. These clinical indices were decreased significantly by treatment in both the ADA and TCZ groups and suppressed bone destruction, as reported previously (20–23). Comparing these 2 therapies, the cumulative probability plots of the ΔTGSS showed that there was a space between each of the curves (Figure 1). There was no significant difference in the rate of number of patients with no progression of TGSS (ΔTGSS ≤ 0) between the ADA and TCZ groups. We next explored a relationship between synovial vascularity and bone radiographic progression in local MCP and PIP joints. We observed synovial vascularity at baseline and the fourth and eighth weeks. Previously we had established a quantitative PDS method (10). All of the ICCs calculated for intra- and interobserver reliability during the PDS measurements were acceptable in the study.

Focusing on each finger joint with positive synovial vascularity at baseline, there was no significant difference between ADA and TCZ for synovial vascularity. We found that the synovial vascularity that did not respond to biologic agents in the local finger joints (NR-group) showed a higher risk for progression of joint destruction compared to the responsive joints (R-group) (Table 2). Additionally, the R-group showed suppression of joint destruction (Figure 3). The 2 biologic agents with different therapeutic mechanisms shared similar outcomes. The clinical implications of our results include an observed improvement of synovial vascularity, suggesting that this physiologic parameter is a potential therapeutic marker of bone destruction in each local finger joint.

In a previous study, we showed that improvement of vascularity by DMARDs was correlated with suppression of radiographic progression (10). In this study, we have shown a correlation between the change in synovial vascularity by biologic agents and radiographic progression. It is noteworthy that the synovial vascularity improvement by the therapies is a sign of therapeutic response. Brown et al (3,24) reported that joints with persistent vascularity positively showed being a risk factor of joint destruction. We further investigated the link between the change in synovial vascularity and that of bone destruction in each finger joint level, confirming a clear correlation between them.

In conclusion, change in synovial vascularity should be a direct marker of therapeutic efficacy. According to the EULAR recommendations for the treatment of RA, tight control of disease activity in the early stage would be necessary to obtain long-term improvement of the disease (25).

In RA, an improvement of synovitis in the short term is a first step toward the better outcome. It is interesting as well whether synovial vascularity is a predictive marker for bone destruction in the long term. We further pursue research on the relationship between synovial vascularity and bone destruction. Although our pilot study was limited to a small number of patients and short-term observation, using synovial vascularity as a guide to make therapeutic decisions could control disease activity and promise better prognosis.

AUTHOR CONTRIBUTIONS

All authors were involved in drafting the article or revising it critically for important intellectual content, and all authors approved the final version to be published. Dr. Fukae had full access to all of the data in the study and takes responsibility for the integrity of the data and the accuracy of the data analysis.

Study conception and design. Fukae, Isobe, Kitano, Ito, Shimizu, Tanimura, Matsuhashi, Kamishima, Atsumi, Koiko.

Acquisition of data. Fukae, Isobe, Kitano, Henmi, Sakamoto, Narita, Ito, Mitsuzaki, Shimizu, Tanimura, Matsuhashi, Kamishima, Atsumi, Koike.

Analysis and interpretation of data. Fukae, Kitano, Henmi, Sakamoto, Narita, Ito, Mitsuzaki, Shimizu, Tanimura, Matsuhashi, Kamishima, Atsumi, Koike.

REFERENCES

1. Felson DT, Anderson JJ, Boers M, Bombardier C, Furst D, Goldsmith C, et al. American College of Rheumatology preliminary definition of improvement in rheumatoid arthritis. Arthritis Rheum 1995;38:727–35.
2. Prevoo ML, van 't Hof MA, Kuper HH, van Leeuwen MA, van de Putte LB, van Riel PL. Modified disease activity scores that include twenty-eight–joint counts: development and validation in a prospective longitudinal study of patients with rheumatoid arthritis. Arthritis Rheum 1995;38:44–8.
3. Brown AK, Conaghan PG, Karim Z, Quinn MA, Ikeda K, Peterfy CG, et al. An explanation for the apparent dissociation between clinical remission and continued structural deterioration in rheumatoid arthritis. Arthritis Rheum 2008;58:2958–67.
4. Koch AE. Angiogenesis: implications for rheumatoid arthritis. Arthritis Rheum 1998;41:951–62.
5. Newman JS, Adler RS, Bude RO, Rubin JM. Detection of soft-tissue hyperemia: value of power Doppler sonography. AJR Am J Roentgenol 1994;163:385–9.
6. Naredo E, Moller I, Cruz A, Carmona L, Garrido J. Power Doppler ultrasonographic monitoring of response to anti–tumor necrosis factor therapy in patients with rheumatoid arthritis. Arthritis Rheum 2008;58:2248–56.
7. Naredo E, Collado P, Cruz A, Palop MJ, Cabero F, Richi P, et al. Longitudinal power Doppler ultrasonographic assessment of joint inflammatory activity in early rheumatoid arthritis: predictive value in disease activity and radiologic progression. Arthritis Rheum 2007;57:116–24.
8. Peluso G, Michelutti A, Bosello S, Gremese E, Tolusso B, Ferraccioli G. Clinical and ultrasonographic remission determines different chances of relapse in early and long standing rheumatoid arthritis. Ann Rheum Dis 2011;70:172–5.

9. Magni-Manzoni S, Epis O, Ravelli A, Klersy C, Visconti C, Lanni S, et al. Comparison of clinical versus ultrasound-determined synovitis in juvenile idiopathic arthritis. Arthritis Rheum 2009;61:1497–504.
10. Fukae J, Kon Y, Henmi M, Sakamoto F, Narita A, Shimizu M, et al. Change of synovial vascularity in a single finger joint assessed by power Doppler sonography correlated with radiographic change in rheumatoid arthritis: comparative study of a novel quantitative score with a semiquantitative score. Arthritis Care Res (Hoboken) 2010;62:657–63.
11. Arnett FC, Edworthy SM, Bloch DA, McShane DJ, Fries JF, Cooper NS, et al. The American Rheumatism Association 1987 revised criteria for the classification of rheumatoid arthritis. Arthritis Rheum 1988;31:315–24.
12. Kamishima T, Tanimura K, Henmi M, Narita A, Sakamoto F, Terae S, et al. Power Doppler ultrasound of rheumatoid synovitis: quantification of vascular signal and analysis of interobserver variability. Skeletal Radiol 2009;38:467–72.
13. Backhaus M, Burmester GR, Gerber T, Grassi W, Machold KP, Swen WA, et al. Guidelines for musculoskeletal ultrasound in rheumatology. Ann Rheum Dis 2001;60:641–9.
14. Genant HK, Jiang Y, Peterfy C, Lu Y, Redei J, Countryman PJ. Assessment of rheumatoid arthritis using a modified scoring method on digitized and original radiographs. Arthritis Rheum 1998;41:1583–90.
15. Bruynesteyn K, Boers M, Kostense P, van der Linden S, van der Heijde D. Deciding on progression of joint damage in paired films of individual patients: smallest detectable difference or change. Ann Rheum Dis 2005;64:179–82.
16. Karonitsch T, Aletaha D, Boers M, Bombardieri S, Combe B, Dougados M, et al. Methods of deriving EULAR/ACR recommendations on reporting disease activity in clinical trials of patients with rheumatoid arthritis. Ann Rheum Dis 2008;67:1365–73.
17. Sokka T, Pincus T. Rheumatoid arthritis: strategy more important than agent. Lancet 2009;374:430–2.
18. Hoff M, Kvien TK, Kalvesten J, Elden A, Haugeberg G. Adalimumab therapy reduces hand bone loss in early rheumatoid arthritis: explorative analyses from the PREMIER study. Ann Rheum Dis 2009;68:1171–6.
19. Nishimoto N, Yoshizaki K, Miyasaka N, Yamamoto K, Kawai S, Takeuchi T, et al. Treatment of rheumatoid arthritis with humanized anti-interleukin-6 receptor antibody: a multicenter, double-blind, placebo-controlled trial. Arthritis Rheum 2004;50:1761–9.
20. Nishimoto N, Hashimoto J, Miyasaka N, Yamamoto K, Kawai S, Takeuchi T, et al. Study of active controlled monotherapy used for rheumatoid arthritis, an IL-6 inhibitor (SAMURAI): evidence of clinical and radiographic benefit from an x ray reader-blinded randomised controlled trial of tocilizumab. Ann Rheum Dis 2007;66:1162–7.
21. Hashimoto J, Garnero P, van der Heijde D, Miyasaka N, Yamamoto K, Kawai S, et al. Humanized anti-interleukin-6-receptor antibody (tocilizumab) monotherapy is more effective in slowing radiographic progression in patients with rheumatoid arthritis at high baseline risk for structural damage evaluated with levels of biomarkers, radiography, and BMI: data from the SAMURAI study. Mod Rheumatol 2011;21:10–5.
22. Moller Dohn U, Boonen A, Hetland ML, Hansen MS, Knudsen LS, Hansen A, et al. Erosive progression is minimal, but erosion healing rare, in patients with rheumatoid arthritis treated with adalimumab: a 1 year investigator-initiated follow-up study using high-resolution computed tomography as the primary outcome measure. Ann Rheum Dis 2009;68:1585–90.
23. Dohn UM, Ejbjerg B, Boonen A, Hetland ML, Hansen MS, Knudsen LS, et al. No overall progression and occasional repair of erosions despite persistent inflammation in adalimumab-treated rheumatoid arthritis patients: results from a longitudinal comparative MRI, ultrasonography, CT and radiography study. Ann Rheum Dis 2011;70:252–8.
24. Brown AK, Quinn MA, Karim Z, Conaghan PG, Peterfy CG, Hensor E, et al. Presence of significant synovitis in rheumatoid arthritis patients with disease-modifying antirheumatic drug–induced clinical remission: evidence from an imaging study may explain structural progression. Arthritis Rheum 2006;54:3761–73.
25. Smolen JS, Boers M, Abadie EC, Breedveld FC, Emery P, Bardin T, et al. Recommendations for an update of 2003 European regulatory requirements for registration of drugs to be used in the treatment of RA. Curr Med Res Opin 2011;27:315–25.

Downloaded from ard.bmj.com on February 18, 2013 - Published by group.bmj.com

ARD Online First, published on January 11, 2013 as 10.1136/annrheumdis-2012-202433

OPEN ACCESS

EXTENDED REPORT

Adalimumab, a human anti-TNF monoclonal antibody, outcome study for the prevention of joint damage in Japanese patients with early rheumatoid arthritis: the HOPEFUL 1 study

Tsutomu Takeuchi,[1] Hisashi Yamanaka,[2] Naoki Ishiguro,[3] Nobuyuki Miyasaka,[4] Masaya Mukai,[5] Tsukasa Matsubara,[6] Shoji Uchida,[7] Hideto Akama,[8] Hartmut Kupper,[9] Vipin Arora,[10] Yoshiya Tanaka[11]

▸ Additional material is published online only. To view please visit the journal online (http://dx.doi.org/10.1136/annrheumdis-2012-202433).

For numbered affiliations see end of article

Correspondence to
Professor Tsutomu Takeuchi, Division of Rheumatology, Department of Internal Medicine, School of Medicine, Keio University, 35 Shinanomachi, Shinjuku-ku, Tokyo 160-8582, Japan; tsutake@z5.keio.jp

Received 2 August 2012
Revised 14 November 2012
Accepted 9 December 2012

To cite: Takeuchi T, Yamanaka H, Ishiguro N, *et al. Ann Rheum Dis* Published Online First: [*please include* Day Month Year] doi:10.1136/annrheumdis-2012-202433

ABSTRACT

Objectives To evaluate the efficacy and safety of adalimumab+methotrexate (MTX) in Japanese patients with early rheumatoid arthritis (RA) who had not previously received MTX or biologics.

Methods This randomised, double-blind, placebo-controlled, multicentre study evaluated adalimumab 40 mg every other week+MTX 6–8 mg every week versus MTX 6–8 mg every week alone for 26 weeks in patients with RA (≤2-year duration). The primary endpoint was inhibition of radiographic progression (change (Δ) from baseline in modified total Sharp score (mTSS)) at week 26.

Results A total of 171 patients received adalimumab+MTX (mean dose, 6.2±0.8 mg/week) and 163 patients received MTX alone (mean dose, 6.6±0.6 mg/week, p<0.001). The mean RA duration was 0.3 years and 315 (94.3%) had high disease activity (DAS28>5.1). Adalimumab+MTX significantly inhibited radiographic progression at week 26 versus MTX alone (ΔmTSS, 1.5±6.1 vs 2.4±3.2, respectively; p<0.001). Significantly more patients in the adalimumab+MTX group (62.0%) did not show radiographic progression (ΔmTSS≤0.5) versus the MTX alone group (35.4%; p<0.001). Patients treated with adalimumab+MTX were significantly more likely to achieve American College of Rheumatology responses and achieve clinical remission, using various definitions, at 26 weeks versus MTX alone. Combination therapy was well tolerated, and no new safety signals were observed.

Conclusions Adalimumab in combination with low-dose MTX was well tolerated and efficacious in suppressing radiographic progression and improving clinical outcomes in Japanese patients with early RA and high disease activity.

INTRODUCTION

Rheumatoid arthritis (RA) is a chronic inflammatory disorder that is associated with joint damage and progressive disability, an increased risk of morbidity related to comorbid conditions, and substantial socioeconomic costs.[1–3] Given the significant impact biologic therapies have had in the treatment of RA, a paradigm shift has emerged toward earlier inclusion of these therapies in the management of RA.[3 4] Furthermore, international guidelines published in 2010 recommend a treat-to-target goal of remission for patients with early RA in order to mitigate radiographic progression and long-term disability.[5] The efficacy and safety of adalimumab, a tumour necrosis factor (TNF)-α inhibitor, administered as monotherapy or in combination with methotrexate (MTX) for the treatment of RA has been well established in clinical trials conducted in Western countries.[6–12] In early RA, the PREMIER and OPTIMA studies demonstrated that initial combination therapy with adalimumab and MTX was superior to MTX alone in inhibiting radiographic progression and improving clinical symptoms.[6 7 12]

Translating efficacy and safety results of RA Western-based studies to an Eastern populace can be potentially misleading given the genetic, medical and environmental differences (eg, body weight) observed between the two populations.[13] A limited number of studies have evaluated the efficacy or effectiveness and safety of adalimumab in Japanese patients. However, these studies either assessed adalimumab monotherapy in moderate-to-severe RA[14] or were retrospective[15] or postmarketing surveillance studies[16] of adalimumab monotherapy or combination therapy in a population with a wide range of RA duration and prior biologic and MTX experience. Thus, a randomised, placebo-controlled study of adalimumab +MTX combination therapy in MTX-naive Japanese patients with early RA was lacking.

The current study, called adalimumab, a human anti-TNF monoclonal antibody, outcome study for the persistent efficacy under allocation to treatment strategies in early RA, or HOPEFUL 1, was conducted to compare the efficacy and safety of early intervention with adalimumab+MTX versus MTX alone for 26 weeks in inhibiting radiographic progression in MTX-naive Japanese patients with RA.

PATIENTS AND METHODS

Patients aged ≥20 years were evaluated during March 2009 and November 2010 from 94 centres. Eligible patients had RA (1987-revised American College of Rheumatology (ACR) criteria),[17] of ≤2-year duration, a tender joint count ≥10, a swollen joint count ≥8, a C reactive protein (CRP) level ≥1.5 mg/dl or erythrocyte sedimentation rate

Copyright Article author (or their employer) 2013. Produced by BMJ Publishing Group Ltd (& EULAR) under licence.

Downloaded from ard.bmj.com on February 18, 2013 - Published by group.bmj.com

(ESR) ≥28 mm/h, and had ≥1 joint erosion or were rheumatoid factor positive. Patients had not previously received MTX, leflunomide or >2 other disease-modifying antirheumatic drugs (DMARDs). Patients who had previously received cyclophosphamide, cyclosporine, azathioprine, tacrolimus or biologic DMARDs (eg, anti-TNF-α therapy) and patients with a chronic infection, interstitial pneumonia, or a history of tuberculosis or malignancy were excluded from the study.

The phase III trial consisted of a randomised, double-blind, placebo-controlled, 26-week phase followed by a 26-week open-label extension phase (clinicaltrials.gov identifier, NCT00870467; only 26-week double-blind data presented). After a 4-week washout period for patients taking eligible DMARDs and a >2-week screening period for all patients, participants were randomised (1 : 1) to receive subcutaneous adalimumab 40 mg or placebo every other week, both administered in combination with oral MTX 6–8 mg/week (adalimumab +MTX vs MTX alone) for 26 weeks. Treatment with MTX was initiated at 6 mg/week and increased to 8 mg/week in patients who did not experience ≥20% decrease from baseline in tender or swollen joint counts on or after week 8, unless investigators indicated a safety concern. In addition, reduction of the MTX dose to 4 mg/week was permitted at the investigator's discretion. All patients received concomitant oral folic acid 5 mg/week. Patients who experienced a >20% increase from baseline in tender and swollen joint counts at weeks 12, 16 or 20 were to discontinue blinded treatment with adalimumab or placebo and were eligible for open-label rescue treatment with adalimumab 40 mg every other week.

The primary endpoint was inhibition of radiographic progression assessed as the change from baseline (Δ) in modified total Sharp score (mTSS) at week 26. All single-emulsion radiographs of the hands (posteroanterior view) and feet (anteroposterior view) obtained from a patient were scored by two independent readers blinded to patient and treatment, as previously described,[6] with the exception that the triquetrum/pisiform joint was not scored for erosions and the first interphalangeal joint was not scored for joint-space narrowing (range, 0–380) (see online supplementary text for more information).

Secondary efficacy endpoints included ACR responses[18 19] by visit; clinical remission (the 28-joint disease activity score with ESR (DAS28-ESR)<2.6) at week 26;[20 21] and change from baseline in the Health Assessment Questionnaire disability index (HAQ-DI)[22] at week 26. Several additional post hoc analyses were conducted, including assessments of the DAS28-CRP, simplified disease activity index (SDAI)[23] and clinical disease activity index (CDAI) scores[24] over time; clinically relevant radiographic progression (ΔmTSS>3); European League Against Rheumatism responses[25] at week 26; and clinical remission, defined as DAS28-CRP<2.6,[26] SDAI≤3.3,[27 28] CDAI≤2.8[28] or meeting Boolean remission criteria,[27] at week 26. Low, medium and high disease activity was also determined using DAS28-ESR, DAS28-CRP, SDAI and CDAI. Adverse events (AEs) and clinical laboratory parameters were routinely monitored during the study. A 28-day follow-up after the completion of or discontinuation from the study and a 70-day follow-up after the last dose of adalimumab administration were conducted to evaluate safety.

Statistics

The primary endpoint was analysed using the Wilcoxon rank sum test for observed data with a separate supportive analysis using linear extrapolation (LE) to impute missing values. Secondary endpoints were analysed using the Fisher's exact test and Wilcoxon rank sum test for discrete variables and continuous variables, respectively. Non-responder imputation was used for binary variables, and the last-observation-carried-forward approach was applied for continuous variables. The safety population included all randomised patients who received ≥1 dose of study medication and had ≥1 efficacy assessment.

To identify baseline predictors of no radiographic progression (mTSS≤0.5) and clinical remission (DAS28-ESR<2.6), univariate logistic regression analysis was performed, applying 24 baseline demographics and disease characteristics. Significant ($p<0.1$) variables in univariate were included in multivariate models. Last, multivariate models were selected based on model fit statistics (Akaike information criterion and r^2) and clinical significance. Adjusted OR and 95% CIs for selected baseline variables were calculated.

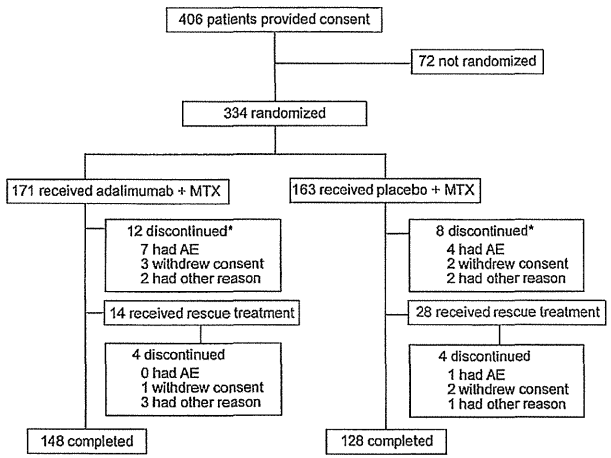

Figure 1 Patient disposition through week 26. *Three adalimumab+MTX patients and one MTX alone patient discontinued from the study by week 26; however, they were included in the efficacy analyses at week 26. AE, adverse event; MTX, methotrexate.

Downloaded from ard.bmj.com on February 18, 2013 - Published by group.bmj.com

RESULTS

Overall, 334 patients were randomised to treatment and received adalimumab+MTX (n=171) or MTX alone (n=163), and 148 (86.5%) and 128 (78.5%) patients completed the double-blind portion of the study, respectively (figure 1). Demographics and baseline characteristics were well matched between treatment groups (table 1). The mean RA disease duration was 0.3 years, and the majority of patients had ≥1 erosion at baseline and high disease activity. The mean MTX dose during the 26-week study was 6.2±0.8 mg/week in the adalimumab+MTX group and 6.6±0.6 mg/week in the MTX alone group ($p<0.001$). After 26 weeks of treatment, 34.5% (59/171) of adalimumab+MTX patients were receiving MTX 8 mg/week versus 65.0% (106/163) of MTX alone patients ($p<0.001$).

Table 1 Demographics and baseline characteristics

Parameter*	Adalimumab+MTX (n=171)	MTX (n=163)
Age±SD (year)	54.0±13.1	54.0±13.2
Females (n (%))	144 (84.2)	128 (78.5)
RA duration±SD (year)	0.3±0.4	0.3±0.4
Weight±SD (kg)	54.4±9.7	56.1±12.3
Previous DMARD use (n (%))	74 (43.3)	87 (53.4)
1 DMARD	57 (33.3)	69 (42.3)
2 DMARDs	17 (9.9)	18 (11.0)
Corticosteroid use at baseline (n (%))	58 (33.9)	49 (30.1)
RF positive (n (%))	146 (85.4)	136 (83.4)
Mean titre±SD (IU/ml)	154.5±202.3	163.7±362.8
Anti-CCP positive (n (%))	145 (84.8)	136 (83.4)
Mean titre±SD (U/ml)	386.2±694.2	241.3±367.2
ESR (mm/h)	59.9±30.1	61.8±29.0
CRP (mg/dl)	2.9±3.0	3.1±3.3
Swollen joint count (n±SD)		
0–28	11.5±4.7	11.8±5.3
0–66	16.5±6.2	17.3±7.7
Tender joint count (n±SD)		
0–28	13.2±5.8	13.2±6.1
0–68	20.7±9.4	21.1±10.2
mTSS	13.6±22.3	13.6±17.4
Erosion score	7.5±11.6	7.3±9.2
Joint space narrowing score	6.2±11.4	6.2±9.4
DAS28-ESR	6.6±0.9	6.6±1.0
DAS28-CRP	5.8±1.0	5.9±1.0
HAQ-DI score	1.1±0.7	1.3±0.8
SDAI score	40.7±12.0	41.4±13.8
CDAI score	37.8±10.9	38.3±12.4
Physician's global assessment of disease activity±SD (mm)	65.8±18.4	66.2±18.8
Patient's global assessment of disease activity±SD (mm)	64.1±24.8	66.4±23.7

*Data are mean±SD unless otherwise indicated.
CCP, cyclic citrullinated peptide; CDAI, clinical disease activity index; CRP, C reactive protein; DAS28-CRP, disease activity score using a 28-joint count and CRP level; DAS28-ESR, disease activity score using a 28-joint count and ESR; DMARD, disease-modifying antirheumatic drug; ESR, erythrocyte sedimentation rate; HAQ-DI, Health Assessment Questionnaire disability index; mTSS, modified total Sharp score; MTX, methotrexate; RA, rheumatoid arthritis; RF, rheumatoid factor; SDAI, simplified disease activity index.

Radiographic progression

Treatment with adalimumab+MTX significantly inhibited radiographic progression (figure 2A) at week 26 versus MTX alone (mean change±SD, 1.5±6.1 vs 2.4±3.2, respectively; $p<0.001$). Results were confirmed by an LE analysis (figure 2A). Changes in radiographic progression during 26 weeks of treatment were also assessed by a cumulative probability plot of ΔmTSS (figure 2B). Fewer adalimumab+MTX patients exhibited radiographic progression (ΔmTSS>0.5), with 62.0% (106/171) of patients showing no radiographic progression versus 35.4% (57/161) of MTX alone patients ($p<0.001$). Furthermore, only 14.0% (24/171) of adalimumab+MTX patients exhibited clinically relevant radiographic progression (ΔmTSS>3) versus 37.3% (60/161) of MTX alone patients ($p<0.001$). In addition, a significantly higher percentage of adalimumab+MTX patients did not experience worsening (≤0.5) in erosion score (73.7% (126/171)) versus MTX alone patients (42.2% (68/161); $p<0.001$). In patients who lacked baseline erosive damage, the continued absence of erosions was reported in more adalimumab+MTX patients versus MTX alone patients (9/9 vs 2/6 patients, respectively; $p=0.01$).

Clinical response

A significantly higher percentage of adalimumab+MTX patients achieved ACR responses versus MTX alone patients at each assessment (figure 3A–C). Significant differences between treatment groups, observed as early as week 2, were maintained through week 26. At week 26, a significantly larger percentage of adalimumab+MTX patients versus MTX alone patients achieved ACR20, ACR50 and ACR70 (figure 3A–C) and ACR90 (12.9% vs 5.5%; $p=0.02$) responses. Significant differences in favour of adalimumab+MTX were also observed from week 2 to 26 for DAS28-ESR, DAS28-CRP, SDAI and CDAI (see online supplementary figure 1A–D). A larger percentage of adalimumab+MTX patients than MTX alone patients demonstrated good or moderate European League Against Rheumatism responses (figure 3D) and were in states of low disease activity or remission after 26 weeks of treatment (figure 3E). Furthermore, a significantly larger percentage of adalimumab+MTX patients versus MTX alone patients satisfied Boolean remission criteria (19.3% vs 8.6%, $p=0.007$). Adalimumab+MTX achieved a 1.8- to 2.2-fold increase in the percentage of patients achieving clinical remission, across all definitions of clinical remission evaluated, versus MTX alone.

A significantly larger decrease from baseline in mean HAQ-DI score, indicative of an improvement in physical function, was observed for adalimumab+MTX patients versus MTX alone patients at week 26 (−0.6±0.6 vs −0.4±0.6; $p<0.001$). Although the significant difference between the two groups was small (0.2 units), the percentage of patients achieving normal functionality (HAQ-DI score<0.5) after 26 weeks of treatment was also significantly higher with adalimumab+MTX (figure 3F).

Factors associated with the absence of radiographic progression or with clinical remission

Disease activity or function baseline variables generally were associated with the absence of radiographic progression (ΔmTSS≤0.5) and with clinical remission (DAS28-ESR<2.6) in both treatment groups (see online supplementary text and online supplementary table 1).

Downloaded from ard.bmj.com on February 18, 2013 - Published by group.bmj.com

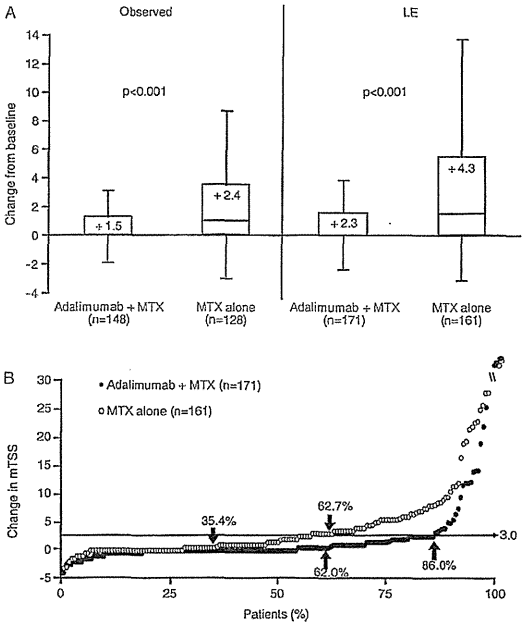

Figure 2 (A) Box plot of change from baseline in mTSS at week 26 with adalimumab+MTX versus MTX alone and (B) cumulative probability plot of mean change from baseline to week 26 in mTSS score (LE). Thickened horizontal lines in (A) indicate median values, the boxes mark the interval between the 25th and 75th percentiles, whiskers indicate the IQR and mean values are reported in the boxes. No radiographic progression (change from baseline in mTSS≤0.5) was reported in 62.0% (106/171) of adalimumab+MTX patients versus 35.4% (57/161) of MTX alone patients (p<0.001). No clinically relevant radiographic progression (change from baseline mTSS≤3) was reported in 86.0% (147/171) of adalimumab+MTX patients versus 62.7% (101/161) of MTX alone patients (p<0.001) (B). LE, linear extrapolation; mTSS, modified total Sharp score; MTX, methotrexate. p Value determined using Wilcoxon rank sum test.

Safety

The mean treatment duration during the double-blind phase was *168.7±36.6 days for adalimumab+MTX patients* (mean cumulative adalimumab dose, *477.4±104.5* mg) and 162.8±38.6 days for MTX alone patients. Overall, there were 376 and 302 AEs reported in the adalimumab+MTX group and the MTX alone group, respectively. There were no significant differences in the percentage of patients with AEs *in the adalimumab+MTX group* (80.7% (138/171)) versus the MTX alone group (71.8% (117/163)), and the incidence of severe AEs was rare (table 2). No significant differences in the incidence of AEs of interest were observed between the two groups, with the exception of injection-site reactions, which were reported in 10.5% of adalimumab+MTX patients and 3.7% of MTX alone patients (p=0.02; table 2). Serious infections were observed in two adalimumab+MTX patients (one case each of pneumonia and infectious enteritis) and one MTX alone patient (*Pneumocystis jiroveci* pneumonia), occurring at rates of 2.5 and 1.4 events per 100 patient-years, respectively. There were no reports of demyelination, tuberculosis or malignancy during the study. One death, due to worsening of interstitial lung disease, occurred in the MTX alone group.

DISCUSSION

The HOPEFUL 1 study was designed to evaluate the efficacy and safety of adalimumab in combination with MTX in Japanese patients with early RA. This is the first description of a clinical trial of anti-TNF therapy+MTX versus MTX alone in MTX-naive Japanese patients with early RA and high disease activity. It is also the first randomised trial evaluating the efficacy of anti-TNF *therapy+low-dose MTX versus low-dose MTX alone for the* inhibition of radiographic progression in any patient population. This study extends observations from Western studies of adalimumab by demonstrating the superiority of adalimumab+MTX to MTX alone for the inhibition of radiographic progression and *improvement in clinical outcomes in Japanese patients with early* RA. Moreover, the combination of adalimumab+MTX significantly improved a wide array of clinical and functional disease activity measures and responses versus MTX alone, with improvements observed as early as the first assessment (week 2) and maintained through the 26-week double-blind trial.

Following 26 weeks of treatment, the mean ΔmTSS (primary endpoint) in adalimumab+MTX patients (1.48) in the current study was significantly smaller than observed in MTX alone patients (2.38). In addition, a similar trend in inhibition of radiographic progression in patients with early RA was observed in the OPTIMA study, with a smaller mean ΔmTSS in adalimumab+MTX patients (0.15) versus MTX alone patients (0.96; p<0.001).[12] The difference between the two treatment groups (0.8) at week 26 was similar to the difference observed in the current study (0.9 (observed)).[12] Furthermore, baseline characteristics, including RA duration, in the two studies were generally similar, but the OPTIMA study had a lower percentage of previous DMARD use.

A similar trend in inhibition of radiographic progression in the current study was observed in the PREMIER study, with a

Downloaded from ard.bmj.com on February 18, 2013 - Published by group.bmj.com

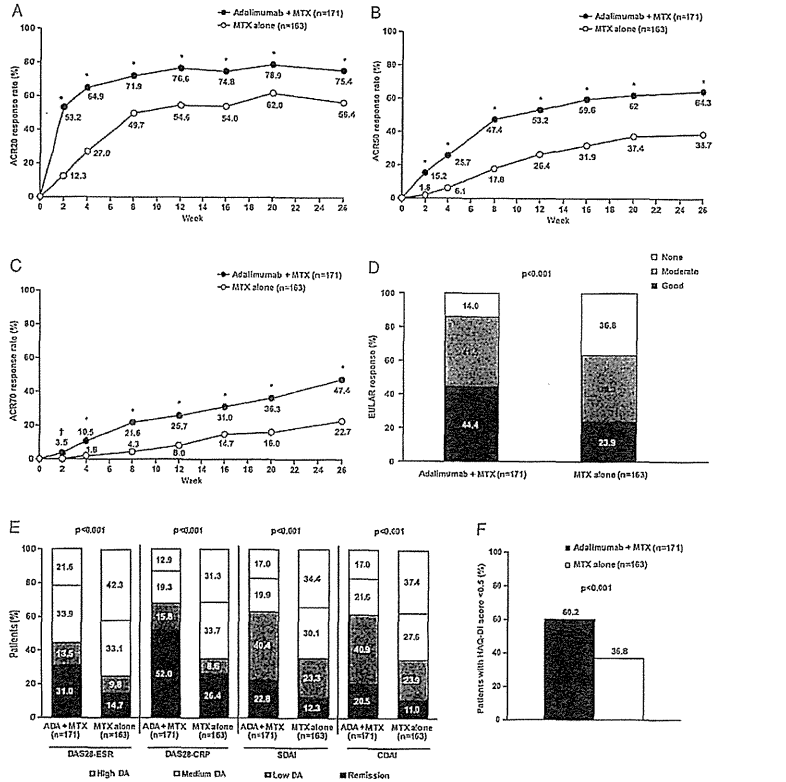

Figure 3 Percentage of patients with an (A) ACR20 response, (B) ACR50 response or (C) ACR70 response over time; (D) the percentage of patients with a EULAR response at week 26; (E) the percentage of patients with low, medium or high disease activity at week 26; and (F) the percentage of patients achieving functional remission (HAQ-DI score<0.5) at week 26. The following values were used to identify remission, low, medium and high disease activity for each clinical assessment in (E): DAS28-ESR or DAS-CRP (<2.6, ≥2.6–<3.2; ≥3.2–≤5.1, >5.1, respectively), SDAI (≤3.3, >3.3–≤11.0, >11.0–≤26.0, >26.0, respectively), and CDAI (≤2.8, >2.8–≤10.0, >10.0–≤22.0, >22.0, respectively). *p<0.001 versus MTX alone. †p=0.03 versus MTX alone. ACR, American College of Rheumatology; ADA, adalimumab; CDAI, clinical disease activity index; DA, disease activity; DAS28-CRP, disease activity score using a 28-joint count and C reactive protein level; DAS28-ESR, disease activity score using a 28-joint count and erythrocyte sedimentation rate; EULAR, European League Against Rheumatism; HAQ-DI, Health Assessment Questionnaire disability index; MTX, methotrexate; SDAI, simplified disease activity index.

smaller mean ΔmTSS in adalimumab+MTX patients (0.8) versus MTX alone patients (3.5; p<0.001). However, the mean difference in radiographic progression between the two treatments groups, although statistically significant, was smaller in the current study (0.9 (observed); 2.0 (LE)) than in the PREMIER study (2.7).

In the current study, the SD for the mean ΔmTSS at week 26 was generally high. When the median ΔmTSS was compared using observed data, results were in good agreement between the PREMIER study (0.0 (adalimumab+MTX) vs 1.3 (MTX alone); data on file) and the current study (0.0 (adalimumab +MTX) vs 1.0 (MTX alone)). Alternatively, the smaller difference in improvement observed in the current study may also be related to the mTSS scoring method used, but this seems unlikely because only two joints assessed in PREMIER were omitted from scoring in the present analysis. The mean duration of RA was also shorter in the current study (0.3 years) versus the PREMIER study (0.7–0.8 years), although the percentage of patients who had previously taken DMARDs was higher (43.3–53.4% vs 31.5–32.5%). There were also slight differences in mean baseline tender and swollen joint counts and CRP levels, which were higher in the PREMIER study and considered

Downloaded from ard.bmj.com on February 18, 2013 - Published by group.bmj.com

Table 2 Adverse events (AEs)

Parameter	Patients (n (%)) Adalimumab+MTX (n=171)	MTX (n=163)
Any AE	138 (80.7)	117 (71.8)
Severe AE	1 (0.6)	1 (0.6)
Serious AE	7 (4.1)	4 (2.4)
Infectious AE	59 (34.5)	48 (29.4)
Serious infection	2 (1.2)	1 (0.6)
AEs leading to study drug discontinuation	7 (4.1)	6 (3.7)
AEs of interest		
Elevated liver function test level	32 (18.7)†	21 (12.9)†
Injection-site reaction	18 (10.5)*	6 (3.7)
Haematological event	7 (4.1)	8 (4.9)
Allergic reaction	1 (0.6)	2 (1.2)
Interstitial lung disease	1 (0.6)	1 (0.6)
Lupus-like syndrome	0	1 (0.6)
Opportunistic infection	0	1 (0.6)

*p=0.02 versus MTX.
†≥94% of events were mild in severity.
MTX, methotrexate.

related to the longer duration of RA at baseline versus the current study. Furthermore, the MTX dose of 6–8 mg/week, although consistent with the dosage commonly administered in Japan at the time the study was conducted, was substantially lower than that commonly administered in Western countries (eg, 15–20 mg/week). In the PREMIER study, MTX was initiated at 7.5 mg/week, increased to 15 mg/week during weeks 4–8, and increased to 20 mg/week starting at week 9. In addition, the mean MTX dose during the 26 weeks of the current study was significantly lower in the adalimumab+MTX group (6.2±0.8 mg/week) versus the MTX alone group (6.6±0.6 mg/week; $p<0.001$), thereby potentially impacting the ΔmTSS and thus the maximal difference observed between the two treatment groups. Therefore, these multiple differences may have contributed to the small difference in radiographic outcomes between the current study and the PREMIER study. Whether the difference in radiographic outcomes can be explained by differences between Japanese and Western populations remains unclear, although this seems unlikely. Longer-term studies may help elucidate potential differences in outcomes.

Since this study was conducted, the maximum approved MTX dosage in Japan has been increased from 8 to 16 mg/week in patients with RA. Therefore, this study provides important information on the efficacy of low-dose MTX and anti-TNF therapy versus low-dose MTX alone for the inhibition of radiographic progression. Data suggest that patients with early RA who may not tolerate higher doses of MTX will likely benefit from adalimumab+low-dose MTX combination therapy.

Given the lower MTX dose prescribed, one could question whether we might only be seeing natural progression in the MTX only arm. It is ethically difficult to include a true placebo arm in clinical trials of ≥6 months duration for early active RA, particularly when MTX is recommended as first-line therapy to achieve clinical remission/low disease activity. Although an important question to ponder, a placebo arm in long-term clinical trials in early active RA appears to be unrealistic, and further research using highly sensitive and reproducible imaging techniques during a short-term placebo-treatment period in early active RA is warranted.

It is also important to note that the current patient population had severe baseline symptoms, including baseline erosions, despite only several months since RA onset. This scenario is becoming increasingly less common in Western populations due to treat-to-target recommendations and earlier intervention. In Japan, general practitioners are still seeing many early RA patients and referrals to rheumatologists are often delayed. In addition, the diagnosis of RA in this trial was based upon 1987 classification criteria. Thus, these factors may have played a role in the conundrum of more severe baseline clinical symptoms yet shorter mean disease duration.

The clinical results of the current study are supported by the HARMONY study, which retrospectively determined the effectiveness and safety of adalimumab 40 mg every other week with or without MTX (mean dose, 8.5 mg/week) in Japanese patients with RA (mean RA duration, 9.0±9.5 years) with or without prior biologic treatment.[15] Although patients in the HARMONY study had more established disease and the study design was retrospective, adalimumab+MTX patients (n=143) had an improvement from baseline in DAS28-ESR score at week 24 (baseline, 5.3; week 24, 3.3), which was within the range but slightly smaller than the improvement observed in the current study at week 26 (baseline, 6.6; week 26, 3.7; see online supplementary figure 1A). Clinical remission rates for adalimumab+MTX patients were also comparable between the HARMONY study (week 24, 35.0%) and the current study (week 26, 31.0%).

The safety profile of the current study was generally consistent with those in previous clinical studies of adalimumab in patients with RA conducted in Japan.[14–16] There were no reports of demyelination, tuberculosis or malignancy, and there were no statistically significant differences in the incidence of serious AEs, serious infections, opportunistic infections or lupus-like reactions between adalimumab+MTX patients versus MTX alone patients. There was a significantly higher incidence of injection-site reactions for adalimumab+MTX patients versus MTX alone patients, but the incidence (10.5%) was similar to that reported for the 167 adalimumab±MTX patients in the HARMONY study (12.0%). The incidence of injection-site reactions in both of these studies was lower than the 30.8% reported for the 91 adalimumab monotherapy patients (40 mg every other week) in the CHANGE study,[14] possibly related to the immunosuppressive effects of concomitant MTX in the current study and in some of the patients in the HARMONY study.

In the multivariate regression analyses (see online supplementary table 1), lower baseline CRP level was identified as a predictor of radiographic non-progression in adalimumab+MTX patients, whereas normal baseline CRP level (≤0.3 mg/dl) appeared to have an increased likelihood of radiographic non-progression. However, no baseline predictors appeared to predict both the lack of progression and clinical remission. Furthermore, baseline mTSS was not an independent predictor for either treatment group in this study.

Overall, adalimumab+MTX was well tolerated in Japanese patients with early RA with no new safety signals and with a safety and tolerability profile similar to that observed in Western populations. Administration of adalimumab in combination with MTX was efficacious in improving radiographic and clinical responses in MTX-naive patients with early RA, high disease activity and poor prognostic factors (eg, rheumatoid factor positive or with baseline erosive damage) through week 26. Given its radiographic, clinical and functional superiority versus MTX monotherapy, consideration should be given to administration of anti-TNF-α and MTX combination therapy in patients with early RA and high disease activity.

Author affiliations
[1]Division of Rheumatology, Department of Internal Medicine, School of Medicine, Keio University, Shinjuku-ku, Tokyo, Japan
[2]Institute of Rheumatology, Tokyo Women's Medical University, Shinjuku-ku, Tokyo, Japan
[3]Department of Orthopedic Surgery, Nagoya University Graduate School and School of Medicine, Showa-ku, Nagoya, Japan
[4]Department of Medicine and Rheumatology, Graduate School of Tokyo Medical and Dental University, Bunkyo-ku, Tokyo, Japan
[5]Division of Rheumatology and Hematology, Department of Medicine, Sapporo City General Hospital, Chuo-ku, Sapporo, Japan
[6]Matsubara Mayflower Hospital, Katou-shi, Hyogo, Japan
[7]Uchida Clinic of Rheumatic Diseases, Sumida-ku, Tokyo, Japan
[8]Eisai Co, Ltd., Bunkyo-ku, Tokyo, Japan
[9]Abbott GmbH & Co KG, Ludwigshafen, Germany
[10]Abbott Laboratories, Abbott Park, Illinois, USA
[11]The First Department of Internal Medicine, School of Medicine, University of Occupational and Environmental Health, Japan, Yahatanishi-ku, Kitakyushu, Japan

Acknowledgements The authors would like to thank all the patients, investigators and support staff who participated in the study, Sourav Santra, PhD, formally of Abbott, who provided statistical support, and Mary Beth C. Moncrief, PhD, of MedThink SciCom, for editorial assistance in the writing of this manuscript; this assistance was funded by Abbott.

Contributors All the authors evaluated the study results, interpreted the data and suggested additional analyses. All authors contributed to the development and critical review of manuscript and approved the final version.

Funding This study was supported by Abbott Japan Co (Tokyo, Japan) and Eisai Co (Tokyo, Japan).

Competing interests TT has received consulting fees, speaking fees, honoraria and/or research grant support from Abbott Japan Co; Astellas Pharma Inc; Astra-Zeneca K.K.; Bristol-Myers Squibb; Chugai Pharmaceutical Co; Daiichi-Sankyo Co; Eisai Co; Janssen Pharmaceutical K.K.; Mitsubishi Tanabe Pharma Corporation; Pfizer Japan Inc; and Takeda Pharmaceutical Co. HY has received research grants from Abbott Japan Co; Bristol-Myers Squibb; Chugai Pharmaceutical Co; Eisai Co; Janssen Pharmaceutical K.K.; Mitsubishi Tanabe Pharma Corporation; Otsuka Pharmaceutical Co; Pfizer Japan Inc; Takeda Industrial Pharmaceutical Co; and UCB Japan Co, and speakers honoraria/consulting fees from Abbott Japan Co; Bristol-Myers Squibb; Chugai Pharmaceutical Co; Eisai Co; Janssen Pharmaceutical K.K.; Mitsubishi Tanabe Pharma Corporation; Otsuka Pharmaceutical Co; Pfizer Japan Inc; Takeda Pharmaceutical Co; and UCB Japan Co. NI has received research grants from Astellas Pharmaceutical; Chugai Pharmaceutical Co; Eisai Co; and Mitsubishi Tanabe Pharmaceutical Co. NM has received research grants from Abbott Japan Co; Astellas Pharmaceutical; Banyu Pharmaceutical; Chugai Pharmaceutical Co; Daiichi Sankyo Pharmaceutical Co; Eisai Co; Janssen Pharmaceuticals; Mitsubishi Tanabe Pharma Corporation; Takeda Pharmaceutical Co; and Teijin Limited. MM has received research grants from Abbott Japan Co; Eli Lilly Japan K.K.; GlaxoSmithKline K.K.; Pfizer Japan Inc; Bristol-Myers Squibb; and Otsuka Pharmaceutical Co, and received compensation for work on this manuscript from Abbott Japan Co. TM has received research grants from Chugai Pharmaceutical Co; Bristol-Myers Squibb; Nippon Kayaku Co; Otsuka Pharmaceutical Co; Takeda Pharmaceutical Co; Eli Lilly Japan K.K.; Eli Lilly and Company; Astellas Pharma Inc; Pfizer Japan Inc; AstraZeneca K.K.; and Santen Pharmaceutical Co, and received compensation for work on this manuscript from Abbott Japan Co. SU has received research grants from Abbott Japan Co, and received compensation for work on this manuscript from Abbott Japan Co. HA is an employee of Eisai Co, Tokyo, Japan. HK is an employee of Abbott GmbH and Co KG, Ludwigshafen, Germany, and may hold Abbott stock or options. VA is an employee of Abbott Laboratories, Abbott Park, Illinois, USA, and may hold Abbott stock or options. YT has received consulting fees, speaking fees and/or honoraria from Mitsubishi Tanabe Pharma Corporation; Abbott Japan Co; Eisai Co; Chugai Pharmaceutical Co; Janssen Pharmaceutical K.K.; Santen Pharmaceutical Co; Pfizer Japan Inc; Astellas Pharma Inc; Daiichi-Sankyo Co; GlaxoSmithKline K.K.; Astra-Zeneca; Otsuka Pharmaceutical Co; Actelion Pharmaceuticals Japan; Eli Lilly Japan K.K.; Nippon Kayaku Co; UCB Japan Co; Quintiles Transnational Japan Co; Ono Pharmaceutical Co; and Novartis Pharma K.K. YT has received research grants from Bristol-Myers Squibb; MSD K.K.; Chugai Pharmaceutical Co; Mitsubishi Tanabe Pharma Corporation; Astellas Pharma Inc; Abbott Japan Co; Eisai Co; and Janssen Pharmaceutical K.K.

Patient consent Obtained.

Ethics approval An institutional review board approved the study at each site.

Provenance and peer review Not commissioned; externally peer reviewed.

Open Access This is an Open Access article distributed in accordance with the Creative Commons Attribution Non Commercial (CC BY-NC 3.0) license, which permits others to distribute, remix, adapt, build upon this work non-commercially, and license their derivative works on different terms, provided the original work is properly cited and the use is non-commercial. See: http://creativecommons.org/licenses/by-nc/3.0/

REFERENCES

1 Filipović I, Walker D, Forster F, *et al*. Quantifying the economic burden of productivity loss in rheumatoid arthritis. *Rheumatology (Oxford)* 2011; 50:1083–90.
2 Scott DL, Wolfe F, Huizinga TWJ. Rheumatoid arthritis. *Lancet* 2010;376:1094–108.
3 Takeuchi T. Revolutionary change in rheumatoid arthritis management with biological therapy. *Keio J Med* 2011;60:75–81.
4 Saag KG, Teng GG, Patkar NM, *et al*. American College of Rheumatology 2008 recommendations for the use of nonbiologic and biologic disease-modifying antirheumatic drugs in rheumatoid arthritis. *Arthritis Rheum* 2008;59:762–84.
5 Smolen JS, Aletaha D, Bijlsma JW, *et al*. For the T2T Expert Committee. Treating rheumatoid arthritis to target: recommendations of an international task force. *Ann Rheum Dis* 2010;69:631–7.
6 Breedveld FC, Weisman MH, Kavanaugh AF, *et al*. For the PREMIER Investigators. The PREMIER study: a multicenter, randomized, double-blind clinical trial of combination therapy with adalimumab plus methotrexate versus methotrexate alone or adalimumab alone in patients with early, aggressive rheumatoid arthritis who had not had previous methotrexate treatment. *Arthritis Rheum* 2006;54:26–37.
7 van der Heijde D, Breedveld FC, Kavanaugh A, *et al*. Disease activity, physical function, and radiographic progression after longterm therapy with adalimumab plus methotrexate: 5-year results of PREMIER. *J Rheumatol* 2010;37:2237–46.
8 Weinblatt ME, Keystone EC, Furst DE, *et al*. Adalimumab, a fully human anti-tumor necrosis factor α monoclonal antibody, for the treatment of rheumatoid arthritis in patients taking concomitant methotrexate: the ARMadalimumab trial. *Arthritis Rheum* 2003;48:35–45.
9 van de Putte LBA, Atkins C, Malaise M, *et al*. Efficacy and safety of adalimumab as monotherapy in patients with rheumatoid arthritis for whom previous disease modifying antirheumatic drug treatment has failed. *Ann Rheum Dis* 2004;63:508–16.
10 Keystone EC, Kavanaugh AF, Sharp JT, *et al*. Radiographic, clinical, and functional outcomes of treatment with adalimumab (a human anti-tumor necrosis factor monoclonal antibody) in patients with active rheumatoid arthritis receiving concomitant methotrexate therapy: a randomized, placebo-controlled, 52-week trial. *Arthritis Rheum* 2004;50:1400–11.
11 Furst DE, Schiff MH, Fleischmann RM, *et al*. Adalimumab, a fully human anti tumor necrosis factor-alpha monoclonal antibody, and concomitant standard antirheumatic therapy for the treatment of rheumatoid arthritis: results of STAR (Safety Trial of Adalimumab in Rheumatoid Arthritis). *J Rheumatol* 2003;30:2563–71.
12 Kavanaugh A, Fleischmann RM, Emery P, *et al*. Clinical, functional and radiographic consequences of achieving stable low disease activity and remission with adalimumab plus methotrexate or methotrexate alone in early rheumatoid arthritis: 26-week results from the randomised, controlled OPTIMA study. *Ann Rheum Dis* 2013;72:64–71.
13 Takeuchi T, Kameda H. The Japanese experience with biologic therapies for rheumatoid arthritis. *Nat Rev Rheumatol* 2010;6:644–52.
14 Miyasaka N, The CHANGE Study Investigators. Clinical investigation in highly disease-affected rheumatoid arthritis patients in Japan with adalimumab applying standard and general evaluation: the CHANGE study. *Mod Rheumatol* 2008;18:252–62.
15 Takeuchi T, Tanaka Y, Kaneko Y, *et al*. Effectiveness and safety of adalimumab in Japanese patients with rheumatoid arthritis: retrospective analyses of data collected during the first year of adalimumab treatment in routine clinical practice (HARMONY study). *Mod Rheumatol* 2012;22:327–38.
16 Koike T, Harigai M, Ishiguro N, *et al*. Safety and effectiveness of adalimumab in Japanese rheumatoid arthritis patients: postmarketing surveillance report of the first 3,000 patients. *Mod Rheumatol* 2012;22:498–508.
17 Arnett FC, Edworthy SM, Bloch DA, *et al*. The American Rheumatism Association 1987 revised criteria for the classification of rheumatoid arthritis. *Arthritis Rheum* 1988;31:315–24.
18 Felson DT, Anderson JJ, Boers M, *et al*. American College of Rheumatology. Preliminary definition of improvement in rheumatoid arthritis. *Arthritis Rheum* 1995;38:727–35.
19 Felson DT, Anderson JJ, Lange ML, *et al*. Should improvement in rheumatoid arthritis clinical trials be defined as fifty percent or seventy percent improvement in core set measures, rather than twenty percent? *Arthritis Rheum* 1998;41:1564–70.
20 Fransen J, Creemers MCW, van Riel PLCM. Remission in rheumatoid arthritis: agreement of the disease activity score (DAS28) with the ARA preliminary remission criteria. *Rheumatology (Oxford)* 2004;43:1252–5.
21 Prevoo ML, van't Hof MA, Kuper HH, *et al*. Modified disease activity scores that include twenty-eight-joint counts. Development and validation in a prospective